

Learning with Neural Tangent Kernels in Near Input Sparsity Time

Amir Zandieh
 Max-Planck Institute for Informatics
 azandieh@mpi-inf.mpg.de

May 4, 2022

Abstract

The Neural Tangent Kernel (NTK) characterizes the behavior of infinitely wide neural nets trained under least squares loss by gradient descent [JGH18]. However, despite its importance, the super-quadratic runtime of kernel methods limits the use of NTK in large-scale learning tasks. To accelerate kernel machines with NTK, we propose a near input sparsity time algorithm that maps the input data to a randomized low-dimensional feature space so that the inner product of the transformed data approximates their NTK evaluation. Furthermore, we propose a feature map for approximating the convolutional counterpart of the NTK [ADH⁺19b], which can transform any image using a runtime that is only linear in the number of pixels. We show that in standard large-scale regression and classification tasks a linear regressor trained on our features outperforms trained NNs and Nystrom method with NTK kernels.

1 Introduction

The Neural Tangent Kernel (NTK), introduced by [JGH18], characterizes the behavior of infinitely wide fully connected neural nets trained by gradient descent. In fact, for least-squares loss, an ultra-wide net trained by gradient descent is equivalent to kernel regression with respect to the NTK. This kernel is shown to be central in theoretical understanding of the generalization and optimization properties of neural networks. More recently, [ADH⁺19b] extended this result by proving an analogous equivalence between convolutional nets with an infinite number of channels and Convolutional NTK (CNTK). Because the NTK and CNTK are obtained from tangent approximation to deep neural networks, it is plausible to expect them to be more powerful and expressive than the classical kernel functions such as Polynomial or Laplacian. Thus, plugging these kernels into kernelized learning methods, such as kernel regression or SVM, can effectively capture the power of a fully-trained deep net by a pure kernel-based method. In fact, [ADH⁺19b] showed that kernel regression using CNTK sets an impressive performance record on CIFAR-10 for kernel methods without trainable kernels and more recently, [ADL⁺19] applied kernel method with neural tangent kernels on a large array of low-data tasks and showed that it consistently beats previous gold standards including fully-trained deep neural nets.

While kernel machines enjoy good generalization and well understood statistical properties, they suffer from scalability challenges as they operate on the kernel matrix (Gram matrix of data), whose size scales quadratically in the size of the training dataset. In particular, for a dataset of n images $x_1, x_2, \dots, x_n \in \mathbb{R}^{d_1 \times d_2}$, only writing down the kernel matrix corresponding to the CNTK requires $\Omega(d_1^2 d_2^2 \cdot n^2)$ operations [ADH⁺19b]. Running regression or PCA on the resulting kernel matrix takes additional $\Omega(n^{w=2.373})$ time. We address this issue by designing feature maps with low-dimensional feature spaces so that the inner product between a pair of transformed data points approximates their kernel evaluation for the important NTK and CNTK kernels.

Problem Definition. For the NTK corresponding to a deep net $\Theta_{ntk} : \mathbb{R}^d \times \mathbb{R}^d \rightarrow \mathbb{R}$, we propose an explicit randomized feature map $\Psi_{ntk} : \mathbb{R}^d \rightarrow \mathbb{R}^s$ with small target dimension s such that, for any pair of points $y, z \in \mathbb{R}^d$:

$$\Pr [\langle \Psi_{ntk}(y), \Psi_{ntk}(z) \rangle \in (1 \pm \epsilon) \cdot \Theta_{ntk}(y, z)] \geq 1 - \delta,$$

We construct feature spaces that uniformly approximate the NTK $\Theta_{ntk}(\cdot, \cdot)$ to within $(1 \pm \epsilon)$ multiplicative factor with probability $1 - \delta$ with only $s = O\left(\epsilon^{-2} \log \frac{1}{\delta}\right)$ dimensions. Furthermore, our feature map can transform any data point $x \in \mathbb{R}^d$ using a runtime which is nearly proportional to the sparsity of that point, i.e., $\tilde{O}(\text{nnz}(x))$ runtime.

Additionally, for the CNTK corresponding to a convolutional deep net $\Theta_{cntk} : \mathbb{R}^{d_1 \times d_2} \times \mathbb{R}^{d_1 \times d_2} \rightarrow \mathbb{R}$, we construct feature spaces that uniformly approximate the CNTK $\Theta_{cntk}(\cdot, \cdot)$ to within $(1 \pm \epsilon)$ multiplicative factor with probability $1 - \delta$ with only $s = O\left(\epsilon^{-2} \log \frac{1}{\delta}\right)$ dimensions. Our feature map can transform any image $x \in \mathbb{R}^{d_1 \times d_2}$ using a runtime which depends nearly linearly on the number of pixels of the image, i.e., $\tilde{O}(d_1 d_2)$ runtime. To the best of our knowledge, there are no previously known data oblivious feature maps for NTK or CNTK with provable guarantees.

Consequently, we can simply transform the input dataset with our feature maps, and then apply fast linear learning methods to approximate the answer of the corresponding nonlinear kernel method with NTK kernels. In particular, the kernel regression can be solved approximately using our feature transform in time $O(s^2 \cdot n)$ which is significantly faster than the exact kernel regression when n is large.

1.1 Contributions

In this paper we design data oblivious feature maps for uniformly approximating the NTK as well as the CNTK:

- We prove that the NTK of a fully connected deep net with ReLU activation is a highly structured object which can be fully characterized by a univariate function $K_{relu} : [-1, 1] \rightarrow \mathbb{R}$, plotted for various network depths in Figure 1. In fact the NTK is a normalized dot-product kernel, i.e., $\Theta_{ntk}(y, z) \equiv \|y\|_2 \|z\|_2 \cdot K_{relu}\left(\frac{\langle y, z \rangle}{\|y\|_2 \|z\|_2}\right)$, see Theorem 1. This specific structure is the key insight behind designing efficient sketching methods for the NTK kernel.
- We design an efficient algorithm for mapping the data points to a low-dimensional features space such that the inner product between a pair of transformed points approximates their NTK evaluation. The features space has dimension $s = O\left(\epsilon^{-2} \log \frac{1}{\delta}\right)$ and our algorithm transforms any data point in time that is nearly proportional to its sparsity, see Theorem 2.
- We propose an efficient algorithm for mapping a dataset of images to a low-dimensional features space such that the inner product between a pair of transformed images approximates their CNTK evaluation. The features space has dimension $s = O\left(\epsilon^{-2} \log \frac{1}{\delta}\right)$ and our algorithm transforms any image using a runtime that is nearly proportional to the number of pixels, see Theorem 3.
- Finally, we investigate our NTK feature maps on standard large-scale regression and classification datasets with over half a million examples and show that our method competes favorably with trained MLPs and Nystrom method with NTK kernel. Furthermore, we demonstrate the power of our CNTK feature map on MNIST dataset and show that our method outperforms trained CNNs.

Our results give the first data oblivious sketching method that can quickly sketch the NTK and CNTK kernels. In particular, our CNTK sketch maps an entire dataset of n images of size $d_1 \times d_2$ pixels to an $s = O^*(1/\epsilon^2)$ -dimensional feature space using a total runtime of $\text{poly}(L, \epsilon^{-1}) \cdot d_1 d_2 \cdot n$. Thus, we can approximately solve the CNTK kernel regression problem in total time $\text{poly}(L, \epsilon^{-1}) \cdot d_1 d_2 \cdot n$. This is extremely faster than exact kernel regression using CNTK, which takes $\Omega(L \cdot (d_1 d_2)^2 \cdot n^2 + n^{\omega=2.373})$, when $d_1 d_2 \cdot n \gg \text{poly}(L, \epsilon^{-1})$.

1.2 Related Work

There has been a long line of work on the correspondence between deep or convolutional neural nets and kernel machines [LBN⁺18, MHR⁺18, NXB⁺18, GARA18, Yan19]. Furthermore, in recent years there has been a lot of effort in understanding the convergence and generalization of neural networks in the over-parameterized regime [DLL⁺19, DZPS18, LL18, DH19, AZLL19, AZLS19, CG19, ADH⁺19a, Yan19, ADL⁺19, BM19], all of which either explicitly or implicitly use the notion of neural tangent kernel [JGH18]. More recently, [ADH⁺19b] gave an efficient procedure to compute the convolutional extension of neural tangent kernel, which they name CNTK. We remark that the over-parametrized neural network theory is not our focus and our aim is merely to accelerate kernel-based learning with NTK and CNTK kernels using sketching techniques.

So far, there is little known about how to speed up learning with these kernels. [NXB⁺18] tried accelerating CNTK computations via Monte Carlo methods. They generate random features by taking the gradient of randomly initialized CNNs with respect to the weight matrices. Although they do not provide a provable guarantee on the number of features needed to have control over the error, one can expect that this method requires a large number of features in order to enter the over-parametrized regime and achieve a good approximation factor. In fact, we can analyze the fully-connected version of this Monte Carlo method. By theorem 3.1 of [ADH⁺19b], in order for the gradient of a randomly initialized fully-connected ReLU network to approximate the NTK kernel up to ϵ , its width needs to be at least $\Omega(L^6/\epsilon^4 \cdot \log(L/\delta))$. The number of weights of such network is in the order of $\Omega(L^{13}/\epsilon^8 \cdot \log^2(L/\delta))$, thus, transforming a single vector $x \in \mathbb{R}^d$ using this method would require $\Omega(L^{13}/\epsilon^8 \cdot \log^2(L/\delta) + L^6/\epsilon^4 \cdot \log(L/\delta) \cdot \text{nnz}(x))$ operations, which is slower than our theorem 2 by a factor of L^3/ϵ^2 . Furthermore, [ADH⁺19b] shows that these random features perform poorly in practice and decrease the classification accuracy by a large margin compared to exact CNTK. More recently, [LSS⁺20] proposed leverage score sampling for the NTK, however, their work is primarily theoretical and does not suggest an efficient way of sampling the features.

In the literature, much work has focused on scaling up kernel methods by producing low-rank approximations to kernel matrices [AM15, ACW17, ZNV⁺20]. A popular approach for accelerating kernel methods is based on Nystrom sampling. We refer the reader to the work of [MM17] and the references therein. This method can efficiently produce a spectral approximation to the kernel matrix, however, it is not data oblivious and needs to read the entire dataset in order to select the landmarks. In contrast, instead of approximating the kernel matrix, our work approximates the kernel function directly using a *data oblivious* random mapping, providing nice advantages, such as one-round distributed protocols and single-pass streaming algorithms.

Another popular line of work on kernel approximation problem is based on the Fourier features method of [RR07]. This method works well in practice and with some modifications can embed the Gaussian kernel near optimally [AKM⁺17], however, it only works for shift-invariant kernels and does not apply to NTK or CNTK.

In linear sketching literature, [ANW14] proposed an oblivious subspace embedding for the polynomial kernel. The runtime of this method, while nearly linear in sparsity of the input dataset, scales exponentially in the degree of the polynomial kernel. In a recent work, [AKK⁺20] improved

the exponential dependence on the kernel's degree to polynomial. This improvement enables them to sketch high degree polynomial kernels and hence led to near-optimal embedding of the Gaussian kernel. In fact, this sketching technology constitutes one of the main ingredients of our proposed sketch for the NTK and CNTK. Additionally, there is an improvement on embedding high-degree polynomial kernel, due to [WZ20], which combines sketching with leverage score sampling to achieve fastest possible runtime. However, since this method is data-dependent and our focus is on oblivious methods we did not use the techniques from this work.

2 Preliminaries and Notations

Definition 2.1 (Tensor product). Given $x \in \mathbb{R}^m$ and $y \in \mathbb{R}^n$ we define the twofold tensor product $x \otimes y$ as

$$x \otimes y = \begin{bmatrix} x_1 y_1 & x_1 y_2 & \cdots & x_1 y_n \\ x_2 y_1 & x_2 y_2 & \cdots & x_2 y_n \\ \vdots & \vdots & & \vdots \\ x_m y_1 & x_m y_2 & \cdots & x_m y_n \end{bmatrix} \in \mathbb{R}^{m \times n}.$$

Tensor product can be naturally extended to matrices, which results in 4-dimensional objects, i.e., for $X \in \mathbb{R}^{m \times n}$ and $Y \in \mathbb{R}^{m' \times n'}$, the tensor product $X \otimes Y$ is in $\mathbb{R}^{m \times n \times m' \times n'}$.

Although tensor products are multidimensional objects, it is often convenient to associate them with single-dimensional vectors. In particular, we often associate $x \otimes y$ with a single dimensional vector $(x_1 y_1, x_2 y_1, \dots, x_m y_1, x_1 y_2, x_2 y_2, \dots, x_m y_2, \dots, x_m y_n)$.

Given $v_1 \in \mathbb{R}^{d_1}, v_2 \in \mathbb{R}^{d_2}, \dots, v_p \in \mathbb{R}^{d_p}$ we define the p -fold tensor product $v_1 \otimes v_2 \otimes \dots \otimes v_p \in \mathbb{R}^{d_1 d_2 \dots d_p}$ in the same fashion. For shorthand, we use the notation $x^{\otimes p}$ to denote $\underbrace{x \otimes x \otimes \dots \otimes x}_{p \text{ terms}}$, the p -fold self-tensoring of x .

Another related operation that we use is the *direct sum* of vectors: $x \oplus y := \begin{bmatrix} x \\ y \end{bmatrix}$. We also use the notation \odot to denote the hadamard product of tensors. For instance, the hadamard product of 3-dimensional tensors $X, Y \in \mathbb{R}^{m \times n \times d}$ is a tensor in $\mathbb{R}^{m \times n \times d}$ defined as $[X \odot Y]_{i,j,l} := X_{i,j,l} \cdot Y_{i,j,l}$. We need notation for **subtensors of a tensor**. For instance, for a 3-dimensioanl tensor $Y \in \mathbb{R}^{m \times n \times d}$ and every $l \in [d]$, we denote by $y_{(:, :, l)}$ the $m \times n$ matrix that is defined as $[Y_{(:, :, l)}]_{i,j} := Y_{i,j,l}$ for $i \in [m], j \in [n]$. For two univariate functions f and g we denote their twofold composition by $f \circ g$, defined as $f \circ g(\alpha) := f(g(\alpha))$. Finally, we use $\mathcal{N}(\mu, \sigma^2)$ to denote the normal distribution with mean μ and variance σ^2 .

3 Fully Connected Neural Tangent Kernel

The main result of this section is an efficient oblivious sketch for the Neural Tangent Kernel (NTK) corresponding to a fully connected multi-layer network. [ADH⁺19b] showed how to exactly compute the L -layered NTK with activation $\sigma : \mathbb{R} \rightarrow \mathbb{R}$ using the following dynamic program:

1. For every $y, z \in \mathbb{R}^d$, let $\Sigma^{(0)}(y, z) := \langle y, z \rangle$ and for every layer $h = 1, 2, \dots, L$, recursively define

the covariance $\Sigma^{(h)} : \mathbb{R}^d \times \mathbb{R}^d \rightarrow \mathbb{R}$ as:

$$\begin{aligned}\Lambda^{(h)}(y, z) &:= \begin{pmatrix} \Sigma^{(h-1)}(y, y) & \Sigma^{(h-1)}(y, z) \\ \Sigma^{(h-1)}(z, y) & \Sigma^{(h-1)}(z, z) \end{pmatrix}, \\ \Sigma^{(h)}(y, z) &:= \frac{\mathbb{E}_{(u, v) \sim \mathcal{N}(0, \Lambda^{(h)}(y, z))} [\sigma(u) \cdot \sigma(v)]}{\mathbb{E}_{x \sim \mathcal{N}(0, 1)} [|\sigma(x)|^2]}.\end{aligned}\tag{1}$$

2. For $h = 1, 2, \dots, L$, define the derivative covariance as,

$$\dot{\Sigma}^{(h)}(y, z) := \frac{\mathbb{E}_{(u, v) \sim \mathcal{N}(0, \Lambda^{(h)}(y, z))} [\dot{\sigma}(u) \cdot \dot{\sigma}(v)]}{\mathbb{E}_{x \sim \mathcal{N}(0, 1)} [|\sigma(x)|^2]}.\tag{2}$$

3. Let $\Theta_{ntk}^{(0)}(y, z) := \Sigma^{(0)}(y, z)$ and for every integer $L \geq 1$, the depth- L NTK expression is defined recursively as:

$$\Theta_{ntk}^{(L)}(y, z) := \Theta_{ntk}^{(L-1)}(y, z) \cdot \dot{\Sigma}^{(L)}(y, z) + \Sigma^{(L)}(y, z).\tag{3}$$

While using this DP, one can compute the kernel value $\Theta_{ntk}^{(L)}(y, z)$ for any pair of vectors $y, z \in \mathbb{R}^d$ using $O(d + L)$ operations, it is hard to gain insight into the structure of this kernel using the expression above. In particular, the NTK expression involves recursive nontrivial expectations which makes it is unclear whether there exist efficient sketching solutions for this kernel in its current form. However, we show that for the important case of ReLU activation $\sigma(\alpha) = \max(\alpha, 0)$, this kernel takes an extremely nice and highly structured form. We prove that the NTK corresponding to ReLU activation can be characterized by the composition of smooth analytic functions that can be approximated very effectively. We show that, in fact, the NTK can be fully characterized by a *univariate function* $K_{relu}^{(L)} : [-1, 1] \rightarrow \mathbb{R}$, and exploiting this special structure is the key to designing efficient sketching methods for this kernel.

3.1 ReLU-NTK

The L -layered NTK corresponding to ReLU activation $\sigma(\alpha) = \max(\alpha, 0)$ can be fully characterized by a univariate function $K_{relu}^{(L)} : [-1, 1] \rightarrow \mathbb{R}$ that we refer to as *ReLU-NTK*. This function, which is closely related to the arc-cosine kerel functions [CS09] and was recently derived in [BM19] is defined as follows:

Definition 3.1 (ReLU-NTK function). For every integer $L > 0$, the L -layered **ReLU-NTK** function $K_{relu}^{(L)} : [-1, 1] \rightarrow \mathbb{R}$ is defined via following procedure:

1. Let functions $\kappa_0(\cdot)$ and $\kappa_1(\cdot)$ be 0^{th} and 1^{st} order arc-cosine kernels [CS09] defined as follows,

$$\kappa_0(\alpha) := \frac{1}{\pi} \cdot (\pi - \arccos(\alpha)) \text{ and } \kappa_1(\alpha) := \frac{1}{\pi} \left(\sqrt{1 - \alpha^2} + \alpha \cdot (\pi - \arccos(\alpha)) \right) \text{ for } \alpha \in [-1, 1].\tag{4}$$

2. Let $\Sigma_{relu}^{(0)}(\alpha) := \alpha$ and for every $h = 1, 2, \dots, L$, define $\Sigma_{relu}^{(h)}(\alpha)$ as follows for every $\alpha \in [-1, 1]$:

$$\Sigma_{relu}^{(h)}(\alpha) := \underbrace{\kappa_1 \circ \kappa_1 \circ \dots \circ \kappa_1}_{h\text{-fold self composition}}(\alpha).\tag{5}$$

3. For every $h = 1, 2, \dots, L$, define $\dot{\Sigma}_{relu}^{(h)}(\alpha)$ as follows:

$$\dot{\Sigma}_{relu}^{(h)}(\alpha) := \kappa_0 \left(\Sigma_{relu}^{(h-1)}(\alpha) \right).\tag{6}$$

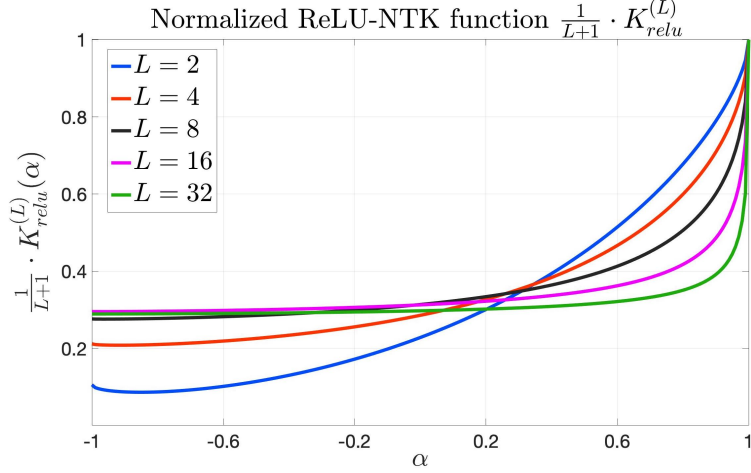


Figure 1: The normalized ReLU-NTK function $\frac{1}{L+1} \cdot K_{relu}^{(L)}$ for various number of layers $L \in \{2, 4, 8, 16, 32\}$.

4. Let $K_{relu}^{(0)}(\alpha) := \Sigma_{relu}^{(0)}(\alpha) = \alpha$ and for $h = 1, 2, \dots, L$, define $K_{relu}^{(h)}(\alpha)$ recursively as follows for $\alpha \in [-1, 1]$:

$$K_{relu}^{(h)}(\alpha) := K_{relu}^{(h-1)}(\alpha) \cdot \dot{\Sigma}_{relu}^{(h)}(\alpha) + \Sigma_{relu}^{(h)}(\alpha). \quad (7)$$

The connection between ReLU-NTK function $K_{relu}^{(L)}$ and the kernel function $\Theta_{ntk}^{(L)}$ is formalized in the following theorem,

Theorem 1. *For every integer $L \geq 1$, if we let $K_{relu}^{(L)} : [-1, 1] \rightarrow \mathbb{R}$ be the ReLU-NTK function as in Definition 3.1, then the Neural Tangent Kernel (NTK) of fully-connected L -layered network with ReLU activation, $\sigma(\alpha) = \max(\alpha, 0)$, satisfies the following for any $y, z \in \mathbb{R}^d$,*

$$\Theta_{ntk}^{(L)}(y, z) \equiv \|y\|_2 \|z\|_2 \cdot K_{relu}^{(L)} \left(\frac{\langle y, z \rangle}{\|y\|_2 \|z\|_2} \right).$$

This theorem is proved in Appendix B. Theorem 1 shows that the NTK is a *normalized dot-product kernel* which can be fully characterized by the univariate function $K_{relu}^{(L)} : [-1, 1] \rightarrow \mathbb{R}$. This function can be efficiently computed using $O(L)$ operations at any desired point $\alpha \in [-1, 1]$. We plot the family of ReLU-NTK functions for a range of different values of $L \in \{2, 4, 8, 16, 32\}$ in Figure 1. In this figure, we plot normalized function $\frac{1}{L+1} \cdot K_{relu}^{(L)}(\alpha)$ (note the $\frac{1}{L+1}$ normalization). It is evident that for relatively larger values of L , the function $K_{relu}^{(L)}(\cdot)$ converges to a *knee shape*. More precisely, $K_{relu}^{(L)}(\alpha)$ has a nearly constant value of approximately $0.3 \cdot (L+1)$ on the interval $\alpha \in [-1, 1 - O(1/L)]$, and on the interval $\alpha \in [1 - O(1/L), 1]$ its value sharply increases and attains $L+1$ at point $\alpha = 1$. Note that the derivative of $K_{relu}^{(L)}(\alpha)$ at point $\alpha = 1$ is $+\infty$. This implies that the NTK $\Theta_{ntk}^{(L)}(y, z)$ has a nearly constant value of approximately $0.3 \cdot (L+1) \cdot \|y\|_2 \|z\|_2$ for any pair of vectors y and z whose angle is larger than $\Omega(1/L)$ while its value sharply rises to $(L+1) \|y\|_2 \|z\|_2$ when vectors y and z are fully aligned.

3.2 NTK Sketch

As shown in Definition 3.1 and Theorem 1, the NTK $\Theta_{ntk}^{(L)}$ is constructed by recursive composition of functions $\kappa_1(\cdot)$ and $\kappa_0(\cdot)$. Thus, we crucially need efficient methods for approximating these functions in order to design efficient sketches for the NTK. Our main tool is to approximate these functions with low degree polynomials via Taylor series expansion, and then apply a linear sketch to the resulting polynomial kernels. We use the sketch introduced in [AKK⁺20] which can be efficiently applied to high-degree polynomial kernels. More precisely, this sketch preserves the norm of vectors in \mathbb{R}^{dp} with high probability and can be applied to tensor product vectors of the form $v_1 \otimes v_2 \otimes \dots \otimes v_p$ very quickly. The approximation guarantee and runtime of this sketch is stated in the following Lemma, which is a minor modification of Theorem 1.2 of [AKK⁺20],

Lemma 1 (Polynomial Sketch). *For every integers $p, d \geq 1$, every $\epsilon, \delta > 0$, there exists a distribution on random matrices $Q^p \in \mathbb{R}^{m \times dp}$ with $m = O\left(\frac{p}{\epsilon^2} \log^3 \frac{1}{\epsilon\delta}\right)$, called **degree- p polynomial sketch**, such that the following hold,*

1. *For any $y \in \mathbb{R}^{dp}$, $\Pr[\|Q^p y\|_2^2 \in (1 \pm \epsilon)\|y\|_2^2] \geq 1 - \delta$.*
2. *For any $x \in \mathbb{R}^d$, if $\mathbf{e}_1 \in \mathbb{R}^d$ is the standard basis vector along the first coordinate, the total time to compute $Q^p(x^{\otimes p-j} \otimes \mathbf{e}_1^{\otimes j})$ for all $j = 0, 1, \dots, p$ is $O\left(\frac{p^2 \log^2 \frac{p}{\epsilon}}{\epsilon^2} \log^3 \frac{1}{\epsilon\delta} + \min\left\{\frac{p^{3/2} \log \frac{1}{\delta}}{\epsilon} \cdot nnz(x), pd \log d\right\}\right)$.*
3. *For any collection of vectors $v_1, v_2, \dots, v_p \in \mathbb{R}^d$, the time to compute $Q^p(v_1 \otimes v_2 \otimes \dots \otimes v_p)$ is bounded by $O\left(\frac{p^2 \log \frac{p}{\epsilon}}{\epsilon^2} \log^3 \frac{1}{\epsilon\delta} + \frac{p^{3/2}}{\epsilon} \cdot d \cdot \log \frac{1}{\delta}\right)$.*

We include the proof of this lemma in Appendix C. We also use the Subsampled Randomized Hadamard Transform (SRHT) [AC09] to reduce the dimensionality of the intermediate vectors that arise in our computations. Next lemma gives the performance of SRHT sketches which is proved, for instance, in Theorem 9 of [CNW16],

Lemma 2 (SRHT Sketch). *For every positive integer d and every $\epsilon, \delta > 0$, there exists a distribution on random matrices $S \in \mathbb{R}^{m \times d}$ with $m = O\left(\frac{1}{\epsilon^2} \cdot \log^2 \frac{1}{\epsilon\delta}\right)$, called **SRHT sketch**, such that for any vector $x \in \mathbb{R}^d$, $\Pr[\|Sx\|_2^2 \in (1 \pm \epsilon)\|x\|_2^2] \geq 1 - \delta$. Moreover, Sx can be computed in time $O\left(\frac{1}{\epsilon^2} \cdot \log^2 \frac{1}{\epsilon\delta} + d \log d\right)$.*

Given the tools we have introduced so far, we can present our oblivious sketch for the depth- L NTK with ReLU activation function. Letting $\Theta_{ntk}^{(L)} : \mathbb{R}^d \times \mathbb{R}^d \rightarrow \mathbb{R}$ be the NTK function, we construct a (random) mapping $\Psi_{ntk}^{(L)} : \mathbb{R}^d \rightarrow \mathbb{R}^s$, called *NTK Sketch*, such that its target dimension s is small and for every pair of vectors $y, z \in \mathbb{R}^d$, $\Pr[\langle \Psi_{ntk}^{(L)}(y), \Psi_{ntk}^{(L)}(z) \rangle \in (1 \pm \epsilon) \cdot \Theta_{ntk}^{(L)}(y, z)] \geq 1 - \delta$. We define our algorithm for recursively constructing this mapping in the following definition,

Definition 3.2 (NTK Sketch Algorithm). For every vector $x \in \mathbb{R}^d$, and every $\epsilon, \delta > 0$, the **NTK Sketch** $\Psi_{ntk}^{(L)}(x)$ is computed recursively as follows,

- Let $s = O\left(\frac{L^2}{\epsilon^2} \log^2 \frac{L}{\epsilon\delta}\right)$, $n = O\left(\frac{L^6}{\epsilon^4} \log^3 \frac{L}{\epsilon\delta}\right)$, $n_1 = O\left(\frac{L^4}{\epsilon^4} \log^3 \frac{L}{\epsilon\delta}\right)$, $r = O\left(\frac{L^6}{\epsilon^4} \log^2 \frac{L}{\epsilon\delta}\right)$, $m = O\left(\frac{L^8}{\epsilon^{16/3}} \log^3 \frac{L}{\epsilon\delta}\right)$, $m_2 = O\left(\frac{L^2}{\epsilon^2} \log^3 \frac{L}{\epsilon\delta}\right)$, $s^* = O\left(\frac{1}{\epsilon^2} \log \frac{1}{\delta}\right)$ be appropriate integers.

- For an integer p , the polynomial functions $P_{\text{relu}}^{(p)}(\cdot)$ and $\dot{P}_{\text{relu}}^{(p)}(\cdot)$ are defined as,

$$\begin{aligned} P_{\text{relu}}^{(p)}(\alpha) &:= \frac{1}{\pi} + \frac{\alpha}{2} + \frac{1}{\pi} \sum_{n=0}^p \frac{(2n)! \cdot \alpha^{2n+2}}{2^{2n}(n!)^2(2n+1)(2n+2)}, \\ \dot{P}_{\text{relu}}^{(p)}(\alpha) &:= \frac{1}{2} + \frac{1}{\pi} \sum_{n=0}^p \frac{(2n)!}{2^{2n}(n!)^2(2n+1)} \cdot \alpha^{2n+1}. \end{aligned} \quad (8)$$

1. Let $Q^1 \in \mathbb{R}^{n \times d}$ be an instance of the degree-1 polynomial sketch with error parameter $O(\epsilon^2/L^3)$ and failure probability $O(\delta/L)$ as per Lemma 1. Additionally, let $S \in \mathbb{R}^{r \times n}$ be an instance of the SRHT with error parameter $O(\epsilon^2/L^3)$ and failure probability $O(\delta/L)$ as in Lemma 2. Compute $\phi^{(0)}(x) \in \mathbb{R}^r$ as follows,

$$\phi^{(0)}(x) \leftarrow \frac{1}{\|x\|_2} \cdot S \cdot Q^1 \cdot x. \quad (9)$$

2. For $q = \lceil 2L^2/\epsilon^{4/3} \rceil$, let $P_{\text{relu}}^{(q)}(\alpha) = \sum_{j=0}^{2q+2} c_j \cdot \alpha^j$ be the degree $2q+2$ polynomial defined in (8). Note that, coefficients $c_0, c_1, \dots, c_{2q+2}$ are non-negative. Let $Q^{2q+2} \in \mathbb{R}^{m \times r^{2q+2}}$ be an instance of the degree- $(2q+2)$ polynomial sketch with error parameter $O(\epsilon^2/L^3)$ and failure probability $O(\delta/qL)$ as in Lemma 1. Also, let $T \in \mathbb{R}^{r \times ((2q+3) \cdot m)}$ be an instance of the SRHT with error parameter $O(\epsilon^2/L^3)$ and failure probability $O(\delta/L)$.

For every $h = 1, 2, \dots, L$ and $l = 0, 1, 2, \dots, 2q+2$, compute the mappings $Z_l^{(h)}(x) \in \mathbb{R}^m$ and $\phi^{(h)}(x) \in \mathbb{R}^r$ as,

$$\begin{aligned} Z_l^{(h)}(x) &\leftarrow Q^{2q+2} \left(\left[\phi^{(h-1)}(x) \right]^{\otimes l} \otimes \mathbf{e}_1^{\otimes 2q+2-l} \right) \\ \phi^{(h)}(x) &\leftarrow T \cdot \left(\bigoplus_{l=0}^{2q+2} \sqrt{c_l} Z_l^{(h)}(x) \right). \end{aligned} \quad (10)$$

3. For $p = \lceil 9L^2/\epsilon^2 \rceil$, let $\dot{P}_{\text{relu}}^{(p)}(\alpha) = \sum_{j=0}^{2p+1} b_j \cdot \alpha^j$ be the degree $2p+1$ polynomial defined in (8). Note that, coefficients $b_0, b_1, \dots, b_{2p+1}$ are non-negative. Let $Q^{2p+1} \in \mathbb{R}^{n_1 \times r^{2p+1}}$ be an instance of the degree- $(2p+1)$ polynomial sketch with error parameter $O(\epsilon/L)$ and failure probability $O(\delta/pL)$ as per Lemma 1. Also, let $W \in \mathbb{R}^{s \times ((2p+2) \cdot n)}$ be an instance of the SRHT with error parameter $O(\epsilon/L)$ and failure probability $O(\delta/L)$ as in Lemma 2.

For every $h = 1, 2, \dots, L$ and $l = 0, 1, 2, \dots, 2p+1$, compute the mappings $Y_l^{(h)}(x) \in \mathbb{R}^n$ and $\dot{\phi}^{(h)}(x) \in \mathbb{R}^s$ as,

$$\begin{aligned} Y_l^{(h)}(x) &\leftarrow Q^{2p+1} \left(\left[\phi^{(h-1)}(x) \right]^{\otimes l} \otimes \mathbf{e}_1^{\otimes 2p+1-l} \right) \\ \dot{\phi}^{(h)}(x) &\leftarrow W \cdot \left(\bigoplus_{l=0}^{2p+1} \sqrt{b_l} Y_l^{(h)}(x) \right). \end{aligned} \quad (11)$$

4. Let $Q^2 \in \mathbb{R}^{m_2 \times s^2}$ be an instance of the degree-2 polynomial sketch with error parameter $O(\epsilon/L)$ and failure probability $O(\delta/L)$ as in Lemma 1. Additionally, let $R \in \mathbb{R}^{s \times (m_2+r)}$ and $V \in \mathbb{R}^{s \times r}$ be independent instances of the SRHT sketch with error parameter $O(\epsilon/L)$ and failure probability $O(\delta/L)$ as in Lemma 2.

For every integer $h = 1, 2, \dots, L$, the mapping $\psi^{(h)}(x) \in \mathbb{R}^s$ is computed recursively as:

$$\begin{aligned}\psi^{(0)}(x) &\leftarrow V \cdot \phi^{(0)}(x), \\ \psi^{(h)}(x) &\leftarrow R \left(Q^2 \left(\psi^{(h-1)}(x) \otimes \dot{\phi}^{(h)}(x) \right) \oplus \phi^{(h)}(x) \right).\end{aligned}\tag{12}$$

5. Let $G \in \mathbb{R}^{s^* \times s}$ be a matrix of i.i.d. normal entries with distribution $\mathcal{N}(0, 1/s^*)$. The mapping $\Psi_{ntk}^{(L)}(x) \in \mathbb{R}^{s^*}$ is computed as

$$\Psi_{ntk}^{(L)}(x) \leftarrow \|x\|_2 \cdot G \cdot \psi^{(L)}(x).\tag{13}$$

Now we present our main theorem on NTK Sketch:

Theorem 2. *For every integers $d \geq 1$ and $L \geq 2$, and any $\epsilon, \delta > 0$, if we let $\Theta_{ntk}^{(L)} : \mathbb{R}^d \times \mathbb{R}^d \rightarrow \mathbb{R}$ be the Neural Tangent Kernel (NTK) corresponding to L -layered neural net with ReLU activation defined in (1), (2), and (3), then there exists a randomized map $\Psi_{ntk}^{(L)} : \mathbb{R}^d \rightarrow \mathbb{R}^{s^*}$ for some $s^* = O\left(\frac{1}{\epsilon^2} \log \frac{1}{\delta}\right)$ such that the following invariants holds,*

1. For any vectors $y, z \in \mathbb{R}^d$:

$$\Pr \left[\left| \left\langle \Psi_{ntk}^{(L)}(y), \Psi_{ntk}^{(L)}(z) \right\rangle - \Theta_{ntk}^{(L)}(y, z) \right| > \epsilon \cdot \Theta_{ntk}^{(L)}(y, z) \right] \leq \delta.$$

2. For every vector $x \in \mathbb{R}^d$, the time to compute $\Psi_{ntk}^{(L)}(x)$ is $O\left(\frac{L^{11}}{\epsilon^7} \cdot \log^3 \frac{L}{\epsilon\delta} + \frac{L^3}{\epsilon^2} \cdot \log \frac{L}{\epsilon\delta} \cdot \text{nnz}(x)\right)$.

For a proof of the above theorem see Appendix C.

4 Convolutional Neural Tangent Kernel

In this section, we design and analyze an efficient oblivious sketch for the Convolutional Neural Tangent Kernel (CNTK), which is the kernel function corresponding to a CNN with infinite number of channels. [ADH⁺19b] gave DP solutions for computing two variants of CNTK; one is the vanilla version which performs no pooling, and the other performs Global Average Pooling (GAP) on its top layer. For conciseness, we focus mainly on the CNTK with GAP, which also exhibits superior empirical performance [ADH⁺19b]. However, we remark that the vanilla CNTK has a very similar structure and hence our techniques can be applied to it, as well. Using CNTK expression, restated in Appendix D, one can compute the kernel value $\Theta_{cntk}^{(L)}(y, z)$ corresponding to any desired activation $\sigma : \mathbb{R} \rightarrow \mathbb{R}$ and any depth L , for any pair of images y, z . However, the number of operations needed for exact computation of the CNTK value $\Theta_{cntk}^{(L)}(y, z)$ is $\Omega(d_1^2 d_2^2 \cdot L)$, which is very slow particularly due to its quadratic dependence on the number of pixels of input images $d_1 d_2$.

The CNTK expression for general activation $\sigma(\cdot)$ looks rather complicated and it is hard to gain insight into its core structure. In particular, it involves recursive computation of various expectations which depend nontrivially on the activation function. This complexity is an obstacle to designing efficient sketching methods for this kernel. Nevertheless, we are fortunately able to show that the CNTK for the important case of ReLU activation is an extremely structured object. We prove that this kernel can be fully characterized in terms of tensoring and composition of smooth univariate kernel functions $\kappa_1 : [-1, 1] \rightarrow \mathbb{R}$ and $\kappa_0 : [-1, 1] \rightarrow \mathbb{R}$ defined in (4) of Definition 3.1, and exploiting this special structure is the main key to designing efficient sketching methods for the CNTK.

4.1 ReLU-CNTK

We prove that the depth- L CNTK corresponding to ReLU activation is highly structured and can be fully characterized in terms of tensoring and composition of functions $\kappa_1(\cdot)$ and $\kappa_0(\cdot)$. We refer to this kernel function as **ReLU-CNTK** and show how to recursively compute it as follows,

Definition 4.1 (ReLU-CNTK). For every positive integers q, L , the L -layered CNTK for ReLU activation function and convolutional filter size of $q \times q$ is defined as follows

1. For $x \in \mathbb{R}^{d_1 \times d_2 \times c}$, every $i \in [d_1]$ and $j \in [d_2]$ let $N_{i,j}^{(0)}(x) := q^2 \cdot \sum_{l=1}^c |x_{i+a,j+b,l}|^2$, and for every $h \geq 1$, recursively define,

$$N_{i,j}^{(h)}(x) := \frac{1}{q^2} \cdot \sum_{a=-\frac{q-1}{2}}^{\frac{q-1}{2}} \sum_{b=-\frac{q-1}{2}}^{\frac{q-1}{2}} N_{i+a,j+b}^{(h-1)}(x). \quad (14)$$

2. Define $\Gamma^{(0)}(y, z) := \sum_{l=1}^c y_{(:, :, l)} \otimes z_{(:, :, l)}$. Let $\kappa_1 : [-1, 1] \rightarrow \mathbb{R}$ be the function defined in (4) of Definition 3.1. For every layer $h = 1, 2, \dots, L$, every $i, i' \in [d_1]$ and $j, j' \in [d_2]$, define $\Gamma^{(h)} : \mathbb{R}^{d_1 \times d_2 \times c} \times \mathbb{R}^{d_1 \times d_2 \times c} \rightarrow \mathbb{R}^{d_1 \times d_2 \times d_1 \times d_2}$ recursively as:

$$\Gamma_{i,j,i',j'}^{(h)}(y, z) := \frac{\sqrt{N_{i,j}^{(h)}(y) \cdot N_{i',j'}^{(h)}(z)}}{q^2} \cdot \kappa_1(A), \quad (15)$$

$$\text{where } A := \frac{\sum_{a=-\frac{q-1}{2}}^{\frac{q-1}{2}} \sum_{b=-\frac{q-1}{2}}^{\frac{q-1}{2}} \Gamma_{i+a,j+b,i'+a,j'+b}^{(h-1)}(y, z)}{\sqrt{N_{i,j}^{(h)}(y) \cdot N_{i',j'}^{(h)}(z)}}.$$

3. Let $\kappa_0 : [-1, 1] \rightarrow \mathbb{R}$ be the function defined in (4) of Definition 3.1. For every $h = 1, 2, \dots, L$, every $i, i' \in [d_1]$ and $j, j' \in [d_2]$, define $\dot{\Gamma}^{(h)}(y, z) \in \mathbb{R}^{d_1 \times d_2 \times d_1 \times d_2}$ as:

$$\dot{\Gamma}_{i,j,i',j'}^{(h)}(y, z) := \frac{1}{q^2} \cdot \kappa_0(A), \quad (16)$$

where A is defined in (15).

4. Let $\Pi^{(0)}(y, z) := 0$ and for every $h = 1, 2, \dots, L-1$, every $i, i' \in [d_1]$ and $j, j' \in [d_2]$, define $\Pi^{(h)} : \mathbb{R}^{d_1 \times d_2 \times c} \times \mathbb{R}^{d_1 \times d_2 \times c} \rightarrow \mathbb{R}^{d_1 \times d_2 \times d_1 \times d_2}$ recursively as:

$$\Pi_{i,j,i',j'}^{(h)}(y, z) := \sum_{a=-\frac{q-1}{2}}^{\frac{q-1}{2}} \sum_{b=-\frac{q-1}{2}}^{\frac{q-1}{2}} B_{i+a,j+b,i'+a,j'+b}, \quad (17)$$

where $B := \Pi^{(h-1)}(y, z) \odot \dot{\Gamma}^{(h)}(y, z) + \Gamma^{(h)}(y, z)$.

Furthermore, for $h = L$ define:

$$\Pi^{(L)}(y, z) := \Pi^{(L-1)}(y, z) \odot \dot{\Gamma}^{(L)}(y, z). \quad (18)$$

5. The final CNTK expressions for ReLU activation is:

$$\Theta_{cntk}^{(L)}(y, z) := \frac{1}{d_1^2 d_2^2} \cdot \sum_{i, i' \in [d_1]} \sum_{j, j' \in [d_2]} \Pi_{i,j,i',j'}^{(L)}(y, z). \quad (19)$$

We prove in Appendix E that the procedure in Definition 4.1 precisely computes the CNTK for ReLU activation function.

4.2 CNTK Sketch

Similar to the NTK Sketch, our main technique for efficiently sketching the CNTK is to first approximate the functions κ_1 and κ_0 with polynomial kernels and then apply a linear sketch to the resulting polynomial kernels using Lemma 1 that can be applied to high-degree polynomial kernels very efficiently. In what follows, we present our oblivious sketch for the L -layered CNTK with ReLU activation function. Since the CNTK has a recursive nature, our sketch will in turn be constructed recursively. To be precise, letting $\Theta_{cntk}^{(L)} : \mathbb{R}^{d_1 \times d_2 \times c} \times \mathbb{R}^{d_1 \times d_2 \times c} \rightarrow \mathbb{R}$ be the ReLU-CNTK function recursively defined in Definition 4.1, we construct a (random) mapping $\Psi_{cntk}^{(L)} : \mathbb{R}^{d_1 \times d_2 \times c} \rightarrow \mathbb{R}^s$, called *CNTK Sketch*, such that its target dimension s is small and for every pair of images $y, z \in \mathbb{R}^{d_1 \times d_2 \times c}$: $\Pr \left[\langle \Psi_{cntk}^{(L)}(y), \Psi_{cntk}^{(L)}(z) \rangle \notin (1 \pm \epsilon) \cdot \Theta_{cntk}^{(L)}(y, z) \right] < \delta$.

We present our algorithm for computing this mapping in the following definition,

Definition 4.2 (CNTK Sketch Algorithm). For every image $x \in \mathbb{R}^{d_1 \times d_2 \times c}$, we compute the *CNTK Sketch*, $\Psi_{cntk}^{(L)}(x)$, recursively as follows,

- Let $s = O \left(\frac{L^2}{\epsilon^2} \log^2 \frac{d_1 d_2 L}{\epsilon \delta} \right)$, $r = O \left(\frac{L^6}{\epsilon^4} \log^2 \frac{d_1 d_2 L}{\epsilon \delta} \right)$, $m_2 = O \left(\frac{L^2}{\epsilon^2} \log^3 \frac{d_1 d_2 L}{\epsilon \delta} \right)$, $n = O \left(\frac{L^4}{\epsilon^4} \log^3 \frac{d_1 d_2 L}{\epsilon \delta} \right)$, $m = O \left(\frac{L^8}{\epsilon^{16/3}} \log^3 \frac{d_1 d_2 L}{\epsilon \delta} \right)$, and $s^* = O \left(\frac{1}{\epsilon^2} \log \frac{1}{\delta} \right)$ be appropriate integers.

1. For every $i \in [d_1]$, $j \in [d_2]$, and $h = 0, 1, 2, \dots, L$ compute $N_{i,j}^{(h)}(x)$ as per (14) of Definition 4.1.
2. Let $S \in \mathbb{R}^{r \times c}$ be an instance of SRHT with error parameter $O \left(\frac{\epsilon^2}{L^3} \right)$ and failure probability $O \left(\frac{\delta}{d_1^2 d_2^2 L} \right)$ as in Lemma 2. For every $i \in [d_1]$ and $j \in [d_2]$, compute $\phi_{i,j}^{(0)}(x) \in \mathbb{R}^r$ as,

$$\phi_{i,j}^{(0)}(x) \leftarrow S \cdot x_{(i,j,:)}. \quad (20)$$

3. For $p = \lceil 2L^2/\epsilon^{4/3} \rceil$, let $P_{relu}^{(p)}(\alpha) = \sum_{l=0}^{2p+2} e_l \cdot \alpha^l$ be the degree $2p+2$ polynomial defined in (8) of Definition 3.2. Note that, coefficients $e_0, e_1, \dots, e_{2p+2}$ are non-negative. Let $Q^{2p+2} \in \mathbb{R}^{m \times (q^2 r)^{2p+2}}$ be an instance of the degree- $(2p+2)$ polynomial sketch with error parameter $O(\epsilon^2/L^3)$ and failure probability $O \left(\frac{\delta}{d_1^2 d_2^2 p L} \right)$ as per Lemma 1. Additionally, let $T \in \mathbb{R}^{r \times ((2p+3) \cdot m)}$ be an instance of the SRHT with error parameter $O(\epsilon^2/L^3)$ and failure probability $O \left(\frac{\delta}{d_1^2 d_2^2 L} \right)$ as in Lemma 2. For every layer $h = 1, 2, \dots, L$, every $i \in [d_1]$ and $j \in [d_2]$, and $l = 0, 1, 2, \dots, 2p+2$ compute the mappings $\mu_{i,j}^{(h)}(x) \in \mathbb{R}^{q^2 r}$, $[Z_{i,j}^{(h)}(x)]_l \in \mathbb{R}^m$ and $\phi_{i,j}^{(h)}(x) \in \mathbb{R}^r$ as,

$$\begin{aligned} \mu_{i,j}^{(h)}(x) &\leftarrow \frac{1}{\sqrt{N_{i,j}^{(h)}(x)}} \cdot \bigoplus_{a=-\frac{q-1}{2}}^{\frac{q-1}{2}} \bigoplus_{b=-\frac{q-1}{2}}^{\frac{q-1}{2}} \phi_{i+a,j+b}^{(h-1)}(x) \\ [Z_{i,j}^{(h)}(x)]_l &\leftarrow Q^{2p+2} \cdot \left(\left[\mu_{i,j}^{(h)}(x) \right]^{\otimes l} \otimes \mathbf{e}_1^{\otimes 2p+2-l} \right), \\ \phi_{i,j}^{(h)}(x) &\leftarrow \frac{\sqrt{N_{i,j}^{(h)}(x)}}{q} \cdot T \cdot \left(\bigoplus_{l=0}^{2p+2} \sqrt{e_l} [Z_{i,j}^{(h)}(x)]_l \right). \end{aligned} \quad (21)$$

4. For $p' = \lceil 9L^2/\epsilon^2 \rceil$, let $\dot{P}_{relu}^{(p')}(x) = \sum_{l=0}^{2p'+1} f_l \cdot \alpha^l$ be the degree $2p'+1$ polynomial defined in (8) of Definition 3.2. Note that, coefficients $f_0, f_1, \dots, f_{2p'+1}$ are non-negative. Let $Q^{2p'+1} \in \mathbb{R}^{n \times (q^2 r)^{2p'+1}}$

be an instance of the degree- $(2p' + 1)$ polynomial sketch with error parameter $O(\epsilon/L)$ and failure probability $O\left(\frac{\delta}{d_1^2 d_2^2 p' L}\right)$ as per Lemma 1. Also, let $W \in \mathbb{R}^{s \times ((2p'+2) \cdot n)}$ be an instance of the SRHT with error parameter $O(\epsilon/L)$ and failure probability $O\left(\frac{\delta}{d_1^2 d_2^2 L}\right)$ as per Lemma 2. For every $h = 1, 2, \dots, L$, every $i \in [d_1]$ and $j \in [d_2]$, and $l = 0, 1, 2, \dots, 2p' + 1$ compute the mappings $[Y_{i,j}^{(h)}(x)]_l \in \mathbb{R}^n$ and $\dot{\phi}_{i,j}^{(h)}(x) \in \mathbb{R}^s$ as,

$$\begin{aligned} [Y_{i,j}^{(h)}(x)]_l &\leftarrow Q^{2p'+1} \cdot \left([\mu_{i,j}^{(h)}(x)]^{\otimes l} \otimes \mathbf{e}_1^{\otimes 2p'+1-l} \right), \\ \dot{\phi}_{i,j}^{(h)}(x) &\leftarrow \frac{1}{q} \cdot W \cdot \left(\bigoplus_{l=0}^{2p'+1} \sqrt{f_l} [Y_{i,j}^{(h)}(x)]_l \right), \end{aligned} \quad (22)$$

where $\mu_{i,j}^{(h)}(x)$ is computed in (21).

5. Let $Q^2 \in \mathbb{R}^{m_2 \times s^2}$ be an instance of the degree-2 polynomial sketch with error parameter $O(\epsilon/L)$ and failure probability $O\left(\frac{\delta}{d_1^2 d_2^2 L}\right)$ as in Lemma 1. Additionally, let $R \in \mathbb{R}^{s \times (q^2(m_2+r))}$ be an instance of the SRHT sketch with error parameter $O(\epsilon/L)$ and failure probability $O\left(\frac{\delta}{d_1^2 d_2^2 L}\right)$ as in Lemma 2.

Let $\psi_{i,j}^{(0)}(x) \leftarrow 0$ and for every $h = 1, 2, \dots, L-1$, and $i \in [d_1], j \in [d_2]$, compute the mapping $\psi_{i,j}^{(h)}(x) \in \mathbb{R}^s$ as:

$$\begin{aligned} \eta_{i,j}^{(h)}(x) &\leftarrow Q^2 \cdot \left(\psi_{i,j}^{(h-1)}(x) \otimes \dot{\phi}_{i,j}^{(h)}(x) \right) \oplus \phi_{i,j}^{(h)}(x), \\ \psi_{i,j}^{(h)}(x) &\leftarrow R \cdot \left(\bigoplus_{a=-\frac{q-1}{2}}^{\frac{q-1}{2}} \bigoplus_{b=-\frac{q-1}{2}}^{\frac{q-1}{2}} \eta_{i+a,j+b}^{(h)}(x) \right). \end{aligned} \quad (23)$$

Furthermore, for $h = L$ compute:

$$\psi_{i,j}^{(L)}(x) \leftarrow Q^2 \cdot \left(\psi_{i,j}^{(L-1)}(x) \otimes \dot{\phi}_{i,j}^{(L)}(x) \right). \quad (24)$$

6. Let $G \in \mathbb{R}^{s^* \times m_2}$ be a random matrix of i.i.d. normal entries with distribution $\mathcal{N}(0, 1/s^*)$. The final *CNTK Sketch* is the following:

$$\Psi_{cntk}^{(L)}(y, z) := \frac{1}{d_1 d_2} \cdot G \cdot \left(\sum_{i \in [d_1]} \sum_{j \in [d_2]} \psi_{i,j}^{(L)}(x) \right). \quad (25)$$

Now we present our main theorem on efficiently sketching the CNTK with ReLU activation function:

Theorem 3. *For every positive integers d_1, d_2, c and $L \geq 2$, and every $\epsilon, \delta > 0$, if we let $\Theta_{cntk}^{(L)} : \mathbb{R}^{d_1 \times d_2 \times c} \times \mathbb{R}^{d_1 \times d_2 \times c} \rightarrow \mathbb{R}$ be the Convolutional Neural Tangent Kernels (CNTK) corresponding to L -layered ReLU convolutional network with GAP given in [ADH⁺19b], then there exist a randomized map $\Psi_{cntk}^{(L)} : \mathbb{R}^{d_1 \times d_2 \times c} \rightarrow \mathbb{R}^{s^*}$ for some $s^* = O\left(\frac{1}{\epsilon^2} \cdot \log \frac{1}{\delta}\right)$ such that:*

1. *For any images $y, z \in \mathbb{R}^{d_1 \times d_2 \times c}$:*

$$\Pr \left[\left\langle \Psi_{cntk}^{(L)}(y), \Psi_{cntk}^{(L)}(z) \right\rangle \notin (1 \pm \epsilon) \cdot \Theta_{cntk}^{(L)}(y, z) \right] \leq \delta.$$

2. *For every image $x \in \mathbb{R}^{d_1 \times d_2 \times c}$, $\Psi_{cntk}^{(L)}(x)$ can be computed in time $O\left(\frac{L^{11}}{\epsilon^7} \cdot (d_1 d_2) \cdot \log^3 \frac{d_1 d_2 L}{\epsilon \delta}\right)$.*

This theorem is proved in Appendix F.

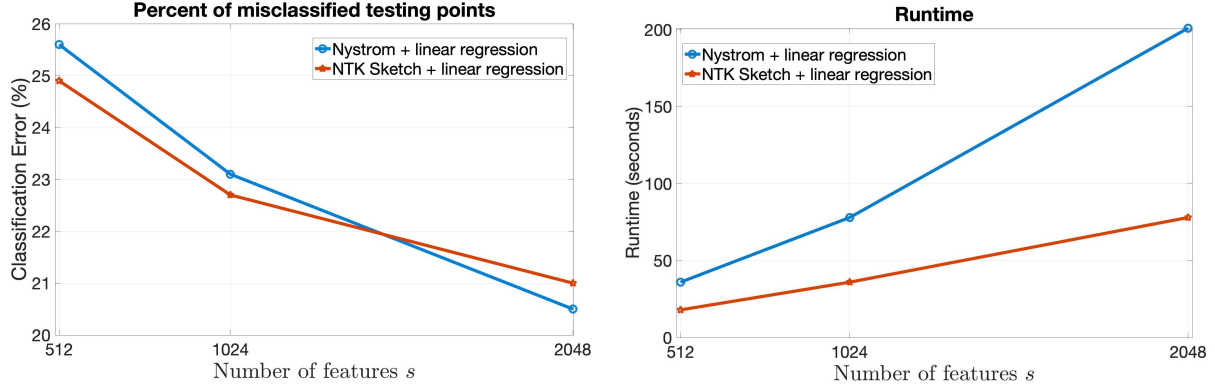


Figure 2: Comparison of test set classification error (left) and total training and estimation runtime (right) on Forest CoverType dataset. The kernel depth for both methods is fixed at $L = 3$.

5 Experiments

In this section, we present the experimental results and show that running least squares regression on the features generated by our methods is an extremely fast and effective way of approximately learning with NTK and CNTK kernel machines. Due to space limit, we only present a small fraction of our experiments here and defer the rest to Appendix A.

NTK Sketch. We compare our NTK Sketch (Theorem2) to Nystrom method of [MM17]. In Figure 2, we compare their performance for various number of features for the depth-3 NTK function $\Theta_{ntk}^{(3)}$ on Forest CoverType dataset, which contains $n = 581'012$ instances in dimension $d = 54$. The top graph in Fig. 2 plots the test set classification error and the bottom graph shows the total training and estimation time. One can observe that the error rate of the NTK Sketch is better when number of features is $s = 512$ or $1'024$ but when the number of features increases to $s = 2'048$ the Nystrom method achieves a slightly better error rate. On the other hand, our method is significantly faster for any number of features. In particular, our method’s runtime scales linearly in the number of features for up to $s = 2'048$ features, while the quadratic behavior of Nystrom method’s runtime is evident in this same range. As a result, our runtime is 3x faster when the number of features is $s = 2'048$. We implemented the Nystrom method very efficiently by using Theorem 1, however, our NTK Sketch outperforms even this highly optimized implementation.

Furthermore, we provide a direct comparison between the approximate kernel matrix generated by our NTK Sketch and the exact NTK kernel matrix. We investigate the “closeness” of our method to the exact NTK by running our sketch on the testing set of MNIST and comparing the resulting approximate kernel matrix to the exact NTK. In figure 3 we plot the relative Frobenius distance between our approximate kernel matrix and exact NTK matrix $\|K - \widehat{K}\|_F/\|K\|_F$ for depths values $L \in \{1, 3\}$. For a target dimension of $s = 8192$, our method produces a kernel matrix that is within 3.3% of the exact kernel matrix in Frobenius norm’s sense.

CNTK Sketch. We base this set of experiments on the MNIST dataset. We compare the performance of our CNTK Sketch (Theorem 3) against SGD-trained CNN for various number of layers L of the CNTK kernel $\Theta_{cntk}^{(L)}$ and number of convolutional layers in its CNN counterpart. The top graph in Figure 4, plots the test set classification error and the bottom graph shows the total training and estimation time. The results correspond to our CNTK Sketch method with $s = 1'024$ features. As can be seen in this figure, our CNTK Sketch combined with linear regression is faster and more accurate than a trained CNN. The gap between our method and CNN widens as we

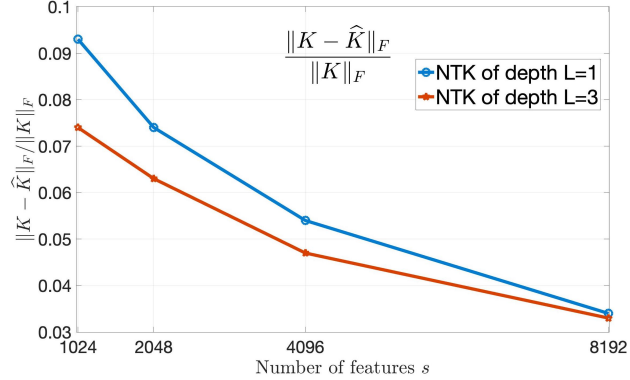


Figure 3: Relative Frobenius distance of our NTK Sketch from exact NTK matrix.

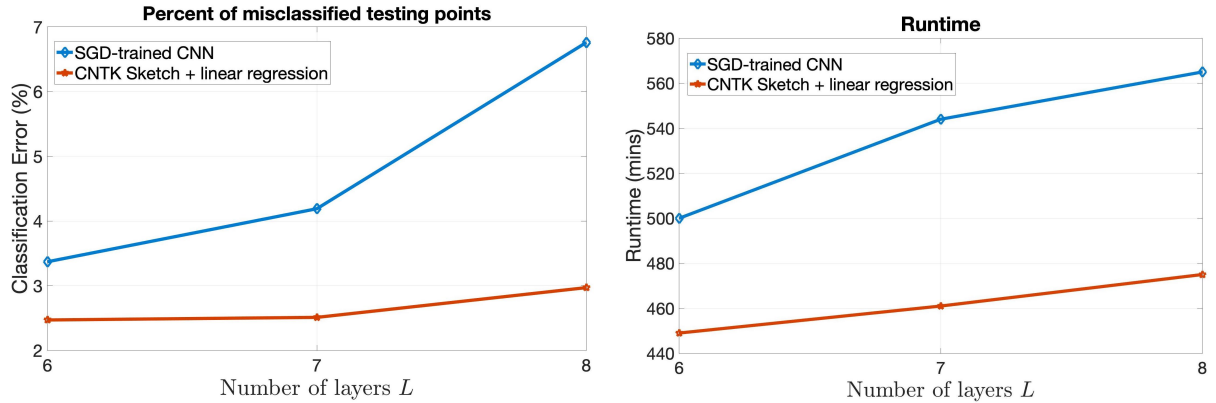


Figure 4: Comparison of test set classification error (left) and total training and estimation runtime (right) on MNIST dataset. The number of features of the CNTK Sketch is fixed at $s = 1'024$.

increase the depth L . This is mainly due to the fact that, for runtime considerations, we limited the number of gradient descent epochs in training the CNN to 300, which seems to be insufficient for networks with larger number of layers.

References

- [AC09] Nir Ailon and Bernard Chazelle. The fast johnson–lindenstrauss transform and approximate nearest neighbors. *SIAM Journal on computing*, 39(1):302–322, 2009.
- [ACW17] Haim Avron, Kenneth L Clarkson, and David P Woodruff. Faster kernel ridge regression using sketching and preconditioning. *SIAM Journal on Matrix Analysis and Applications*, 38(4):1116–1138, 2017.
- [ADH⁺19a] Sanjeev Arora, Simon Du, Wei Hu, Zhiyuan Li, and Ruosong Wang. Fine-grained analysis of optimization and generalization for overparameterized two-layer neural networks. In *International Conference on Machine Learning*, pages 322–332, 2019.
- [ADH⁺19b] Sanjeev Arora, Simon S Du, Wei Hu, Zhiyuan Li, Russ R Salakhutdinov, and Ruosong Wang. On exact computation with an infinitely wide neural net. In *Advances in Neural Information Processing Systems*, pages 8141–8150, 2019.

[ADL⁺19] Sanjeev Arora, Simon S Du, Zhiyuan Li, Ruslan Salakhutdinov, Ruosong Wang, and Dingli Yu. Harnessing the power of infinitely wide deep nets on small-data tasks. In *International Conference on Learning Representations*, 2019.

[AKK⁺20] Thomas D Ahle, Michael Kapralov, Jakob BT Knudsen, Rasmus Pagh, Ameya Velingker, David P Woodruff, and Amir Zandieh. Oblivious sketching of high-degree polynomial kernels. In *Proceedings of the Fourteenth Annual ACM-SIAM Symposium on Discrete Algorithms*, pages 141–160. SIAM, 2020.

[AKM⁺17] Haim Avron, Michael Kapralov, Cameron Musco, Christopher Musco, Ameya Velingker, and Amir Zandieh. Random fourier features for kernel ridge regression: Approximation bounds and statistical guarantees. In *International Conference on Machine Learning*, pages 253–262. PMLR, 2017.

[AM15] Ahmed Alaoui and Michael W Mahoney. Fast randomized kernel ridge regression with statistical guarantees. *Advances in Neural Information Processing Systems*, 28:775–783, 2015.

[ANW14] Haim Avron, Huy Nguyen, and David Woodruff. Subspace embeddings for the polynomial kernel. *Advances in neural information processing systems*, 27:2258–2266, 2014.

[AZLL19] Zeyuan Allen-Zhu, Yuanzhi Li, and Yingyu Liang. Learning and generalization in overparameterized neural networks, going beyond two layers. In *Advances in neural information processing systems*, pages 6158–6169, 2019.

[AZLS19] Zeyuan Allen-Zhu, Yuanzhi Li, and Zhao Song. A convergence theory for deep learning via over-parameterization. In *International Conference on Machine Learning*, pages 242–252. PMLR, 2019.

[BM19] Alberto Bietti and Julien Mairal. On the inductive bias of neural tangent kernels. In *NeurIPS 2019-Thirty-third Conference on Neural Information Processing Systems*, volume 32, pages 12873–12884, 2019.

[CG19] Yuan Cao and Quanquan Gu. A generalization theory of gradient descent for learning overparameterized deep relu networks. *arXiv preprint arXiv:1902.01384*, 2, 2019.

[CNW16] Michael B Cohen, Jelani Nelson, and David P Woodruff. Optimal approximate matrix product in terms of stable rank. In *43rd International Colloquium on Automata, Languages, and Programming (ICALP 2016)*. Schloss Dagstuhl-Leibniz-Zentrum fuer Informatik, 2016.

[CS09] Youngmin Cho and Lawrence K Saul. Kernel methods for deep learning. In *Proceedings of the 22nd International Conference on Neural Information Processing Systems*, pages 342–350, 2009.

[DG03] Sanjoy Dasgupta and Anupam Gupta. An elementary proof of a theorem of johnson and lindenstrauss. *Random Structures & Algorithms*, 22(1):60–65, 2003.

[DH19] Simon Du and Wei Hu. Width provably matters in optimization for deep linear neural networks. In *International Conference on Machine Learning*, pages 1655–1664, 2019.

[DLL⁺19] Simon Du, Jason Lee, Haochuan Li, Liwei Wang, and Xiyu Zhai. Gradient descent finds global minima of deep neural networks. In *International Conference on Machine Learning*, pages 1675–1685. PMLR, 2019.

[DZPS18] Simon S Du, Xiyu Zhai, Barnabas Poczos, and Aarti Singh. Gradient descent provably optimizes over-parameterized neural networks. In *International Conference on Learning Representations*, 2018.

[GARA18] Adrià Garriga-Alonso, Carl Edward Rasmussen, and Laurence Aitchison. Deep convolutional networks as shallow gaussian processes. In *International Conference on Learning Representations*, 2018.

[JGH18] Arthur Jacot, Franck Gabriel, and Clément Hongler. Neural tangent kernel: Convergence and generalization in neural networks. In *Advances in neural information processing systems*, pages 8571–8580, 2018.

[LBN⁺18] Jaehoon Lee, Yasaman Bahri, Roman Novak, Samuel S Schoenholz, Jeffrey Pennington, and Jascha Sohl-Dickstein. Deep neural networks as gaussian processes. In *International Conference on Learning Representations*, 2018.

[LL18] Yuanzhi Li and Yingyu Liang. Learning overparameterized neural networks via stochastic gradient descent on structured data. In *Advances in Neural Information Processing Systems*, pages 8157–8166, 2018.

[LSS⁺20] Jason D Lee, Ruoqi Shen, Zhao Song, Mengdi Wang, and Zheng Yu. Generalized leverage score sampling for neural networks. *arXiv preprint arXiv:2009.09829*, 2020.

[MHR⁺18] Alexander G de G Matthews, Jiri Hron, Mark Rowland, Richard E Turner, and Zoubin Ghahramani. Gaussian process behaviour in wide deep neural networks. In *International Conference on Learning Representations*, 2018.

[MM17] Cameron Musco and Christopher Musco. Recursive sampling for the nystrom method. In *Advances in Neural Information Processing Systems*, pages 3833–3845, 2017.

[NN13] Jelani Nelson and Huy L Nguyêñ. Osnap: Faster numerical linear algebra algorithms via sparser subspace embeddings. In *2013 ieee 54th annual symposium on foundations of computer science*, pages 117–126. IEEE, 2013.

[NXB⁺18] Roman Novak, Lechao Xiao, Yasaman Bahri, Jaehoon Lee, Greg Yang, Jiri Hron, Daniel A Abolafia, Jeffrey Pennington, and Jascha Sohl-dickstein. Bayesian deep convolutional networks with many channels are gaussian processes. In *International Conference on Learning Representations*, 2018.

[RR07] Ali Rahimi and Benjamin Recht. Random features for large-scale kernel machines. *Advances in neural information processing systems*, 20:1177–1184, 2007.

[WZ20] David Woodruff and Amir Zandieh. Near input sparsity time kernel embeddings via adaptive sampling. In *International Conference on Machine Learning*, pages 10324–10333. PMLR, 2020.

[Yan19] Greg Yang. Scaling limits of wide neural networks with weight sharing: Gaussian process behavior, gradient independence, and neural tangent kernel derivation. *arXiv preprint arXiv:1902.04760*, 2019.

[ZNV⁺20] Amir Zandieh, Navid Nouri, Ameya Velingker, Michael Kapralov, and Ilya Razenshteyn. Scaling up kernel ridge regression via locality sensitive hashing. In Silvia Chiappa and Roberto Calandra, editors, *Proceedings of the Twenty Third International Conference on Artificial Intelligence and Statistics*, volume 108 of *Proceedings of Machine Learning Research*, pages 4088–4097. PMLR, 26–28 Aug 2020.

A Experiments

In this section we present the experimental results and show that running least squares regression on the features generated by our method is an extremely fast and effective way of approximating the learning with NTK and CNTK kernel machines. We compare our NTK Sketch method against other competing methods for various large-scale classification and regression tasks in section A.1. Moreover, we present the experimental performance of our CNTK Sketch method for classification of images and compare it against trained CNNs in section A.2.

Setup. We ran all our experiments on a single r5.2xlarge AWS EC2 instance which has 8 vCPU’s and 64GB of memory. This computational infrastructure is not particularly powerful and in fact equivalent to this processing power can be found even in modern laptops. The experiments demonstrate that our method can easily scale to datasets of over half a million training examples without needing powerful workstations. For implementation of all experiments we only used standard PyTorch and NumPy packages. Since our NTK and CNTK Sketches as well as the methods that we compare ourselves to, are randomized, we ran all experiments 5 times with different random seeds and report the average error over all runs.

We remark that for classification tasks, we encode the problem into a regression problem and then solve the regression. More precisely, if we have a classification problem with t classes, then we encode the desired label for the j^{th} class as the vector $(\underbrace{-0.1, -0.1, \dots, -0.1}_{j-1 \text{ terms}}, +0.9, \underbrace{-0.1, -0.1, \dots, -0.1}_{t-j \text{ terms}})$, for

every $j \in [t]$. Then we train regressors to estimate these labels for each datapoint. This same encoding was previously used in [N XB⁺18] and [ADH⁺19b] to reduce classification problems to regression.

A.1 Empirical Results – NTK Sketch

In this set of experiments we train regressors and classifiers by first applying our NTK Sketch from Theorem 2 to the dataset of training points and forming a features matrix $Z \in \mathbb{R}^{n \times s}$ whose rows are the feature vectors obtained by transforming each of the training points. Then we solve the linear least squares problem $\min_w \|Zw - y\|_2^2 + \lambda\|w\|_2^2$, where y denotes the desired labels – i.e., for regression problem, $y \in \mathbb{R}^n$ is a vector whose elements are the desired outputs and for t -class classification, $y \in \mathbb{R}^{n \times t}$ is a matrix whose rows are the desired labels of the training points.

Note that the exact kernel regression scales cubically in the number of training points, therefore, even for datasets with over $n = 10'000$ samples, the runtime of the exact kernel method with NTK kernel would be several orders of magnitude slower than our method. Thus, to have a meaningful comparison, instead of comparing our method to the exact kernel regression, we compare it against the Nystrom method of [MM17] which has excellent empirical performance. This method, by adaptively reading a small number of rows of the kernel matrix, generates a low-rank approximation to the kernel matrix. Specifically, to generate a rank- s approximation to the kernel matrix, this method needs to read only $O(s \log n)$ rows from the kernel matrix adaptively. Hence, the runtime of this method is $\tilde{O}(s^2 \cdot n + n \cdot s \cdot T)$, where T is the kernel evaluation time which is $O(L + d)$ in case of L layered NTK kernel and d -dimensional datasets. Due to its linear dependence on n , this method is significantly faster than regression using exact kernel matrix computation when $s = o(n)$.

Remark on efficient implementation of Nystrom method using Theorem 1. We implemented the Nystrom method with NTK kernel extremely efficiently by using Theorem 1. This theorem shows that in order to compute the kernel value for any pair of input points it is enough to normalize those points, then compute their inner product and then apply the ReLU-NTK function

$K_{relu}^{(L)} : [-1, 1] \rightarrow \mathbb{R}$ on the resulting inner product and then rescale the result with the norms of the points. This suggests an extremely efficient way of computing any collection of rows of the NTK kernel matrix, which in turn leads to accelerating the Nystrom method. We first compute the ReLU-NTK function $K_{relu}^{(L)}$ on a very fine grid on the interval $[-1, 1]$ and store these values in a look up table to be used for approximating the ReLU-NTK function to high precision later. For instance, this function can be easily evaluated on a grid of 10'000 point in a fraction of a second. Now to compute the kernel value for any pair of points we first normalize them and then compute their inner product. Then the NTK value is the product of the norms of the points and the value in the look up table that is stored at the position that corresponds to the inner product value. This way, every element of the kernel matrix can be computed extremely fast compared to the DP of [ADH⁺19b]. In particular, this will speed up kernel computation by a factor of L , where L is the depth of NTK. The experiments show that our NTK Sketch outperforms even this highly optimized implementation of the Nystrom method.

Another method that we compare our NTK Sketch against, is fully trained Multilayer Perceptron (MLP). The MLPs that we use in our experiments have ReLU activation and their width in all hidden layers is 512. While the NTK kernel corresponds to an ultra-wide MLP, we remark that for efficiency purposes and to have an MLP whose runtime can compete with our method we fix the width to 512 in all experiments. We train the MLP using stochastic gradient descent (SGD) with the quadratic loss function and using no data augmentation. Tricks like batch normalization, dropout, etc. are not used for proper comparison. In all experiments, we train the MLP using learning rates chosen from $\{2^{-10}, 2^{-9}, \dots, 2^0, 2^1, 2^2\}$ and report the best testing error.

We base the experiments of this section on three large-scale classification and regression datasets and present the results on each dataset in separate paragraphs as follows,

MNIST Classification. This is a handwritten digits classification dataset with $n = 60'000$ training samples and 10'000 testing samples. Each sample is an image of 28×28 pixels. In this experiment we vectorize the images of this dataset and treat them as vectors of dimension $d = 784$. First we compare the testing set classification accuracy of different methods in Figure 5. This plot illustrates the percent of misclassified testing points for various number of layers L of the NTK kernel $\Theta_{ntk}^{(L)}$ and number of hidden layers in its MLP counterpart. The results correspond to our NTK Sketch method with $s = 8'192$ features. To have a fair comparison we set the number of landmarks of the Nystrom method to the same $s = 8'192$. Furthermore, the MLP was trained with gradient descent for 300 epochs. As can be seen in this figure, the accuracy of projecting the data into feature space using our NTK Sketch and then solving linear regression in the feature space is nearly insensitive to the number of layers for $L \in \{1, 2, 3\}$. The same holds for the Nystrom method with NTK kernel. However, the trained MLP achieves its best performance for $L = 2$. This figure shows that the performance of our method is nearly as good as the Nystrom method and both our method and Nystrom method outperform a fully trained MLP on the MNIST dataset.

In Figure 6 we compare our NTK Sketch with the Nystrom NTK approximation method more extensively. We compare the performance of the two methods for various number of features (or number of landmarks in case of Nystrom method) for the depth-1 NTK kernel $\Theta_{ntk}^{(1)}$. The left graph of Fig. 6 plots the classification error on the testing set and the right graph plots the total training and estimation time. The runtime includes the total time to project the entire dataset into feature space and then solve a linear least squares problem in feature space and construct an estimator. One can observe that the error rate of Nystrom method is better than our method when the number of features is small but as the number of features increases the NTK Sketch closes the gap and for $s = 8'192$ features, produces nearly identical result. In terms of runtime on the other hand,

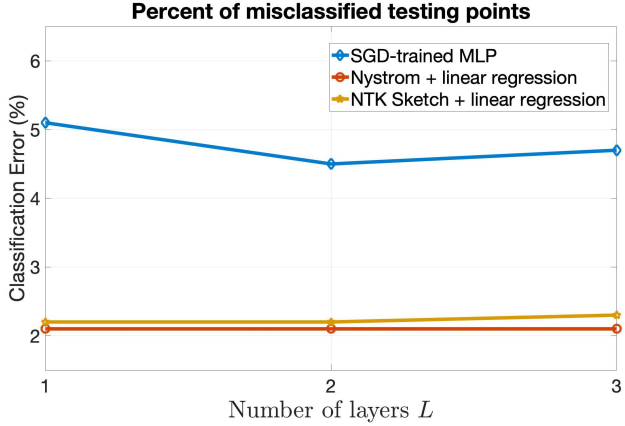


Figure 5: Comparison of test set classification error of different methods on MNIST dataset. The number of features for both NTK Sketch and Nystrom method is fixed at $s = 8'192$.

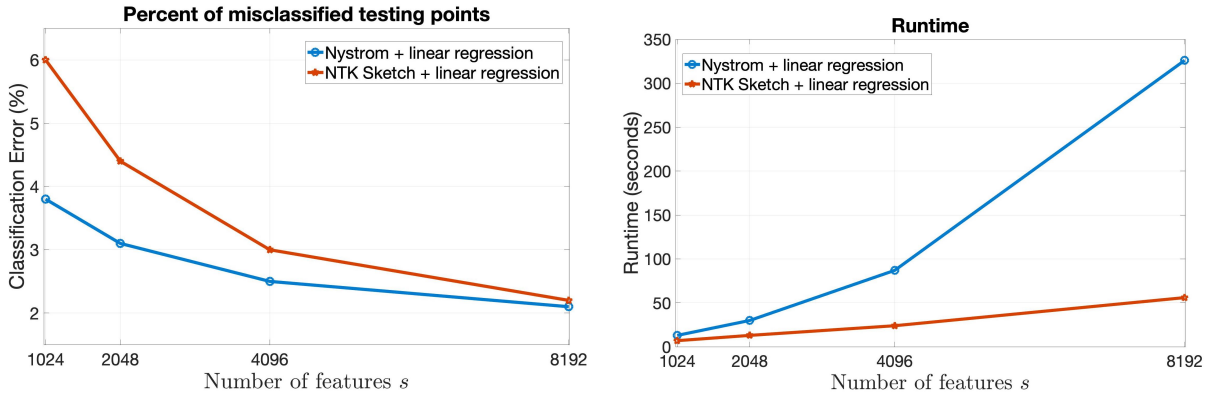


Figure 6: Comparison of NTK Sketch and Nystrom method for various number of features. The kernel depth for both NTK Sketch and Nystrom method is fixed at $L = 1$. The left plot shows classification error on the testing points of MNIST dataset and the right plot shows the total time to compute features and train the estimators by solving least squares problem.

our method significantly outperforms the Nystrom method. In particular, our method's empirical runtime scales linearly in the number of features for up to $s = 8'192$ features, while the quadratic behavior of Nystrom method's runtime is evident in this same range. As a result, our runtime is 6x faster when the number of features is $s = 8'192$.

Location of CT Slices Regression. This is a regression dataset from UCI repository containing $n = 53'500$ instances extracted from CT images. The datapoints are vectors of dimension $d = 384$. The goal is to estimate the relative location of the CT slice on the axial axis of the human body. In Figure 7 we plot the testing RMSE of different methods for various depths L of the NTK kernel $\Theta_{ntk}^{(L)}$ and its MLP counterpart. The results correspond to running our NTK Sketch as well as the Nystrom method with $s = 8'192$ features. Furthermore, the MLP was trained with gradient descent for 400 epochs. One can see that the accuracy of the Nystrom method with NTK kernel is slightly

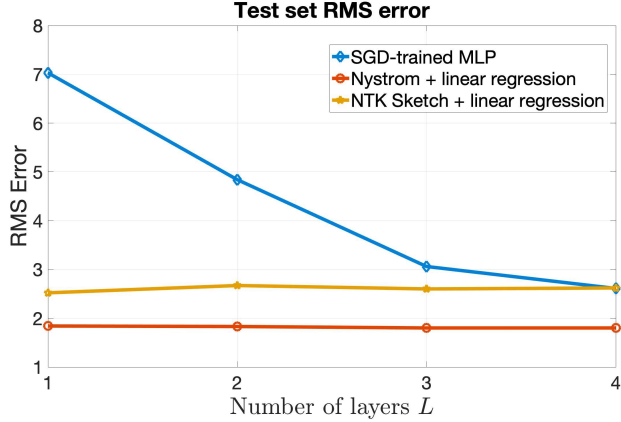


Figure 7: Comparison of testing RMSE of different methods on CT Location dataset. The number of features for both NTK Sketch and Nystrom method is fixed at $s = 8'192$.

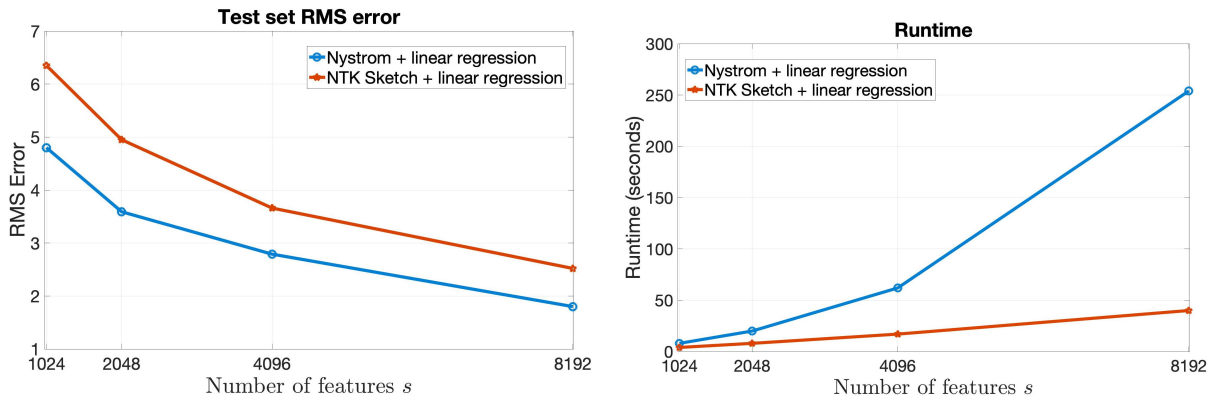


Figure 8: Comparison of NTK Sketch and Nystrom method for various number of features. The kernel depth for both NTK Sketch and Nystrom method is fixed at $L = 3$. The left plot shows RMSE on the testing points of CT Location dataset and the right plot shows the total time to compute features and train the estimators by solving a least squares problem.

better than our NTK Sketch. Additionally, our method outperforms the MLP at smaller depths but as the number of layers increase the MLP improves and at depth $L = 4$ achieves the same accuracy as the NTK Sketch.

In Figure 8, we compare the performance of our NTK Sketch with the Nystrom method for various number of features for the depth-3 NTK $\Theta_{ntk}^{(3)}$. The left graph in Fig. 8 plots the testing RMSE and the right graph shows the total training and estimation time. One can observe that the error rate of Nystrom method is better than our method, while on the other hand, our method is significantly faster. In particular, our method's empirical runtime scales linearly in the number of features for up to $s = 8'192$ features, while the quadratic behavior of Nystrom method's runtime is evident in this same range. As a result, our runtime is over 6x faster when the number of features is $s = 8'192$.

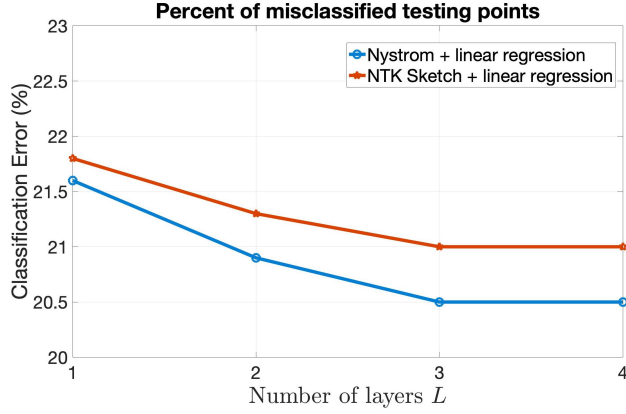


Figure 9: Comparison of test set classification error of different methods on Forest CoverType dataset. The number of features for both NTK Sketch and Nystrom method is fixed at $s = 2'048$.

Forest CoverType Classification. This is a classification dataset from UCI repository containing $n = 581'012$ instances. The datapoints are vectors of dimension $d = 54$. The goal is to estimate the CoverType of the forests which can be one of seven possible categories. In Figure 9 we plot the percent of misclassified testing points by different methods for various depths L of the NTK kernel $\Theta_{ntk}^{(L)}$. The results correspond to running our NTK Sketch as well as the Nystrom method with $s = 2'048$ features. One can see that the accuracy of the Nystrom method with NTK kernel is slightly better than our NTK Sketch. The advantage of the Nystrom method to our NTK Sketch is less than half a percent in classification error rate.

In Figure 10, we compare the performance of our NTK Sketch with the Nystrom method for various number of features for the depth-3 NTK $\Theta_{ntk}^{(3)}$. The left graph in Fig. 10 plots the test set classification error and the right graph shows the total training and estimation time. One can observe that the error rate of the NTK Sketch is better when number of features is $s = 512$ or $1'024$ but when the number of features increases to $s = 2'048$ the Nystrom method achieves a slightly better error rate. On the other hand, our method is significantly faster for any number of features. In particular, our method’s runtime scales linearly in the number of features for up to $s = 2'048$ features, while the quadratic behavior of Nystrom method’s runtime is evident in this same range. As a result, our runtime is 3x faster when the number of features is $s = 2'048$.

A.2 Empirical Results – CNTK Sketch

We base the experiments of this section on MNIST handwritten digits classification dataset which contains $n = 60'000$ training samples and $10'000$ testing samples. Each sample is an image of 28×28 pixels. In this set of experiments we train our classifier by first applying the CNTK Sketch from Theorem 3 to training points and forming a features matrix $Z \in \mathbb{R}^{n \times s}$ whose rows are the feature vectors obtained by transforming each point, and then solving the linear least squares problem $\min_{w \in \mathbb{R}^{s \times t}} \|Zw - y\|_2^2 + \lambda \|w\|_2^2$, where $y \in \mathbb{R}^{n \times t}$ denotes the desired labels – i.e., a matrix whose rows are the desired labels of the training points and $t = 10$ is the number of classes.

We compare our CNTK Sketch against fully trained Convolutional Neural Network (CNN). The CNNs that we use in our experiments have ReLU activation and their number of channels in all convolutional layers is 64. While the CNTK kernel corresponds to an ultra-wide CNN, we remark

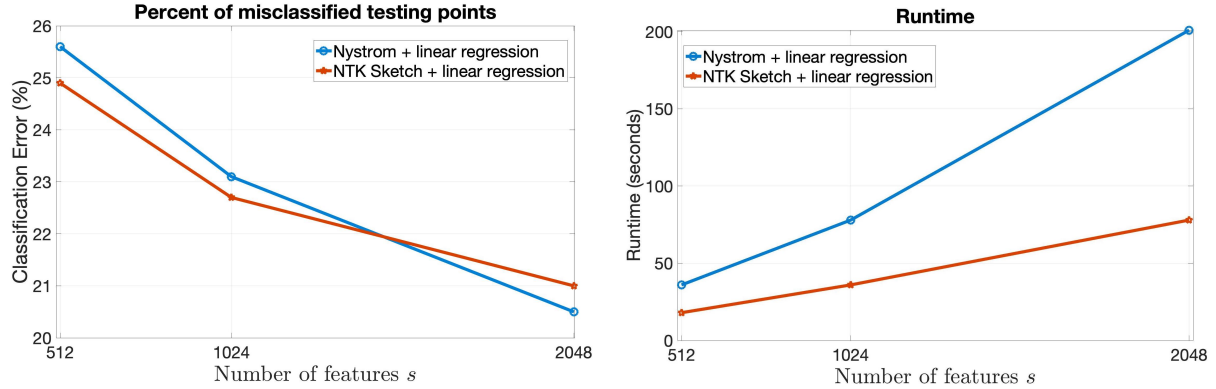


Figure 10: Comparison of NTK Sketch and Nystrom method for various number of features. The kernel depth for both NTK Sketch and Nystrom method is fixed at $L = 3$. The left plot shows classification error rate on the testing points of Forest CoverType dataset and the right plot shows the total time to compute features and train the estimators.

that for efficiency purposes and to have a CNN whose runtime can compete with our method we fix the number of channels to 64 in all experiments. We train the CNN using stochastic gradient descent (SGD) with the quadratic loss function and using no data augmentation and no tricks like batch normalization, dropout, etc. In all experiments, we train the CNN using learning rates chosen from $\{2^{-10}, 2^{-9}, \dots, 2^0, 2^1, 2^2\}$ and report the best testing error. We limited the number of training epochs to 300 to make the runtime of CNN comparable to our CNTK Sketch. This resulted in slight compromise in the accuracy in favor of faster runtime.

Remark on exact computation and Nystrom approximation of CNTK kernel matrix. First we remark that due to cubic runtime complexity, the exact kernel regression with CNTK kernel is out of the question and we did not include the exact method in this set of experiments. On the other hand, the Nystrom method of [MM17] does not suffer from this issue and its runtime has a linear dependence on the size of training set. This method adaptively reads a small number of rows of the kernel matrix and generates a low-rank approximation to the kernel matrix. Specifically, to generate a rank- s approximation to the kernel matrix, this method only needs to access $O(s \log n)$ rows of the kernel matrix. However, the computation of CNTK kernel value is very expensive. In particular, evaluating the depth- L CNTK $\Theta_{cntk}^{(L)}$ on a pair of input images of size $d_1 \times d_2$ requires $\Omega((d_1 d_2)^2 \cdot L)$ operations. Note that while the runtime of our CNTK Sketch scales only linearly in the number of pixels, the CNTK computation time depends quadratically on the number of pixels of input images. Consequently, our CNTK Sketch can be orders of magnitude faster than Nystrom method with similar number of landmarks. More precisely, we attempted to run the Nystrom method with CNTK kernel on MNIST dataset but found that computing a single row of the kernel matrix takes over 15 minutes which implies that the Nystrom method with 400 landmarks would require over 100 hours of runtime. This has no chance of competing with our CNTK Sketch or trained CNNs and thus we did not include Nystrom method in this set of experiments.

First we compare the performance of our CNTK Sketch with SGD-trained CNN for various number of layers L of the CNTK kernel $\Theta_{cntk}^{(L)}$ and number of convolutional layers in its CNN counterpart. The left graph in Fig. 11, plots the test set classification error and the right graph shows the total training and estimation time. The results correspond to our CNTK Sketch method

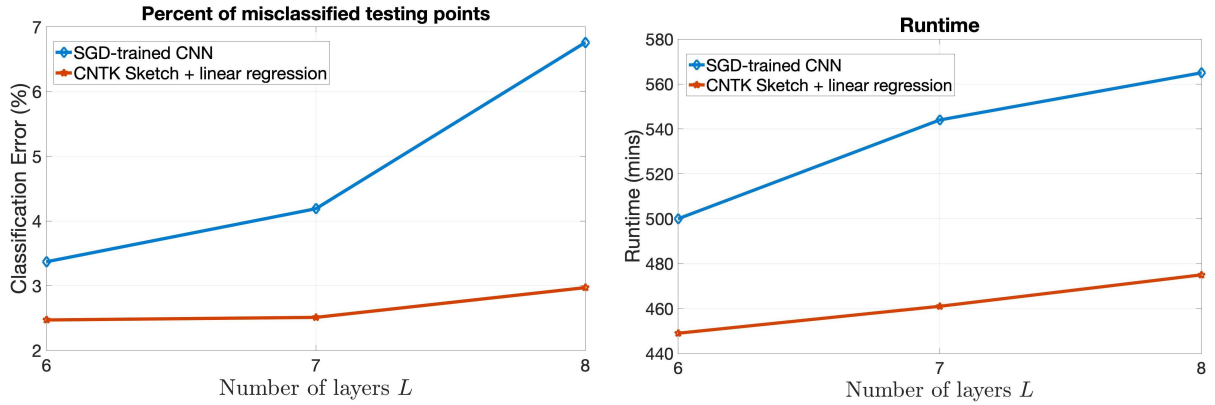


Figure 11: Comparison of test set classification error (left plot) and total training and estimation runtime (right plot) of different methods on MNIST dataset. The number of features of the CNTK Sketch is fixed at $s = 1'024$.

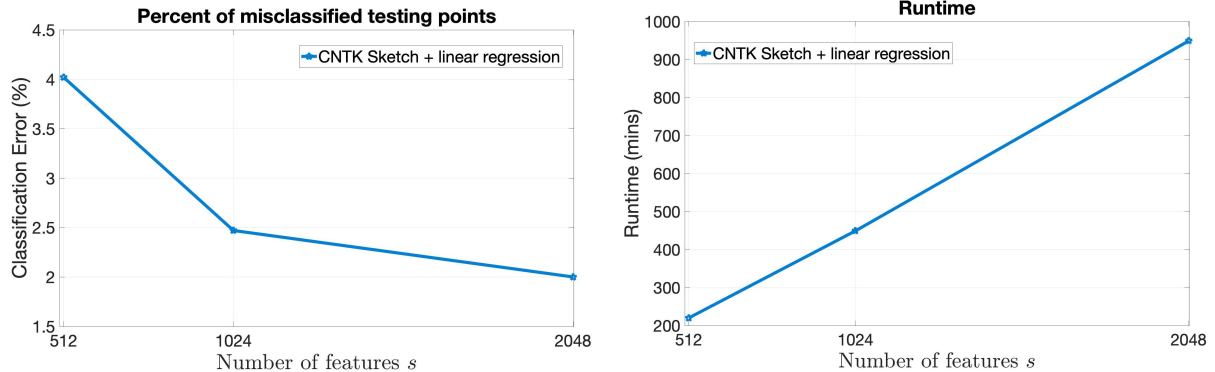


Figure 12: Performance of CNTK Sketch for various number of features. The kernel depth is fixed at $L = 6$. The left plot shows classification error rate on the testing points of MNIST dataset and the right plot shows the total time to compute features and train the estimator by solving a least squares problem.

with $s = 1'024$ features. As can be seen in this figure, projecting the data into feature space using our CNTK Sketch and then solving linear regression in the feature space is both faster and more accurate than training a CNN for any depth $L \in \{6, 7, 8\}$. This figure shows that both methods achieve their best performance when $L = 6$. The gap between the classification accuracy of our method and CNN widens as we increase the depth L . This is mainly due to the fact that we limited the number of gradient descent epochs in training CNN to 300 and this seems to be insufficient for networks with larger number of layers. However, note that even for this choice of epoch number the runtime of CNN is slower than our method.

Next, we investigate the effect of number of features in performance of our CNTK Sketch for the depth-6 CNTK $\Theta_{cntk}^{(6)}$, in Figure 12. The left graph in Fig. 12 plots the test set classification error and the right graph shows the total training and estimation time. One can observe that our method's runtime scales linearly in the number of features for up to $s = 2'048$ features.

B ReLU-NTK Expression

In this section we prove Theorem 1. First note that the main component of the DP given in (1), (2), and (3) for computing the NTK of fully connected network is what we call the *Activation Covariance*. The activation covariance is defined with respect to the activation $\sigma(\cdot)$ as follows,

Definition B.1 (Activation Covariance). For any continuous activation function $\sigma : \mathbb{R} \rightarrow \mathbb{R}$, we define the *Activation Covariance* function $k_\sigma : \mathbb{R}^d \times \mathbb{R}^d \rightarrow \mathbb{R}$ as follows:

$$k_\sigma(y, z) := \mathbb{E}_{w \sim \mathcal{N}(0, I_d)} [\sigma(w^\top y) \cdot \sigma(w^\top z)] \quad \text{for every } y, z \in \mathbb{R}^d,$$

where $\mathcal{N}(0, I_d)$ denotes a d -dimensional isotropic normal distribution. Additionally, we define the *Derivative Activation Covariance* function $\dot{k}_\sigma : \mathbb{R}^d \times \mathbb{R}^d \rightarrow \mathbb{R}$ as follows:

$$\dot{k}_\sigma(y, z) := \mathbb{E}_{w \sim \mathcal{N}(0, I_d)} [\dot{\sigma}(w^\top y) \cdot \dot{\sigma}(w^\top z)] \quad \text{for every } y, z \in \mathbb{R}^d.$$

It is worth noting that one can prove the activation covariance function k_σ as well as the derivative activation covariance function \dot{k}_σ are positive definite and hence they both define valid kernel functions in \mathbb{R}^d . The connection between the ReLU activation covariance functions and arc-cosine kernel functions defined in (4) of Definition 3.1 is proved in [CS09]. We restate this result in the following claim,

Claim 1 (Covariance of ReLU Activation). *For ReLU activation function $\sigma(\alpha) = \max(\alpha, 0)$, let k_σ and \dot{k}_σ denote the activation covariance function and the derivative activation covariance function defined in Definition B.1. If we let $\kappa_0(\cdot)$ and $\kappa_1(\cdot)$ be the zeroth and first order arc-cosine kernels defined in (4) of Definition 3.1, then for every positive integer d and every $y, z \in \mathbb{R}^d$ we have:*

$$k_\sigma(y, z) = \frac{\|y\|_2 \|z\|_2}{2} \cdot \kappa_1 \left(\frac{\langle y, z \rangle}{\|y\|_2 \|z\|_2} \right)$$

and

$$\dot{k}_\sigma(y, z) = \frac{1}{2} \cdot \kappa_0 \left(\frac{\langle y, z \rangle}{\|y\|_2 \|z\|_2} \right).$$

Remark. Observe that $\kappa_0(\alpha) = \frac{d}{d\alpha}(\kappa_1(\alpha))$.

Now we are ready to prove theorem 1:

Proof of Theorem 1: Consider the NTK expression given in (1), (2), and (3). We first prove by induction on $h = 0, 1, 2, \dots, L$ that the covariance function $\Sigma^{(h)}(y, z)$ defined in (1) satisfies:

$$\Sigma^{(h)}(y, z) = \|y\|_2 \|z\|_2 \cdot \Sigma_{\text{relu}}^{(h)} \left(\frac{\langle y, z \rangle}{\|y\|_2 \|z\|_2} \right).$$

The **base of induction** is trivial for $h = 0$ because $\Sigma^{(0)}(y, z) = \langle y, z \rangle = \|y\|_2 \|z\|_2 \cdot \Sigma_{\text{relu}}^{(0)} \left(\frac{\langle y, z \rangle}{\|y\|_2 \|z\|_2} \right)$.

To prove the **inductive step**, suppose that the inductive hypothesis holds for $h - 1$, i.e.,

$$\Sigma^{(h-1)}(y, z) = \|y\|_2 \|z\|_2 \cdot \Sigma_{\text{relu}}^{(h-1)} \left(\frac{\langle y, z \rangle}{\|y\|_2 \|z\|_2} \right)$$

The 2×2 covariance matrix $\Lambda^{(h)}(y, z)$, defined in (1), can be decomposed as $\Lambda^{(h)}(y, z) = \begin{pmatrix} f^\top \\ g^\top \end{pmatrix} \begin{pmatrix} f & g \end{pmatrix}$, where $f, g \in \mathbb{R}^2$. Now note that $\|f\|_2^2 = \Sigma^{(h-1)}(y, y)$, hence, by inductive hypothesis, we have,

$$\|f\|_2^2 = \|y\|_2^2 \cdot \Sigma_{\text{relu}}^{(h-1)} \left(\frac{\langle y, y \rangle}{\|y\|_2^2} \right) = \|y\|_2^2 \cdot \Sigma_{\text{relu}}^{(h-1)}(1) = \|y\|_2^2.$$

Using a similar argument we have $\|g\|_2^2 = \|z\|_2^2$. Therefore, by Claim 1, we can write

$$\begin{aligned}\Sigma^{(h)}(y, z) &= \frac{1}{\mathbb{E}_{x \sim \mathcal{N}(0,1)} [|\sigma(x)|^2]} \cdot \mathbb{E}_{w \sim \mathcal{N}(0, I_2)} [\sigma(w^\top f) \cdot \sigma(w^\top g)] \\ &= \frac{2}{\kappa_1(1)} \cdot \mathbb{E}_{w \sim \mathcal{N}(0, I_2)} [\sigma(w^\top f) \cdot \sigma(w^\top g)] \\ &= \|f\|_2 \|g\|_2 \cdot \kappa_1 \left(\frac{\langle f, g \rangle}{\|f\|_2 \|g\|_2} \right) = \|y\|_2 \|z\|_2 \cdot \kappa_1 \left(\frac{\langle f, g \rangle}{\|y\|_2 \|z\|_2} \right).\end{aligned}$$

Since we assumed that $\Lambda^{(h)}(y, z) = \begin{pmatrix} f^\top \\ g^\top \end{pmatrix} \cdot (f \quad g)$, we have $\langle f, g \rangle = \Sigma^{(h-1)}(y, z)$. By inductive hypothesis along with (5), we find that

$$\Sigma^{(h)}(y, z) = \|y\|_2 \|z\|_2 \cdot \kappa_1 \left(\Sigma_{\text{relu}}^{(h-1)} \left(\frac{\langle y, z \rangle}{\|y\|_2 \|z\|_2} \right) \right) = \|y\|_2 \|z\|_2 \cdot \Sigma_{\text{relu}}^{(h)} \left(\frac{\langle y, z \rangle}{\|y\|_2 \|z\|_2} \right),$$

which completes the induction and proves that for every $h \in \{0, 1, 2, \dots, L\}$,

$$\Sigma^{(h)}(y, z) = \|y\|_2 \|z\|_2 \cdot \Sigma_{\text{relu}}^{(h)} \left(\frac{\langle y, z \rangle}{\|y\|_2 \|z\|_2} \right). \quad (26)$$

For obtaining the final NTK expression we also need to simplify the derivative covariance function defined in (2). Recall that we proved before, the covariance matrix $\Lambda^{(h)}(y, z)$ can be decomposed as $\Lambda^{(h)}(y, z) = \begin{pmatrix} f^\top \\ g^\top \end{pmatrix} \cdot (f \quad g)$, where $f, g \in \mathbb{R}^2$ with $\|f\|_2 = \|y\|_2$ and $\|g\|_2 = \|z\|_2$. Therefore, by Claim 1, we can write

$$\begin{aligned}\dot{\Sigma}^{(h)}(y, z) &= \frac{1}{\mathbb{E}_{x \sim \mathcal{N}(0,1)} [|\sigma(x)|^2]} \cdot \mathbb{E}_{w \sim \mathcal{N}(0, I_2)} [\dot{\sigma}(w^\top f) \cdot \dot{\sigma}(w^\top g)] \\ &= \frac{2}{\kappa_1(1)} \cdot \mathbb{E}_{w \sim \mathcal{N}(0, I_2)} [\dot{\sigma}(w^\top f) \cdot \dot{\sigma}(w^\top g)] \\ &= \kappa_0 \left(\frac{\langle f, g \rangle}{\|y\|_2 \|z\|_2} \right).\end{aligned}$$

Since we assumed that $\Lambda^{(h)}(y, z) = \begin{pmatrix} f^\top \\ g^\top \end{pmatrix} \cdot (f \quad g)$, $\langle f, g \rangle = \Sigma^{(h-1)}(y, z) = \|y\|_2 \|z\|_2 \cdot \Sigma_{\text{relu}}^{(h-1)} \left(\frac{\langle y, z \rangle}{\|y\|_2 \|z\|_2} \right)$. Therefore, by (6), for every $h \in \{1, 2, \dots, L\}$,

$$\dot{\Sigma}^{(h)}(y, z) = \kappa_0 \left(\Sigma_{\text{relu}}^{(h-1)} \left(\frac{\langle y, z \rangle}{\|y\|_2 \|z\|_2} \right) \right) = \dot{\Sigma}_{\text{relu}}^{(h)} \left(\frac{\langle y, z \rangle}{\|y\|_2 \|z\|_2} \right). \quad (27)$$

Now we prove by induction on integer L that the NTK with L layers and ReLU activation given in (3) satisfies

$$\Theta_{\text{ntk}}^{(L)}(y, z) = \|y\|_2 \|z\|_2 \cdot K_{\text{relu}}^{(L)} \left(\frac{\langle y, z \rangle}{\|y\|_2 \|z\|_2} \right).$$

The **base of induction**, trivially holds because, by (26):

$$\Theta_{\text{ntk}}^{(0)}(y, z) = \Sigma^{(0)}(y, z) = \|y\|_2 \|z\|_2 \cdot K_{\text{relu}}^{(0)} \left(\frac{\langle y, z \rangle}{\|y\|_2 \|z\|_2} \right).$$

To prove the **inductive step**, suppose that the inductive hypothesis holds for $L - 1$, that is $\Theta_{ntk}^{(L-1)}(y, z) = \|y\|_2\|z\|_2 \cdot K_{relu}^{(L-1)}\left(\frac{\langle y, z \rangle}{\|y\|_2\|z\|_2}\right)$. Now using the recursive definition of $\Theta_{ntk}^{(L)}(y, z)$ given in (3) along with (26) and (27) we can write,

$$\begin{aligned}\Theta_{ntk}^{(L)}(y, z) &= \Theta_{ntk}^{(L-1)}(y, z) \cdot \dot{\Sigma}^{(L)}(y, z) + \Sigma^{(L)}(y, z) \\ &= \|y\|_2\|z\|_2 \cdot K_{relu}^{(L-1)}\left(\frac{\langle y, z \rangle}{\|y\|_2\|z\|_2}\right) \cdot \dot{\Sigma}_{relu}^{(h)}\left(\frac{\langle y, z \rangle}{\|y\|_2\|z\|_2}\right) + \|y\|_2\|z\|_2 \cdot \Sigma_{relu}^{(h)}\left(\frac{\langle y, z \rangle}{\|y\|_2\|z\|_2}\right) \\ &\equiv \|y\|_2\|z\|_2 \cdot K_{relu}^{(L)}\left(\frac{\langle y, z \rangle}{\|y\|_2\|z\|_2}\right),\end{aligned}$$

which gives the theorem. \square

C NTK Sketch: Claims and Invariants

We start by proving that the polynomials $P_{relu}^{(p)}(\cdot)$ and $\dot{P}_{relu}^{(p)}(\cdot)$ defined in (8) of Definition 3.2 closely approximate the functions $\kappa_1(\cdot)$ and $\kappa_0(\cdot)$ on the interval $[-1, 1]$,

Lemma 3 (Polynomial Approximations to κ_1 and κ_0). *If we let $k_{relu}(\cdot)$ and $\kappa_0(\cdot)$ be defined as in (4) of Definition 3.1, then for any integer $p \geq \frac{1}{9\epsilon^{2/3}}$, the polynomial $P_{relu}^{(p)}(\cdot)$ defined in (8) of Definition 3.2 satisfies,*

$$\max_{\alpha \in [-1, 1]} |P_{relu}^{(p)}(\alpha) - \kappa_1(\alpha)| \leq \epsilon.$$

Moreover, for any integer $p \geq \frac{1}{26\epsilon^2}$, the polynomial $\dot{P}_{relu}^{(p)}(\cdot)$ defined as in (8) of Definition 3.2, satisfies,

$$\max_{\alpha \in [-1, 1]} |\dot{P}_{relu}^{(p)}(\alpha) - \kappa_0(\alpha)| \leq \epsilon.$$

Proof. We start by Taylor series expansion of $\kappa_0(\cdot)$ at $\alpha = 0$, $\kappa_0(\alpha) = \frac{1}{2} + \frac{1}{\pi} \cdot \sum_{n=0}^{\infty} \frac{(2n)!}{2^{2n} \cdot (n!)^2 \cdot (2n+1)} \cdot \alpha^{2n+1}$. Therefore, we have

$$\begin{aligned}\max_{\alpha \in [-1, 1]} |\dot{P}_{relu}^{(p)}(\alpha) - \kappa_0(\alpha)| &= \frac{1}{\pi} \cdot \sum_{n=p+1}^{\infty} \frac{(2n)!}{2^{2n} \cdot (n!)^2 \cdot (2n+1)} \\ &\leq \frac{1}{\pi} \cdot \sum_{n=p+1}^{\infty} \frac{e \cdot e^{-2n} \cdot (2n)^{2n+1/2}}{2\pi \cdot 2^{2n} \cdot e^{-2n} \cdot n^{2n+1} \cdot (2n+1)} \\ &= \frac{e}{\sqrt{2}\pi^2} \cdot \sum_{n=p+1}^{\infty} \frac{1}{\sqrt{n} \cdot (2n+1)} \\ &\leq \frac{e}{\sqrt{2}\pi^2} \cdot \int_p^{\infty} \frac{1}{\sqrt{x} \cdot (2x+1)} dx \\ &\leq \frac{e}{\sqrt{2}\pi^2} \cdot \frac{1}{\sqrt{p}} \leq \epsilon.\end{aligned}$$

To prove the second part of the lemma, we consider the Taylor expansion of $\kappa_1(\cdot)$ at $\alpha = 0$. Observe that $\kappa_0(\alpha) = \frac{d}{d\alpha}(\kappa_1(\alpha))$, therefore, the Taylor series of $\kappa_1(\alpha)$ can be obtained from the Taylor series of $\kappa_0(\alpha)$ as follows,

$$\kappa_1(\alpha) = \frac{1}{\pi} + \frac{\alpha}{2} + \frac{1}{\pi} \cdot \sum_{n=0}^{\infty} \frac{(2n)!}{2^{2n} \cdot (n!)^2 \cdot (2n+1) \cdot (2n+2)} \cdot \alpha^{2n+2}.$$

Hence, we have

$$\begin{aligned}
\max_{\alpha \in [-1, 1]} |P_{\text{relu}}^{(p)}(\alpha) - \kappa_1(\alpha)| &= \frac{1}{\pi} \cdot \sum_{n=p+1}^{\infty} \frac{(2n)!}{2^{2n} \cdot (n!)^2 \cdot (2n+1) \cdot (2n+2)} \\
&\leq \frac{1}{\pi} \cdot \sum_{n=p+1}^{\infty} \frac{e \cdot e^{-2n} \cdot (2n)^{2n+1/2}}{2\pi \cdot 2^{2n} \cdot e^{-2n} \cdot n^{2n+1} \cdot (2n+1) \cdot (2n+2)} \\
&= \frac{e}{\sqrt{2}\pi^2} \cdot \sum_{n=p+1}^{\infty} \frac{1}{\sqrt{n} \cdot (2n+1) \cdot (2n+2)} \\
&\leq \frac{e}{\sqrt{2}\pi^2} \cdot \int_p^{\infty} \frac{1}{\sqrt{x} \cdot (2x+1) \cdot (2x+2)} dx \\
&\leq \frac{e}{\sqrt{2}\pi^2} \cdot \frac{1}{6 \cdot p^{3/2}} \leq \epsilon.
\end{aligned}$$

□

Therefore, it is possible to approximate the function $\kappa_0(\cdot)$ up to error ϵ using a polynomial of degree $O\left(\frac{1}{\epsilon^2}\right)$. Also if we want to approximate $\kappa_1(\cdot)$ using a polynomial up to error ϵ on the interval $[-1, 1]$, it suffices to use a polynomial of degree $O\left(\frac{1}{\epsilon^{2/3}}\right)$. One can see that since the Taylor expansion of κ_1 and κ_0 contain non-negative coefficients only, both of these functions are positive definite. Additionally, the Polynomial approximations $P_{\text{relu}}^{(p)}$ and $\dot{P}_{\text{relu}}^{(p)}$ given in (8) of Definition 3.2 are positive definite functions for any value of $p \geq 0$.

In order to prove Theorem 2, we also need the following lemma on the error sensitivity of polynomials $P_{\text{relu}}^{(p)}$ and $\dot{P}_{\text{relu}}^{(p)}$,

Lemma 4 (Sensitivity of $P_{\text{relu}}^{(p)}$ and $\dot{P}_{\text{relu}}^{(p)}$). *For any integer $p \geq 3$, any $\alpha \in [-1, 1]$, and any α' such that $|\alpha - \alpha'| \leq \frac{1}{6p}$, if we let the polynomials $P_{\text{relu}}^{(p)}(\alpha)$ and $\dot{P}_{\text{relu}}^{(p)}(\alpha)$ be defined as in (8) of Definition 3.2, then*

$$|P_{\text{relu}}^{(p)}(\alpha) - P_{\text{relu}}^{(p)}(\alpha')| \leq |\alpha - \alpha'|,$$

and

$$|\dot{P}_{\text{relu}}^{(p)}(\alpha) - \dot{P}_{\text{relu}}^{(p)}(\alpha')| \leq \sqrt{p} \cdot |\alpha - \alpha'|.$$

Proof. Note that an α' that satisfies the preconditions of the lemma, is in the range $\left[-1 - \frac{1}{6p}, 1 + \frac{1}{6p}\right]$. Now we bound the derivative of the polynomial $\dot{P}_{\text{relu}}^{(p)}$ on the interval $\left[-1 - \frac{1}{6p}, 1 + \frac{1}{6p}\right]$,

$$\begin{aligned}
\max_{\alpha \in \left[-1 - \frac{1}{6p}, 1 + \frac{1}{6p}\right]} \left| \frac{d}{d\alpha} \left(\dot{P}_{\text{relu}}^{(p)}(\alpha) \right) \right| &= \frac{1}{\pi} \cdot \sum_{n=0}^p \frac{(2n)!}{2^{2n} \cdot (n!)^2} \cdot \left(1 + \frac{1}{6p} \right)^{2n} \\
&\leq \frac{1}{\pi} + \frac{e^{4/3}}{\sqrt{2}\pi^2} \cdot \sum_{n=1}^p \frac{1}{\sqrt{n}} \\
&\leq \frac{1}{\pi} + \frac{e^{4/3}}{\sqrt{2}\pi^2} \cdot \int_0^p \frac{1}{\sqrt{x}} dx \\
&\leq \sqrt{p},
\end{aligned}$$

therefore, the second statement of lemma holds.

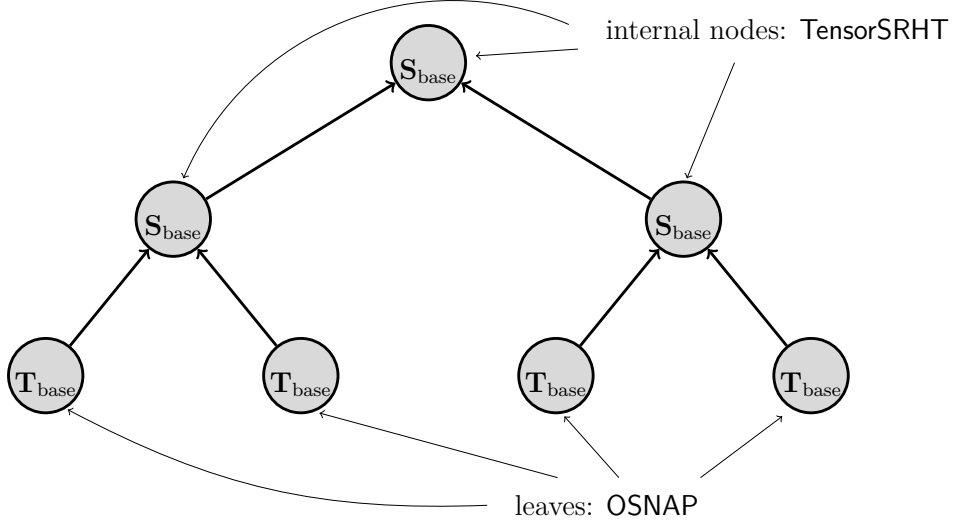


Figure 13: The structure of sketch Q^p proposed in Theorem 1.2 of [AKK⁺20]: the sketch matrices in nodes of the tree labeled with S_{base} and T_{base} are independent instances of TensorSRHT and OSNAP, respectively.

To prove the first statement of lemma, we bound the derivative of the polynomial $P_{\text{relu}}^{(p)}$ on the interval $\left[-1 - \frac{1}{6p}, 1 + \frac{1}{6p}\right]$ as follows,

$$\begin{aligned}
\max_{\alpha \in \left[-1 - \frac{1}{6p}, 1 + \frac{1}{6p}\right]} \left| \frac{d}{d\alpha} \left(P_{\text{relu}}^{(p)}(\alpha) \right) \right| &= \frac{1}{\pi} \cdot \sum_{n=0}^p \frac{(2n)!}{2^{2n} \cdot (n!)^2 \cdot (2n+1)} \cdot \left(1 + \frac{1}{6p} \right)^{2n+1} \\
&\leq \frac{19}{18\pi} + \frac{e^{25/18}}{\sqrt{2\pi^2}} \cdot \sum_{n=1}^p \frac{1}{\sqrt{n} \cdot (2n+1)} \\
&\leq \frac{19}{18\pi} + \frac{e^{25/18}}{\sqrt{2\pi^2}} \cdot \int_0^p \frac{1}{\sqrt{x} \cdot (2x+1)} dx \\
&\leq 1,
\end{aligned}$$

therefore, the second statement of the lemma follows. \square

Now we present the proof of Lemma 1,

Proof of Lemma 1: By invoking Theorem 1.2 of [AKK⁺20], we find that there exists a random sketch $Q^p \in \mathbb{R}^{m \times d^p}$ such that $m = C \cdot \frac{p}{\epsilon^2} \log^3 \frac{1}{\epsilon\delta}$, for some absolute constant C , and for any $y \in \mathbb{R}^{d^p}$,

$$\Pr \left[\|Q^p y\|_2^2 \in (1 \pm \epsilon) \|y\|_2^2 \right] \geq 1 - \delta.$$

This immediately proves the first statement of the lemma.

As shown in [AKK⁺20], the sketch Q^p can be applied to tensor product vectors of the form $v_1 \otimes v_2 \otimes \dots \otimes v_p$ by recursive application of $O(p)$ independent instances of OSNAP transform [NN13] and a novel variant of the SRHT sketch, proposed in [AKK⁺20] called TensorSRHT, on vectors v_i and their sketched versions. The sketch Q^p , as shown in Figure 13, can be represented by a binary tree with p leaves where the leaves are OSNAP sketches and the internal nodes are the TensorSRHT. The use of OSNAP in the leaves of this sketch structure ensures excellent runtime for sketching

sparse input vectors. However, note that if the input vectors are not sparse, i.e., $\text{nnz}(v_i) = \tilde{\Omega}(d)$ for input vectors v_i , then we can simply remove the OSNAP sketches from the leaves of this structure and achieve improved runtime, without hurting the approximation guarantee. Therefore, the sketch Q^p that satisfies the statement of the lemma is exactly the one introduced in [AKK⁺20] for sparse input vectors and for non-sparse inputs is obtained by removing the OSNAP transforms from the leaves of the sketch structure given in Figure 13.

Runtime Analysis: By Theorem 1.2 of [AKK⁺20], for any vector $x \in \mathbb{R}^d$, $Q^p x^{\otimes p}$ can be computed in time $O\left(pm \log m + \frac{p^{3/2}}{\epsilon} \log \frac{1}{\delta} \cdot \text{nnz}(x)\right)$. From the binary tree structure of the sketch, shown in Figure 13, it follows that once we compute $Q^p x^{\otimes p}$, then $Q^p(x^{\otimes p-1} \otimes \mathbf{e}_1)$ can be computed by updating the path from one of the leaves to the root of the binary tree which amounts to applying an instance of OSNAP transform on the \mathbf{e}_1 vector and then applying $O(\log p)$ instances of TensorSRHT on the intermediate nodes of the tree. This can be computed in a total additional runtime of $O(m \log m \log p)$. By this argument, it follows that $Q^p(x^{\otimes p-j} \otimes \mathbf{e}_1^j)$ can be computed sequentially for all $j = 0, 1, 2, \dots, p$ in total time $O\left(pm \log p \log m + \frac{p^{3/2}}{\epsilon} \log \frac{1}{\delta} \cdot \text{nnz}(x)\right)$. By plugging in the value $m = O\left(\frac{p}{\epsilon^2} \log^3 \frac{1}{\epsilon \delta}\right)$, this runtime will be $O\left(\frac{p^2 \log^2 \frac{p}{\epsilon}}{\epsilon^2} \log^3 \frac{1}{\epsilon \delta} + \frac{p^{3/2}}{\epsilon} \log \frac{1}{\delta} \cdot \text{nnz}(x)\right)$, which gives the second statement of the lemma for sparse input vectors x . If x is non-sparse, as we discussed in the above paragraph, we just need to omit the OSNAP transforms from our sketch construction which translates into a runtime of $O\left(\frac{p^2 \log^2 \frac{p}{\epsilon}}{\epsilon^2} \log^3 \frac{1}{\epsilon \delta} + pd \log d\right)$. Therefore, the final runtime bound is $O\left(\frac{p^2 \log^2 \frac{p}{\epsilon}}{\epsilon^2} \log^3 \frac{1}{\epsilon \delta} + \min\left\{\frac{p^{3/2}}{\epsilon} \log \frac{1}{\delta} \cdot \text{nnz}(x), pd \log d\right\}\right)$, which proves the second statement of the lemma.

Furthermore, the sketch Q^p can be applied to tensor product of any collection of p vectors. The time to apply Q^p to the tensor product $v_1 \otimes v_2 \otimes \dots \otimes v_p$ consists of time of applying OSNAP to each of the vectors v_1, v_2, \dots, v_p and time of applying $O(p)$ instances of TensorSRHT to intermediate vectors which are of size m . This runtime can be upper bounded by $O\left(\frac{p^2 \log \frac{p}{\epsilon}}{\epsilon^2} \log^3 \frac{1}{\epsilon \delta} + \frac{p^{3/2}}{\epsilon} d \cdot \log \frac{1}{\delta}\right)$, which proves the third statement of the lemma. \square

For the rest of this section, we need two basic properties of tensor products and direct sums. For vectors x, y, z, w with conforming sizes, the tensor product satisfies the useful property that $\langle x \otimes y, z \otimes w \rangle = \langle x, z \rangle \cdot \langle y, w \rangle$. Also, $\langle x \oplus y, z \oplus w \rangle = \langle x, z \rangle + \langle y, w \rangle$.

Now we are in a position to analyze the invariants that are maintained throughout the execution of NTK Sketch algorithm (Definition 3.2):

Lemma 5 (Invariants of the NTK Sketch algorithm). *For every positive integers d and L , every $\epsilon, \delta > 0$, every vectors $y, z \in \mathbb{R}^d$, if we let $\Sigma_{\text{relu}}^{(h)} : [-1, 1] \rightarrow \mathbb{R}$ and $K_{\text{relu}}^{(h)} : [-1, 1] \rightarrow \mathbb{R}$ be the functions defined in (5) and (7) of Definition 3.1, then with probability at least $1 - \delta$ the following invariants hold for every $h = 0, 1, 2, \dots, L$:*

1. *The mapping $\phi^{(h)}(\cdot)$ computed by the NTK Sketch algorithm in (9) and (10) of Definition 3.2 satisfy*

$$\left| \left\langle \phi^{(h)}(y), \phi^{(h)}(z) \right\rangle - \Sigma_{\text{relu}}^{(h)} \left(\frac{\langle y, z \rangle}{\|y\|_2 \|z\|_2} \right) \right| \leq (h+1) \cdot \frac{\epsilon^2}{60L^3}.$$

2. *The mapping $\psi^{(h)}(\cdot)$ computed by the NTK Sketch algorithm in (12) of Definition 3.2 satisfy*

$$\left| \left\langle \psi^{(h)}(y), \psi^{(h)}(z) \right\rangle - K_{\text{relu}}^{(h)} \left(\frac{\langle y, z \rangle}{\|y\|_2 \|z\|_2} \right) \right| \leq \epsilon \cdot \frac{h^2 + 1}{10L}.$$

Proof. The proof is by induction on the value of $h = 0, 1, 2, \dots, L$. More formally, consider the following statements for every $h = 0, 1, 2, \dots, L$:

P₁(h) :

$$\begin{aligned} \left| \left\langle \phi^{(h)}(y), \phi^{(h)}(z) \right\rangle - \Sigma_{relu}^{(h)} \left(\frac{\langle y, z \rangle}{\|y\|_2 \|z\|_2} \right) \right| &\leq (h+1) \cdot \frac{\epsilon^2}{60L^3}, \\ \left| \left\| \phi^{(h)}(y) \right\|_2^2 - 1 \right| &\leq (h+1) \cdot \frac{\epsilon^2}{60L^3}, \text{ and } \left| \left\| \phi^{(h)}(z) \right\|_2^2 - 1 \right| \leq (h+1) \cdot \frac{\epsilon^2}{60L^3}. \end{aligned}$$

P₂(h) :

$$\begin{aligned} \left| \left\langle \psi^{(h)}(y), \psi^{(h)}(z) \right\rangle - K_{relu}^{(h)} \left(\frac{\langle y, z \rangle}{\|y\|_2 \|z\|_2} \right) \right| &\leq \epsilon \cdot \frac{h^2 + 1}{10L}, \\ \left| \left\| \psi^{(h)}(y) \right\|_2^2 - K_{relu}^{(h)}(1) \right| &\leq \epsilon \cdot \frac{h^2 + 1}{10L}, \text{ and } \left| \left\| \psi^{(h)}(z) \right\|_2^2 - K_{relu}^{(h)}(1) \right| \leq \epsilon \cdot \frac{h^2 + 1}{10L}. \end{aligned}$$

We prove by induction that the following holds,

$$\Pr[P_1(0)] \geq 1 - O(\delta/L), \text{ and } \Pr[P_2(0)|P_1(0)] \geq 1 - O(\delta/L),$$

Additionally, we prove that for every $h = 1, 2, \dots, L$,

$$\Pr[P_1(h)|P_1(h-1)] \geq 1 - O(\delta/L), \text{ and } \Pr[P_2(h)|P_2(h-1), P_1(h), P_1(h-1)] \geq 1 - O(\delta/L).$$

The **base of induction** corresponds to $h = 0$. By (9), $\phi^{(0)}(y) = \frac{1}{\|y\|_2} \cdot S \cdot Q^1 \cdot y$ and $\phi^{(0)}(z) = \frac{1}{\|z\|_2} \cdot S \cdot Q^1 \cdot z$, thus, Lemma 2 implies the following

$$\Pr \left[\left| \left\langle \phi^{(0)}(y), \phi^{(0)}(z) \right\rangle - \frac{1}{\|y\|_2 \|z\|_2} \cdot \langle Q^1 y, Q^1 z \rangle \right| \leq O \left(\epsilon^2 / L^3 \right) \cdot \frac{\|Q^1 y\|_2 \|Q^1 z\|_2}{\|y\|_2 \|z\|_2} \right] \geq 1 - O(\delta/L).$$

By using the above together with Lemma 1 and union bound as well as triangle inequality we find that the following holds,

$$\Pr \left[\left| \left\langle \phi^{(0)}(y), \phi^{(0)}(z) \right\rangle - \frac{\langle y, z \rangle}{\|y\|_2 \|z\|_2} \right| \leq O \left(\epsilon^2 / L^3 \right) \right] \geq 1 - O(\delta/L).$$

Similarly, we can prove

$$\Pr \left[\left| \left\| \phi^{(0)}(y) \right\|_2^2 - 1 \right| \leq O \left(\epsilon^2 / L^3 \right) \right] \geq 1 - O(\delta/L), \text{ and } \Pr \left[\left| \left\| \phi^{(0)}(z) \right\|_2^2 - 1 \right| \leq O \left(\epsilon^2 / L^3 \right) \right] \geq 1 - O(\delta/L).$$

This together with union bound proves the base of induction for statement $P_1(h)$, i.e., $\Pr[P_1(0)] \geq 1 - O(\delta/L)$.

Moreover, by (12), $\psi^{(0)}(y) = V \cdot \phi^{(0)}(y)$ and $\psi^{(0)}(z) = V \cdot \phi^{(0)}(z)$, thus, Lemma 2 implies that,

$$\Pr \left[\left| \left\langle \psi^{(0)}(y), \psi^{(0)}(z) \right\rangle - \left\langle \phi^{(0)}(y), \phi^{(0)}(z) \right\rangle \right| \leq O \left(\epsilon / L \right) \cdot \left\| \phi^{(0)}(y) \right\|_2 \left\| \phi^{(0)}(z) \right\|_2 \right] \geq 1 - O(\delta/L).$$

By conditioninig on $P_1(0)$ and using the above together with triangle inequality it follows that,

$$\Pr \left[\left| \left\langle \psi^{(0)}(y), \psi^{(0)}(z) \right\rangle - K_{relu}^{(0)} \left(\frac{\langle y, z \rangle}{\|y\|_2 \|z\|_2} \right) \right| \leq \frac{\epsilon}{10L} \right] \geq 1 - O(\delta/L).$$

Similarly we can prove that with probability at least $1 - O(\delta/L)$ we have $\left| \left\| \psi^{(0)}(y) \right\|_2^2 - K_{\text{relu}}^{(0)}(1) \right| \leq \frac{\epsilon}{10L}$ and $\left| \left\| \psi^{(0)}(z) \right\|_2^2 - K_{\text{relu}}^{(0)}(1) \right| \leq \frac{\epsilon}{10L}$, which proves the base of induction for the second statement, i.e., $\Pr[P_2(0)|P_1(0)] \geq 1 - O(\delta/L)$. This completes the base of induction.

We proceed by proving the **inductive step**. That is, by assuming the inductive hypothesis for $h-1$, we prove that statements $P_1(h)$ and $P_2(h)$ hold. More precisely, first we condition on the statement $P_1(h-1)$ being true for some $h \geq 1$, and then prove that $P_1(h)$ holds with probability at least $1 - O(\delta/L)$. Next we show that conditioned on statements $P_2(h-1), P_1(h), P_1(h-1)$ being true, $P_2(h)$ holds with probability at least $1 - O(\delta/L)$.

First, note that by Lemma 2 and using (10) we have the following,

$$\Pr \left[\left| \left\langle \phi^{(h)}(y), \phi^{(h)}(z) \right\rangle - \sum_{j=0}^{2q+2} c_j \left\langle Z_j^{(h)}(y), Z_j^{(h)}(z) \right\rangle \right| \leq O \left(\frac{\epsilon^2}{L^3} \right) \cdot A \right] \geq 1 - O(\delta/L), \quad (28)$$

where $A := \sqrt{\sum_{j=0}^{2q+2} c_j \|Z_j^{(h)}(y)\|_2^2} \cdot \sqrt{\sum_{j=0}^{2q+2} c_j \|Z_j^{(h)}(z)\|_2^2}$ and the collection of vectors $\{Z_j^{(h)}(y)\}_{j=0}^{2q+2}$ and $\{Z_j^{(h)}(z)\}_{j=0}^{2q+2}$ and coefficients $c_0, c_1, c_2, \dots, c_{2q+2}$ are defined as per (10). By Lemma 1 together with union bound, the following inequalities hold true simultaneously for all $j \in \{0, 1, 2, \dots, 2q+2\}$, with probability at least $1 - O\left(\frac{\delta}{L}\right)$:

$$\begin{aligned} & \left| \left\langle Z_j^{(h)}(y), Z_j^{(h)}(z) \right\rangle - \left\langle \phi^{(h-1)}(y), \phi^{(h-1)}(z) \right\rangle^j \right| \leq O \left(\frac{\epsilon^2}{L^3} \right) \cdot \left\| \phi^{(h-1)}(y) \right\|_2^j \left\| \phi^{(h-1)}(z) \right\|_2^j \\ & \left\| Z_j^{(h)}(y) \right\|_2^2 \leq \frac{11}{10} \cdot \left\| \phi^{(h-1)}(y) \right\|_2^{2j} \\ & \left\| Z_j^{(h)}(z) \right\|_2^2 \leq \frac{11}{10} \cdot \left\| \phi^{(h-1)}(z) \right\|_2^{2j} \end{aligned} \quad (29)$$

Therefore, by plugging (29) back to (28) and using union bound, triangle inequality and Cauchy–Schwarz inequality we find that,

$$\Pr \left[\left| \left\langle \phi^{(h)}(y), \phi^{(h)}(z) \right\rangle - P_{\text{relu}}^{(q)} \left(\left\langle \phi^{(h-1)}(y), \phi^{(h-1)}(z) \right\rangle \right) \right| \leq O \left(\frac{\epsilon^2}{L^3} \right) \cdot B \right] \geq 1 - O(\delta/L), \quad (30)$$

where $B := \sqrt{P_{\text{relu}}^{(q)}(\|\phi^{(h-1)}(y)\|_2^2) \cdot P_{\text{relu}}^{(q)}(\|\phi^{(h-1)}(z)\|_2^2)}$ and $P_{\text{relu}}^{(q)}(\alpha) = \sum_{j=0}^{2q+2} c_j \cdot \alpha^j$ is the polynomial defined in (8). Using the inductive hypothesis $P_1(h-1)$, we have $\left| \left\| \phi^{(h-1)}(y) \right\|_2^2 - 1 \right| \leq h \cdot \frac{\epsilon^2}{60L^3}$ and $\left| \left\| \phi^{(h-1)}(z) \right\|_2^2 - 1 \right| \leq h \cdot \frac{\epsilon^2}{60L^3}$. Therefore, by Lemma 4 we have $\left| P_{\text{relu}}^{(q)}(\|\phi^{(h-1)}(y)\|_2^2) - P_{\text{relu}}^{(q)}(1) \right| \leq h \cdot \frac{\epsilon^2}{60L^3}$ and $\left| P_{\text{relu}}^{(q)}(\|\phi^{(h-1)}(z)\|_2^2) - P_{\text{relu}}^{(q)}(1) \right| \leq h \cdot \frac{\epsilon^2}{60L^3}$. Consequently, because $P_{\text{relu}}^{(q)}(1) \leq P_{\text{relu}}^{(+\infty)}(1) = 1$, we find that

$$B \leq \frac{11}{10}.$$

By plugging this into (30) we have,

$$\Pr \left[\left| \left\langle \phi^{(h)}(y), \phi^{(h)}(z) \right\rangle - P_{\text{relu}}^{(q)} \left(\left\langle \phi^{(h-1)}(y), \phi^{(h-1)}(z) \right\rangle \right) \right| \leq O \left(\frac{\epsilon^2}{L^3} \right) \right] \geq 1 - O(\delta/L). \quad (31)$$

Furthermore, inductive hypothesis $P_1(h-1)$ implies $\left| \left\langle \phi^{(h-1)}(y), \phi^{(h-1)}(z) \right\rangle - \Sigma_{\text{relu}}^{(h-1)} \left(\frac{\langle y, z \rangle}{\|y\|_2 \|z\|_2} \right) \right| \leq h \cdot \frac{\epsilon^2}{60L^3}$, hence, by invoking Lemma 4 we find that,

$$\left| P_{\text{relu}}^{(q)} \left(\left\langle \phi^{(h-1)}(y), \phi^{(h-1)}(z) \right\rangle \right) - P_{\text{relu}}^{(q)} \left(\Sigma_{\text{relu}}^{(h-1)} \left(\frac{\langle y, z \rangle}{\|y\|_2 \|z\|_2} \right) \right) \right| \leq h \cdot \frac{\epsilon^2}{60L^3}.$$

By incorporating the above inequality into (31) using triangle inequality we find that,

$$\Pr \left[\left| \left\langle \phi^{(h)}(y), \phi^{(h)}(z) \right\rangle - P_{\text{relu}}^{(q)} \left(\Sigma_{\text{relu}}^{(h-1)} \left(\frac{\langle y, z \rangle}{\|y\|_2 \|z\|_2} \right) \right) \right| \leq h \cdot \frac{\epsilon^2}{60L^3} + O \left(\frac{\epsilon^2}{L^3} \right) \right] \geq 1 - O(\delta/L). \quad (32)$$

Now, by invoking Lemma 3 and using the fact that $q = \lceil 2L^2/\epsilon^{4/3} \rceil$ we have,

$$\left| P_{\text{relu}}^{(q)} \left(\Sigma_{\text{relu}}^{(h-1)} \left(\frac{\langle y, z \rangle}{\|y\|_2 \|z\|_2} \right) \right) - k_{\text{relu}} \left(\Sigma_{\text{relu}}^{(h-1)} \left(\frac{\langle y, z \rangle}{\|y\|_2 \|z\|_2} \right) \right) \right| \leq \frac{\epsilon^2}{76L^3}.$$

By combining the above inequality with (32) using triangle inequality and using the fact that $k_{\text{relu}} \left(\Sigma_{\text{relu}}^{(h-1)} \left(\frac{\langle y, z \rangle}{\|y\|_2 \|z\|_2} \right) \right) = \Sigma_{\text{relu}}^{(h)} \left(\frac{\langle y, z \rangle}{\|y\|_2 \|z\|_2} \right)$ (by (5)), we get the following bound,

$$\Pr \left[\left| \left\langle \phi^{(h)}(y), \phi^{(h)}(z) \right\rangle - \Sigma_{\text{relu}}^{(h)} \left(\frac{\langle y, z \rangle}{\|y\|_2 \|z\|_2} \right) \right| \leq (h+1) \cdot \frac{\epsilon^2}{60L^3} \right] \geq 1 - O(\delta/L).$$

Similarly, we can prove that

$$\Pr \left[\left| \left\| \phi^{(h)}(y) \right\|_2^2 - 1 \right| \leq \frac{(h+1) \cdot \epsilon^2}{60L^4} \right] \geq 1 - O \left(\frac{\delta}{L} \right), \text{ and } \Pr \left[\left| \left\| \phi^{(h)}(z) \right\|_2^2 - 1 \right| \leq \frac{(h+1) \cdot \epsilon^2}{60L^3} \right] \geq 1 - O \left(\frac{\delta}{L} \right).$$

This is sufficient to prove the inductive step by union bound, i.e., $\Pr[P_1(h)|P_1(h-1)] \geq 1 - O(\delta/L)$.

Now we prove the inductive step for statement $P_2(h)$, that is, we prove that conditioned on $P_2(h-1), P_1(h), P_1(h-1)$, statement $P_2(h)$ holds with probability at least $1 - O(\delta/L)$. First, note that by Lemma 2 and using (11) we have,

$$\Pr \left[\left| \left\langle \dot{\phi}^{(h)}(y), \dot{\phi}^{(h)}(z) \right\rangle - \sum_{j=0}^{2p+1} b_j \left\langle Y_j^{(h)}(y), Y_j^{(h)}(z) \right\rangle \right| \leq O \left(\frac{\epsilon}{L} \right) \cdot \widehat{A} \right] \geq 1 - O(\delta/L), \quad (33)$$

where $\widehat{A} := \sqrt{\sum_{j=0}^{2p+1} b_j \|Y_j^{(h)}(y)\|_2^2} \cdot \sqrt{\sum_{j=0}^{2p+1} b_j \|Y_j^{(h)}(z)\|_2^2}$ and the collection of vectors $\{Y_j^{(h)}(y)\}_{j=0}^{2p+1}$ and $\{Y_j^{(h)}(z)\}_{j=0}^{2p+1}$ and coefficients $b_0, b_1, b_2, \dots, b_{2p+1}$ are defined as per (11). By invoking Lemma 1 along with union bound, with probability at least $1 - O \left(\frac{\delta}{L} \right)$, the following inequalities hold true simultaneously for all $j \in \{0, 1, 2, \dots, 2p+1\}$

$$\begin{aligned} & \left| \left\langle Y_j^{(h)}(y), Y_j^{(h)}(z) \right\rangle - \left\langle \phi^{(h-1)}(y), \phi^{(h-1)}(z) \right\rangle^j \right| \leq O \left(\frac{\epsilon}{L} \right) \cdot \left\| \phi^{(h-1)}(y) \right\|_2^j \left\| \phi^{(h-1)}(z) \right\|_2^j \\ & \|Y_j^{(h)}(y)\|_2^2 \leq \frac{11}{10} \cdot \left\| \phi^{(h-1)}(y) \right\|_2^{2j} \\ & \|Y_j^{(h)}(z)\|_2^2 \leq \frac{11}{10} \cdot \left\| \phi^{(h-1)}(z) \right\|_2^{2j} \end{aligned} \quad (34)$$

Therefore, by plugging (34) into (33) and using union bound, triangle inequality and Cauchy–Schwarz inequality we find that,

$$\Pr \left[\left| \left\langle \dot{\phi}^{(h)}(y), \dot{\phi}^{(h)}(z) \right\rangle - \dot{P}_{\text{relu}}^{(p)} \left(\left\langle \phi^{(h-1)}(y), \phi^{(h-1)}(z) \right\rangle \right) \right| \leq O \left(\frac{\epsilon}{L} \right) \cdot \widehat{B} \right] \geq 1 - O(\delta/L), \quad (35)$$

where $\widehat{B} := \sqrt{\dot{P}_{\text{relu}}^{(p)}(\|\phi^{(h-1)}(y)\|_2^2) \cdot \dot{P}_{\text{relu}}^{(p)}(\|\phi^{(h-1)}(z)\|_2^2)}$ and $\dot{P}_{\text{relu}}^{(p)}(\alpha) = \sum_{j=0}^{2p+1} b_j \cdot \alpha^j$ is the polynomial defined in (8). By inductive hypothesis $P_1(h-1)$ we have $\left| \left\| \phi^{(h-1)}(y) \right\|_2^2 - 1 \right| \leq h \cdot \frac{\epsilon^2}{60L^3}$ and $\left| \left\| \phi^{(h-1)}(z) \right\|_2^2 - 1 \right| \leq h \cdot \frac{\epsilon^2}{60L^3}$. Therefore, using the fact that $p = \lceil 9L^2/\epsilon^2 \rceil$ and Lemma 4, $\left| \dot{P}_{\text{relu}}^{(p)}(\|\phi^{(h-1)}(y)\|_2^2) - \dot{P}_{\text{relu}}^{(p)}(1) \right| \leq \frac{h\cdot\epsilon}{20L^2}$ and $\left| \dot{P}_{\text{relu}}^{(p)}(\|\phi^{(h-1)}(z)\|_2^2) - \dot{P}_{\text{relu}}^{(p)}(1) \right| \leq \frac{h\cdot\epsilon}{20L^2}$. Consequently, because $\dot{P}_{\text{relu}}^{(p)}(1) \leq \dot{P}_{\text{relu}}^{(+\infty)}(1) = 1$, we find that

$$\widehat{B} \leq \frac{11}{10}.$$

By plugging this into (35) we have,

$$\Pr \left[\left| \left\langle \dot{\phi}^{(h)}(y), \dot{\phi}^{(h)}(z) \right\rangle - \dot{P}_{\text{relu}}^{(p)} \left(\left\langle \phi^{(h-1)}(y), \phi^{(h-1)}(z) \right\rangle \right) \right| \leq O \left(\frac{\epsilon}{L} \right) \right] \geq 1 - O(\delta/L). \quad (36)$$

Furthermore, inductive hypothesis $P_1(h-1)$ implies $\left| \left\langle \phi^{(h-1)}(y), \phi^{(h-1)}(z) \right\rangle - \Sigma_{\text{relu}}^{(h-1)} \left(\frac{\langle y, z \rangle}{\|y\|_2 \|z\|_2} \right) \right| \leq h \cdot \frac{\epsilon^2}{60L^3}$, hence, by invoking Lemma 4 we find that,

$$\left| \dot{P}_{\text{relu}}^{(p)} \left(\left\langle \phi^{(h-1)}(y), \phi^{(h-1)}(z) \right\rangle \right) - \dot{P}_{\text{relu}}^{(p)} \left(\Sigma_{\text{relu}}^{(h-1)} \left(\frac{\langle y, z \rangle}{\|y\|_2 \|z\|_2} \right) \right) \right| \leq \frac{h \cdot \epsilon}{20L^2}.$$

By plugging the above inequality into (36) using triangle inequality we find that,

$$\Pr \left[\left| \left\langle \dot{\phi}^{(h)}(y), \dot{\phi}^{(h)}(z) \right\rangle - \dot{P}_{\text{relu}}^{(p)} \left(\Sigma_{\text{relu}}^{(h-1)} \left(\frac{\langle y, z \rangle}{\|y\|_2 \|z\|_2} \right) \right) \right| \leq \frac{h \cdot \epsilon}{20L^2} + O \left(\frac{\epsilon}{L} \right) \right] \geq 1 - O(\delta/L). \quad (37)$$

Now, by invoking Lemma 3 and using the fact that $p = \lceil 9L^2/\epsilon^2 \rceil$ we have,

$$\left| \dot{P}_{\text{relu}}^{(p)} \left(\Sigma_{\text{relu}}^{(h-1)} \left(\frac{\langle y, z \rangle}{\|y\|_2 \|z\|_2} \right) \right) - \dot{k}_{\text{relu}} \left(\Sigma_{\text{relu}}^{(h-1)} \left(\frac{\langle y, z \rangle}{\|y\|_2 \|z\|_2} \right) \right) \right| \leq \frac{\epsilon}{15L}.$$

By combining the above inequality with (37) using triangle inequality and using the fact that $\dot{k}_{\text{relu}} \left(\Sigma_{\text{relu}}^{(h-1)} \left(\frac{\langle y, z \rangle}{\|y\|_2 \|z\|_2} \right) \right) = \dot{\Sigma}_{\text{relu}}^{(h)} \left(\frac{\langle y, z \rangle}{\|y\|_2 \|z\|_2} \right)$ (by (6)) we get the following bound,

$$\Pr \left[\left| \left\langle \dot{\phi}^{(h)}(y), \dot{\phi}^{(h)}(z) \right\rangle - \dot{\Sigma}_{\text{relu}}^{(h)} \left(\frac{\langle y, z \rangle}{\|y\|_2 \|z\|_2} \right) \right| \leq \frac{\epsilon}{8L} \right] \geq 1 - O(\delta/L). \quad (38)$$

Similarly we can show that,

$$\begin{aligned} \Pr \left[\left| \left\| \dot{\phi}^{(h)}(y) \right\| - 1 \right| \leq \frac{\epsilon}{8L} \right] &\geq 1 - O(\delta/L), \\ \Pr \left[\left| \left\| \dot{\phi}^{(h)}(z) \right\| - 1 \right| \leq \frac{\epsilon}{8L} \right] &\geq 1 - O(\delta/L). \end{aligned} \quad (39)$$

If we let $f := \psi^{(h-1)}(y) \otimes \dot{\phi}^{(h)}(y)$ and $g := \psi^{(h-1)}(z) \otimes \dot{\phi}^{(h)}(z)$, then by Lemma 2 and using (12) we have the following,

$$\Pr \left[\left| \left\langle \psi^{(h)}(y), \psi^{(h)}(z) \right\rangle - \left\langle Q^2 f \oplus \phi^{(h)}(y), Q^2 g \oplus \phi^{(h)}(z) \right\rangle \right| \leq O(\epsilon/L) \cdot D \right] \geq 1 - O(\delta/L), \quad (40)$$

where $D := \left\| Q^2 f \oplus \phi^{(h)}(y) \right\|_2 \left\| Q^2 g \oplus \phi^{(h)}(z) \right\|_2$. By the fact that we conditioned on $P_1(h)$, we have,

$$D \leq \sqrt{\|Q^2 f\|_2^2 + \frac{11}{10}} \cdot \sqrt{\|Q^2 g\|_2^2 + \frac{11}{10}}.$$

By Lemma 1, we can further upper bound the above as follows,

$$D \leq \frac{11}{10} \cdot \sqrt{\|f\|_2^2 + 1} \cdot \sqrt{\|g\|_2^2 + 1}.$$

Now note that because we conditioned on $P_2(h-1)$ and using (39), with probability at least $1 - O(\delta/L)$ the following holds:

$$\|f\|_2^2 = \left\| \psi^{(h-1)}(y) \right\|_2^2 \left\| \dot{\phi}^{(h)}(y) \right\|_2^2 \leq \frac{11}{10} \cdot K_{relu}^{(h-1)}(1) = 11h/10.$$

Similarly, $\|g\|_2^2 \leq 11h/10$ with probability at least $1 - O(\delta/L)$, thus, by union bound:

$$\Pr[D \leq 2(h+1) | P_2(h-1), P_1(h), P_1(h-1)] \geq 1 - O(\delta/L).$$

Therefore, by combining the above with (40) via union bound we find that,

$$\Pr \left[\left| \left\langle \psi^{(h)}(y), \psi^{(h)}(z) \right\rangle - \left\langle Q^2 f \oplus \phi^{(h)}(y), Q^2 g \oplus \phi^{(h)}(z) \right\rangle \right| \leq O(\epsilon h/L) \right] \geq 1 - O(\delta/L), \quad (41)$$

Now note that $\left\langle Q^2 f \oplus \phi^{(h)}(y), Q^2 g \oplus \phi^{(h)}(z) \right\rangle = \langle Q^2 f, Q^2 g \rangle + \left\langle \phi^{(h)}(y), \phi^{(h)}(z) \right\rangle$. We proceed by bounding the term $|\langle Q^2 f, Q^2 g \rangle - \langle f, g \rangle|$ using Lemma 1, as follows,

$$\Pr \left[\left| \langle Q^2 f, Q^2 g \rangle - \langle f, g \rangle \right| \leq O(\epsilon/L) \cdot \|f\|_2 \|g\|_2 \right] \geq 1 - O(\delta/L).$$

We proved that conditioned on $P_2(h-1)$ and $P_1(h-1)$, $\|f\|_2^2 \leq 11h/10$ and $\|g\|_2^2 \leq 11h/10$ with probability at least $1 - O(\delta/L)$. Hence, by union bound we find that,

$$\Pr \left[\left| \langle Q^2 f, Q^2 g \rangle - \langle f, g \rangle \right| \leq O(\epsilon h/L) \middle| P_2(h-1), P_1(h-1) \right] \geq 1 - O(\delta/L). \quad (42)$$

Note that $\langle f, g \rangle = \left\langle \psi^{(h-1)}(y), \psi^{(h-1)}(z) \right\rangle \cdot \left\langle \dot{\phi}^{(h)}(y), \dot{\phi}^{(h)}(z) \right\rangle$, thus by conditioning on inductive hypothesis $P_2(h-1)$ and (38) we have,

$$\left| \langle f, g \rangle - K_{relu}^{(h-1)} \left(\frac{\langle y, z \rangle}{\|y\|_2 \|z\|_2} \right) \cdot \dot{\Sigma}_{relu}^{(h)} \left(\frac{\langle y, z \rangle}{\|y\|_2 \|z\|_2} \right) \right| \leq \frac{\epsilon}{8L} \cdot \left(h + \epsilon \cdot \frac{(h-1)^2 + 1}{10L} \right) + \epsilon \cdot \frac{(h-1)^2 + 1}{10L}$$

By combining the above inequality, (42), $P_1(h)$, and (41) using triangle inequality and union bound we get the following inequality,

$$\Pr \left[\left| \left\langle \psi^{(h)}(y), \psi^{(h)}(z) \right\rangle - K_{relu}^{(h-1)} \left(\frac{\langle y, z \rangle}{\|y\|_2 \|z\|_2} \right) \cdot \dot{\Sigma}_{relu}^{(h)} \left(\frac{\langle y, z \rangle}{\|y\|_2 \|z\|_2} \right) - \Sigma_{relu}^{(h)} \left(\frac{\langle y, z \rangle}{\|y\|_2 \|z\|_2} \right) \right| \leq \epsilon \cdot \frac{h^2 + 1}{10L} \right] \geq 1 - O(\delta/L).$$

By noting that $K_{relu}^{(h-1)}(\cdot) \cdot \dot{\Sigma}_{relu}^{(h)}(\cdot) + \Sigma_{relu}^{(h)}(\cdot) = K_{relu}^{(h)}(\cdot)$ (see (7)) we have indeed proved that

$$\Pr \left[\left| \left\langle \psi^{(h)}(y), \psi^{(h)}(z) \right\rangle - K_{relu}^{(h)} \left(\frac{\langle y, z \rangle}{\|y\|_2 \|z\|_2} \right) \right| \leq \epsilon \cdot \frac{h^2 + 1}{10L} \right] \geq 1 - O(\delta/L).$$

Similarly we can prove the following inequalities hold with probability at least $1 - O(\delta/L)$,

$$\left| \left\| \psi^{(h)}(y) \right\|_2^2 - K_{\text{relu}}^{(h)}(1) \right| \leq \epsilon \cdot \frac{h^2 + 1}{10L}, \text{ and } \left| \left\| \psi^{(h)}(z) \right\|_2^2 - K_{\text{relu}}^{(h)}(1) \right| \leq \epsilon \cdot \frac{h^2 + 1}{10L}.$$

This proves the inductive step for the statement $P_2(h)$ follows, i.e.,

$$\Pr[P_2(h) | P_2(h-1), P_1(h), P_1(h-1)] \geq 1 - O(\delta/L).$$

Therefore, by union bounding over all $h = 0, 1, 2, \dots, L$, it follows that the statements of the lemma hold simultaneously for all h with probability at least $1 - \delta$, which completes the proof. \square

We now analyze the runtime of the NTK Sketch algorithm:

Lemma 6 (Runtime of the NTK Sketch). *For every positive integers d and L , every $\epsilon, \delta > 0$, every vector $x \in \mathbb{R}^d$, the time to compute the NTK sketch $\Psi_{\text{ntk}}^{(L)}(x) \in \mathbb{R}^{s^*}$, for $s^* = O\left(\frac{1}{\epsilon^2} \cdot \log \frac{1}{\delta}\right)$, using the procedure given in Definition 3.2 is bounded by,*

$$O\left(\frac{L^{11}}{\epsilon^7} \cdot \log^3 \frac{L}{\epsilon\delta} + \frac{L^3}{\epsilon^2} \cdot \log \frac{L}{\epsilon\delta} \cdot \text{nnz}(x)\right).$$

Proof. There are three main components to the runtime of this procedure that we have to account for. The first is the time to apply the sketch Q^1 to x in (9). By Lemma 1, the runtime of computing $Q^1 \cdot x$ is $O\left(\frac{L^6}{\epsilon^4} \cdot \log^3 \frac{L}{\epsilon\delta} + \frac{L^3}{\epsilon^2} \cdot \log \frac{L}{\epsilon\delta} \cdot \text{nnz}(x)\right)$. The second heavy operation corresponds to computing vectors $Z_j^{(h)}(x) = Q^{2q+2} \cdot \left(\left[\phi^{(h-1)}(x)\right]^{\otimes j} \otimes \mathbf{e}_1^{\otimes 2q+2-j}\right)$ for $j = 0, 1, 2, \dots, 2q+2$ and $h = 1, 2, \dots, L$ in (10). By Lemma 1, the time to compute $Z_j^{(h)}(x)$ for a fixed h and all $j = 0, 1, 2, \dots, 2q+2$ is bounded by,

$$O\left(L^{10}/\epsilon^{20/3} \cdot \log^2(L/\epsilon) \log^3 \frac{L}{\epsilon\delta} + L^8/\epsilon^{16/3} \cdot \log^3 \frac{L}{\epsilon\delta}\right) = O\left(\frac{L^{10}}{\epsilon^7} \cdot \log^3 \frac{L}{\epsilon\delta}\right).$$

The total time to compute vectors $Z_j^{(h)}(x)$ for all $h = 1, 2, \dots, L$ and all $j = 0, 1, 2, \dots, 2q+2$ is thus $O\left(\frac{L^{11}}{\epsilon^7} \cdot \log^3 \frac{L}{\epsilon\delta}\right)$. Finally, the last computationally expensive operation is computing vectors $Y_j^{(h)}(x) = Q^{2p+1} \cdot \left(\left[\phi^{(h-1)}(x)\right]^{\otimes j} \otimes \mathbf{e}_1^{\otimes 2p+1-j}\right)$ for $j = 0, 1, 2, \dots, 2p+1$ and $h = 1, 2, \dots, L$ in (11). By Lemma 1, the runtime of computing $Y_j^{(h)}(x)$ for a fixed h and all $j = 0, 1, 2, \dots, 2p+1$ is bounded by,

$$O\left(\frac{L^6}{\epsilon^6} \cdot \log^2(L/\epsilon) \log^3 \frac{L}{\epsilon\delta} + \frac{L^8}{\epsilon^6} \cdot \log^3 \frac{L}{\epsilon\delta}\right) = O\left(\frac{L^8}{\epsilon^6} \cdot \log^3 \frac{L}{\epsilon\delta}\right).$$

Hence, the total time to compute vectors $Y_j^{(h)}(x)$ for all $h = 1, 2, \dots, L$ and all $j = 0, 1, 2, \dots, 2p+1$ is $O\left(\frac{L^9}{\epsilon^6} \cdot \log^3 \frac{L}{\epsilon\delta}\right)$. The total runtime of the NTK Sketch is obtained by summing up these three contributions. \square

Now we are ready to prove the main theorem on the NTK Sketch,

Proof of Theorem 2: Let $\psi^{(L)} : \mathbb{R}^d \rightarrow \mathbb{R}^s$ for $s = O\left(\frac{L^4}{\epsilon^2} \cdot \log^2 \frac{L}{\epsilon\delta}\right)$ be the mapping defined in (12) of Definition 3.2. By (13), the NTK Sketch $\Psi_{ntk}^{(L)}(x)$ is defined as

$$\Psi_{ntk}^{(L)}(x) := \|x\|_2 \cdot G \cdot \psi^{(L)}(x).$$

Because G is a matrix of i.i.d normal entries with $s^* = C \cdot \frac{1}{\epsilon^2} \cdot \log \frac{1}{\delta}$ rows for large enough constant C , by [DG03], G is a JL transform and hence $\Psi_{ntk}^{(L)}$ satisfies the following,

$$\Pr \left[\left| \left\langle \Psi_{ntk}^{(L)}(y), \Psi_{ntk}^{(L)}(z) \right\rangle - \|y\|_2 \|z\|_2 \cdot \left\langle \psi^{(L)}(y), \psi^{(L)}(z) \right\rangle \right| \leq O(\epsilon) \cdot A \right] \geq 1 - O(\delta),$$

where $A := \|y\|_2 \|z\|_2 \left\| \psi^{(L)}(y) \right\|_2 \left\| \psi^{(L)}(z) \right\|_2$. By Lemma 5 and using the fact that $K_{relu}^{(L)}(1) = L + 1$, the following bounds hold with probability at least $1 - O(\delta)$:

$$\left\| \psi^{(L)}(y) \right\|_2^2 \leq \frac{11}{10} \cdot (L + 1), \text{ and } \left\| \psi^{(L)}(z) \right\|_2^2 \leq \frac{11}{10} \cdot (L + 1).$$

Therefore, by union bound we find that,

$$\Pr \left[\left| \left\langle \Psi_{ntk}^{(L)}(y), \Psi_{ntk}^{(L)}(z) \right\rangle - \|y\|_2 \|z\|_2 \cdot \left\langle \psi^{(L)}(y), \psi^{(L)}(z) \right\rangle \right| \leq O(\epsilon L) \cdot \|y\|_2 \|z\|_2 \right] \geq 1 - O(\delta).$$

Additionally, by Lemma 5, the following holds with probability at least $1 - O(\delta)$:

$$\left| \left\langle \psi^{(L)}(y), \psi^{(L)}(z) \right\rangle - K_{relu}^{(L)} \left(\frac{\langle y, z \rangle}{\|y\|_2 \|z\|_2} \right) \right| \leq \frac{\epsilon(L + 1)}{10}.$$

Hence by union bound and triangle inequality we have,

$$\Pr \left[\left| \left\langle \Psi_{ntk}^{(L)}(y), \Psi_{ntk}^{(L)}(z) \right\rangle - \|y\|_2 \|z\|_2 \cdot K_{relu}^{(L)} \left(\frac{\langle y, z \rangle}{\|y\|_2 \|z\|_2} \right) \right| \leq \frac{\epsilon(L + 1)}{9} \cdot \|y\|_2 \|z\|_2 \right] \geq 1 - O(\delta).$$

Now note that by Theorem 1, $\|y\|_2 \|z\|_2 \cdot K_{relu}^{(L)} \left(\frac{\langle y, z \rangle}{\|y\|_2 \|z\|_2} \right) = \Theta_{ntk}^{(L)}(y, z)$, and also note that for every $L \geq 3$ and any $\alpha \in [-1, 1]$, $K_{relu}^{(L)}(\alpha) \geq (L + 1)/9$, therefore,

$$\Pr \left[\left| \left\langle \Psi_{ntk}^{(L)}(y), \Psi_{ntk}^{(L)}(z) \right\rangle - \Theta_{ntk}^{(L)}(y, z) \right| \leq \epsilon \cdot \Theta_{ntk}^{(L)}(y, z) \right] \geq 1 - \delta.$$

Remark on the fact that $K_{relu}^{(L)}(\alpha) \geq (L + 1)/9$ for every $L \geq 2$ and any $\alpha \in [-1, 1]$.
Note that from the definition of $\Sigma_{relu}^{(h)}$ in (5), we have that for any $\alpha \in [-1, 1]$: $\Sigma_{relu}^{(0)}(\alpha) \geq -1$, $\Sigma_{relu}^{(1)}(\alpha) \geq 0$, $\Sigma_{relu}^{(2)}(\alpha) \geq \frac{1}{\pi}$, and $\Sigma_{relu}^{(h)}(\alpha) \geq \frac{1}{2}$ for every $h \geq 3$ because $\kappa_1(\cdot)$ is a monotonically increasing function on the interval $[-1, 1]$. Moreover, using the definition of $\dot{\Sigma}_{relu}^{(h)}$ in (6), we have that for any $\alpha \in [-1, 1]$: $\dot{\Sigma}_{relu}^{(1)}(\alpha) \geq 0$, $\dot{\Sigma}_{relu}^{(2)}(\alpha) \geq \frac{1}{2}$, and $\dot{\Sigma}_{relu}^{(h)}(\alpha) \geq \frac{3}{5}$ for every $h \geq 3$ because $\kappa_1(\cdot)$ is a monotonically increasing function on the interval $[-1, 1]$. By an inductive proof and using the definition of $K_{relu}^{(L)}$ in (7), we can show that $K_{relu}^{(L)}(\alpha) \geq (L + 1)/9$ for every $L \geq 2$ and any $\alpha \in [-1, 1]$

Runtime: By Lemma 6, time to compute the NTK Sketch is $O\left(\frac{L^{11}}{\epsilon^7} \log^3 \frac{L}{\epsilon\delta} + \frac{L^3}{\epsilon^2} \log \frac{L}{\epsilon\delta} \cdot \text{nnz}(x)\right)$.

□

D CNTK's Dynamic Program

In this section we restate the DP proposed in [ADH⁺19b] for computing the L -layered CNTK kernel corresponding to an arbitrary activation function $\sigma : \mathbb{R} \rightarrow \mathbb{R}$ and convolutional filters of size $q \times q$, with global average pooling (GAP):

1. Let $y, z \in \mathbb{R}^{d_1 \times d_2 \times c}$ be two input images, where c is the number of channels ($c = 3$ for standard color images). Define $\Gamma^{(0)} : \mathbb{R}^{d_1 \times d_2 \times c} \times \mathbb{R}^{d_1 \times d_2 \times c} \rightarrow \mathbb{R}^{d_1 \times d_2 \times d_1 \times d_2}$ and $\Sigma^{(0)} : \mathbb{R}^{d_1 \times d_2 \times c} \times \mathbb{R}^{d_1 \times d_2 \times c} \rightarrow \mathbb{R}^{d_1 \times d_2 \times d_1 \times d_2}$ as follows for every $i, i' \in [d_1]$ and $j, j' \in [d_2]$:

$$\Gamma^{(0)}(y, z) := \sum_{l=1}^c y_{(:, :, l)} \otimes z_{(:, :, l)}, \text{ and } \Sigma_{i, j, i', j'}^{(0)}(y, z) := \sum_{a=-\frac{q-1}{2}}^{\frac{q-1}{2}} \sum_{b=-\frac{q-1}{2}}^{\frac{q-1}{2}} \Gamma_{i+a, j+b, i'+a, j'+b}^{(0)}(y, z). \quad (43)$$

2. For every layer $h = 1, 2, \dots, L$ of the network and every $i, i' \in [d_1]$ and $j, j' \in [d_2]$, define $\Gamma^{(h)} : \mathbb{R}^{d_1 \times d_2 \times c} \times \mathbb{R}^{d_1 \times d_2 \times c} \rightarrow \mathbb{R}^{d_1 \times d_2 \times d_1 \times d_2}$ recursively as:

$$\begin{aligned} \Lambda_{i, j, i', j'}^{(h)}(y, z) &:= \begin{pmatrix} \Sigma_{i, j, i, j}^{(h-1)}(y, y) & \Sigma_{i, j, i', j'}^{(h-1)}(y, z) \\ \Sigma_{i', j', i, j}^{(h-1)}(z, y) & \Sigma_{i', j', i', j'}^{(h-1)}(z, z) \end{pmatrix}, \\ \Gamma_{i, j, i', j'}^{(h)}(y, z) &:= \frac{1}{q^2 \cdot \mathbb{E}_{w \sim \mathcal{N}(0, 1)} [|\sigma(w)|^2]} \cdot \mathbb{E}_{(u, v) \sim \mathcal{N}\left(0, \Lambda_{i, j, i', j'}^{(h)}(y, z)\right)} [\sigma(u) \cdot \sigma(v)], \\ \Sigma_{i, j, i', j'}^{(h)}(y, z) &:= \sum_{a=-\frac{q-1}{2}}^{\frac{q-1}{2}} \sum_{b=-\frac{q-1}{2}}^{\frac{q-1}{2}} \Gamma_{i+a, j+b, i'+a, j'+b}^{(h)}(y, z), \end{aligned} \quad (44)$$

3. For every $h = 1, 2, \dots, L$, every $i, i' \in [d_1]$ and $j, j' \in [d_2]$, define $\dot{\Gamma}^{(h)}(y, z) \in \mathbb{R}^{d_1 \times d_2 \times d_1 \times d_2}$ as:

$$\dot{\Gamma}_{i, j, i', j'}^{(h)}(y, z) := \frac{1}{q^2 \cdot \mathbb{E}_{w \sim \mathcal{N}(0, 1)} [|\sigma(w)|^2]} \cdot \mathbb{E}_{(u, v) \sim \mathcal{N}\left(0, \Lambda_{i, j, i', j'}^{(h)}(y, z)\right)} [\dot{\sigma}(u) \cdot \dot{\sigma}(v)]. \quad (45)$$

4. Let $\Pi^{(0)}(y, z) := 0$ and for every $h = 1, 2, \dots, L-1$, every $i, i' \in [d_1]$ and $j, j' \in [d_2]$, define $\Pi^{(h)} : \mathbb{R}^{d_1 \times d_2 \times c} \times \mathbb{R}^{d_1 \times d_2 \times c} \rightarrow \mathbb{R}^{d_1 \times d_2 \times d_1 \times d_2}$ recursively as:

$$\Pi_{i, j, i', j'}^{(h)}(y, z) := \sum_{a=-\frac{q-1}{2}}^{\frac{q-1}{2}} \sum_{b=-\frac{q-1}{2}}^{\frac{q-1}{2}} [\Pi^{(h-1)}(y, z) \odot \dot{\Gamma}^{(h)}(y, z) + \Gamma^{(h)}(y, z)]_{i+a, j+b, i'+a, j'+b}, \quad (46)$$

also let $\Pi^{(L)}(y, z) := \Pi^{(L-1)}(y, z) \odot \dot{\Gamma}^{(L)}(y, z)$.

5. The final CNTK expressions is defined as:

$$\Theta_{cntk}^{(L)}(y, z) := \frac{1}{d_1^2 d_2^2} \cdot \sum_{i, i' \in [d_1]} \sum_{j, j' \in [d_2]} \Pi_{i, j, i', j'}^{(L)}(y, z). \quad (47)$$

E ReLU-CNTK Expression

In this section we prove that Definition 4.1 computes the CNTK kernel function corresponding to ReLU activation and additionally, we present useful corollaries and consequences of this fact.

Lemma 7. For every positive integers d_1, d_2, c , odd integer q , and every integer $h \geq 0$, if the activation function is ReLU $\sigma(\alpha) = \max(\alpha, 0)$, then the tensor covariances $\Gamma^{(h)}, \dot{\Gamma}^{(h)}(y, z) : \mathbb{R}^{d_1 \times d_2 \times c} \times \mathbb{R}^{d_1 \times d_2 \times c} \rightarrow \mathbb{R}^{d_1 \times d_2 \times d_1 \times d_2}$ defined in (44) and (45), are precisely equal to the tensor covariances defined in (15) and (16) of Definition 4.1, respectively.

Proof. To prove the lemma, we first show by induction on $h = 1, 2, \dots$ that $N_{i,j}^{(h)}(x) \equiv \Sigma_{i,j,i,j}^{(h-1)}(x, x)$ for every $x \in \mathbb{R}^{d_1 \times d_2 \times c}$ and every $i \in [d_1]$ and $j \in [d_2]$, where $\Sigma^{(h-1)}(x, x)$ is defined as per (43) and (44). The **base of induction** trivially holds for $h = 1$ because by definition of $N^{(1)}(x)$ and (43) we have,

$$N_{i,j}^{(1)}(x) = \sum_{a=-\frac{q-1}{2}}^{\frac{q-1}{2}} \sum_{b=-\frac{q-1}{2}}^{\frac{q-1}{2}} \sum_{l=1}^c |x_{i+a,j+b,l}|^2 \equiv \Sigma_{i,j,i,j}^{(0)}(x, x).$$

To prove the **inductive step**, suppose that the inductive hypothesis $N_{i,j}^{(h-1)}(x) = \Sigma_{i,j,i,j}^{(h-1)}(x, x)$ holds for some $h \geq 2$. Now we show that conditioned on the inductive hypothesis, the inductive claim holds. By (44), we have,

$$\begin{aligned} \Sigma_{i,j,i,j}^{(h-1)}(x, x) &= \sum_{a=-\frac{q-1}{2}}^{\frac{q-1}{2}} \sum_{b=-\frac{q-1}{2}}^{\frac{q-1}{2}} \Gamma_{i+a,j+b,i+a,j+b}^{(h-1)}(x, x) \\ &= \sum_{a=-\frac{q-1}{2}}^{\frac{q-1}{2}} \sum_{b=-\frac{q-1}{2}}^{\frac{q-1}{2}} \frac{1}{q^2 \cdot \mathbb{E}_{w \sim \mathcal{N}(0,1)} [|\sigma(w)|^2]} \cdot \mathbb{E}_{(u,v) \sim \mathcal{N}\left(0, \Lambda_{i+a,j+b,i+a,j+b}^{(h-1)}(x, x)\right)} [\sigma(u) \cdot \sigma(v)] \\ &= \sum_{a=-\frac{q-1}{2}}^{\frac{q-1}{2}} \sum_{b=-\frac{q-1}{2}}^{\frac{q-1}{2}} \frac{1}{q^2 \cdot \mathbb{E}_{w \sim \mathcal{N}(0,1)} [|\max(0, w)|^2]} \cdot \mathbb{E}_{u \sim \mathcal{N}\left(0, \Sigma_{i+a,j+b,i+a,j+b}^{(h-2)}(x, x)\right)} [|\max(0, u)|^2] \\ &= \sum_{a=-\frac{q-1}{2}}^{\frac{q-1}{2}} \sum_{b=-\frac{q-1}{2}}^{\frac{q-1}{2}} \frac{1}{q^2} \cdot \Sigma_{i+a,j+b,i+a,j+b}^{(h-2)}(x, x) \\ &= \sum_{a=-\frac{q-1}{2}}^{\frac{q-1}{2}} \sum_{b=-\frac{q-1}{2}}^{\frac{q-1}{2}} \frac{1}{q^2} \cdot N_{i+a,j+b}^{(h-1)}(x) \equiv N_{i,j}^{(h)}(x). \end{aligned} \tag{by (14)}$$

Therefore, this proves that $N_{i,j}^{(h)}(x) \equiv \Sigma_{i,j,i,j}^{(h-1)}(x, x)$ for every x and every integer $h \geq 1$.

Now, note that the 2×2 covariance matrix $\Lambda_{i,j,i',j'}^{(h)}(y, z)$, defined in (44), can be decomposed as $\Lambda_{i,j,i',j'}^{(h)}(y, z) = \begin{pmatrix} f^\top \\ g^\top \end{pmatrix} \cdot \begin{pmatrix} f & g \end{pmatrix}$, where $f, g \in \mathbb{R}^2$. Also note that $\|f\|_2^2 = \Sigma_{i,j,i,j}^{(h-1)}(y, y)$ and $\|g\|_2^2 = \Sigma_{i',j',i',j'}^{(h-1)}(z, z)$, hence, by what we proved above, we have,

$$\|f\|_2^2 = N_{i,j}^{(h)}(y), \text{ and } \|g\|_2^2 = N_{i',j'}^{(h)}(z).$$

Therefore, by Claim 1, we can write:

$$\begin{aligned}
\Gamma_{i,j,i',j'}^{(h)}(y, z) &= \frac{1}{q^2 \cdot \mathbb{E}_{w \sim \mathcal{N}(0,1)} [|\sigma(w)|^2]} \cdot \mathbb{E}_{(u,v) \sim \mathcal{N}\left(0, \Lambda_{i,j,i',j'}^{(h)}(y, z)\right)} [\sigma(u) \cdot \sigma(v)] \\
&= \frac{1}{q^2 \cdot \mathbb{E}_{w \sim \mathcal{N}(0,1)} [|\sigma(w)|^2]} \cdot \mathbb{E}_{u \sim \mathcal{N}(0, I_d)} [\sigma(u^\top f) \cdot \sigma(u^\top g)] \\
&= \frac{2 \cdot \|f\|_2 \cdot \|g\|_2}{q^2 \cdot \kappa_1(1)} \cdot \frac{1}{2} \cdot \kappa_1 \left(\frac{\langle f, g \rangle}{\|f\|_2 \cdot \|g\|_2} \right) \\
&= \frac{\sqrt{N_{i,j}^{(h)}(y) \cdot N_{i',j'}^{(h)}(z)}}{q^2} \cdot \kappa_1 \left(\frac{\Sigma_{i,j,i',j'}^{(h-1)}(y, z)}{\sqrt{N_{i,j}^{(h)}(y) \cdot N_{i',j'}^{(h)}(z)}} \right) \\
&= \frac{\sqrt{N_{i,j}^{(h)}(y) \cdot N_{i',j'}^{(h)}(z)}}{q^2} \cdot \kappa_1 \left(\frac{\sum_{a=-\frac{q-1}{2}}^{\frac{q-1}{2}} \sum_{b=-\frac{q-1}{2}}^{\frac{q-1}{2}} \Gamma_{i+a,j+b,i'+a,j'+b}^{(h-1)}(y, z)}{\sqrt{N_{i,j}^{(h)}(y) \cdot N_{i',j'}^{(h)}(z)}} \right),
\end{aligned}$$

where the third line follows from Claim 1 and fourth line follows because we have $\langle f, g \rangle = \Sigma_{i,j,i',j'}^{(h-1)}(y, z)$. The fifth line above follows from (44). This proves the equivalence between the tensor covariance defined in (44) and the one defined in (15) of Definition 4.1. Similarly, by using Claim 1, we can prove the statement of the lemma about $\dot{\Gamma}_{i,j,i',j'}^{(h)}(y, z)$ as follows,

$$\begin{aligned}
\dot{\Gamma}_{i,j,i',j'}^{(h)}(y, z) &= \frac{1}{q^2 \cdot \mathbb{E}_{w \sim \mathcal{N}(0,1)} [|\sigma(w)|^2]} \cdot \mathbb{E}_{(u,v) \sim \mathcal{N}\left(0, \Lambda_{i,j,i',j'}^{(h)}(y, z)\right)} [\dot{\sigma}(u) \cdot \dot{\sigma}(v)] \\
&= \frac{1}{q^2 \cdot \mathbb{E}_{w \sim \mathcal{N}(0,1)} [|\sigma(w)|^2]} \cdot \mathbb{E}_{u \sim \mathcal{N}(0, I_d)} [\dot{\sigma}(u^\top f) \cdot \dot{\sigma}(u^\top g)] \\
&= \frac{2}{q^2 \cdot \kappa_1(1)} \cdot \frac{1}{2} \cdot \kappa_0 \left(\frac{\langle f, g \rangle}{\|f\|_2 \cdot \|g\|_2} \right) \\
&= \frac{1}{q^2} \cdot \kappa_0 \left(\frac{\Sigma_{i,j,i',j'}^{(h-1)}(y, z)}{\sqrt{N_{i,j}^{(h)}(y) \cdot N_{i',j'}^{(h)}(z)}} \right) \\
&= \frac{1}{q^2} \cdot \kappa_0 \left(\frac{\sum_{a=-\frac{q-1}{2}}^{\frac{q-1}{2}} \sum_{b=-\frac{q-1}{2}}^{\frac{q-1}{2}} \Gamma_{i+a,j+b,i'+a,j'+b}^{(h-1)}(y, z)}{\sqrt{N_{i,j}^{(h)}(y) \cdot N_{i',j'}^{(h)}(z)}} \right),
\end{aligned}$$

□

Corollary 2 (Consequence of Lemma 7). *Consider the preconditions of Lemma 7. For every $x \in \mathbb{R}^{d_1 \times d_2 \times c}$, $N_{i,j}^{(h)}(x) \equiv \sum_{a=-\frac{q-1}{2}}^{\frac{q-1}{2}} \sum_{b=-\frac{q-1}{2}}^{\frac{q-1}{2}} \Gamma_{i+a,j+b,i+a,j+b}^{(h-1)}(x, x)$.*

We describes some of the basic properties of the function $\Gamma^{(h)}(y, z)$ defined in (15) in the following lemma,

Lemma 8 (Properties of $\Gamma^{(h)}(y, z)$). *For every images $y, z \in \mathbb{R}^{d_1 \times d_2 \times c}$, every integer $h \geq 0$ and every $i, i' \in [d_1]$ and $j, j' \in [d_2]$ the following properties are satisfied by functions $\Gamma^{(h)}$ and $N^{(h)}$ defined in (15) and (14) of Definition 4.1:*

1. **Cauchy–Schwarz inequality:** $|\Gamma_{i,j,i',j'}^{(h)}(y, z)| \leq \frac{\sqrt{N_{i,j}^{(h)}(y) \cdot N_{i',j'}^{(h)}(z)}}{q^2}$.

2. **Norm value:** $\Gamma_{i,j,i,j}^{(h)}(y, y) = \frac{N_{i,j}^{(h)}(y)}{q^2} \geq 0$.

Proof. We prove the lemma by induction on h . The **base of induction** corresponds to $h = 0$. In the base case, by (14) and (15) and Cauchy–Schwarz inequality, we have

$$\begin{aligned} \left| \Gamma_{i,j,i',j'}^{(0)}(y, z) \right| &\equiv \left| \sum_{l=1}^c y_{i,j,l} \cdot z_{i',j',l} \right| \\ &\leq \sqrt{\sum_{l=1}^c |y_{i,j,l}|^2 \cdot \sum_{l=1}^c |z_{i',j',l}|^2} \\ &= \frac{\sqrt{N_{i,j}^{(0)}(y) \cdot N_{i',j'}^{(0)}(z)}}{q^2}. \end{aligned}$$

This proves the base for the first statement. Additionally we have, $\Gamma_{i,j,i,j}^{(0)}(y, y) = \sum_{l=1}^c y_{i,j,l}^2 = \frac{N_{i,j}^{(0)}(y)}{q^2} \geq 0$ which proves the base for the second statement of the lemma. Now, in order to prove the inductive step, suppose that statements of the lemma hold for $h - 1$, where $h \geq 1$. Then, conditioned on this, we prove that the lemma holds for h . First note that by conditioning on the inductive hypothesis, applying Cauchy–Schwarz inequality, and using the definition of $N^{(h)}$ in (14), we can write

$$\begin{aligned} \left| \frac{\sum_{a=-\frac{q-1}{2}}^{\frac{q-1}{2}} \sum_{b=-\frac{q-1}{2}}^{\frac{q-1}{2}} \Gamma_{i+a,j+b,i'+a,j'+b}^{(h-1)}(y, z)}{\sqrt{N_{i,j}^{(h)}(y) \cdot N_{i',j'}^{(h)}(z)}} \right| &\leq \frac{\sum_{a=-\frac{q-1}{2}}^{\frac{q-1}{2}} \sum_{b=-\frac{q-1}{2}}^{\frac{q-1}{2}} \sqrt{\frac{N_{i+a,j+b}^{(h-1)}(y)}{q^2} \cdot \frac{N_{i'+a,j'+b}^{(h-1)}(z)}{q^2}}}{\sqrt{N_{i,j}^{(h)}(y) \cdot N_{i',j'}^{(h)}(z)}} \\ &\leq 1. \end{aligned}$$

Thus, by monotonicity of function $\kappa_1 : [-1, 1] \rightarrow \mathbb{R}$, we can write,

$$\begin{aligned} \left| \Gamma_{i,j,i',j'}^{(h)}(y, z) \right| &\equiv \frac{\sqrt{N_{i,j}^{(h)}(y) \cdot N_{i',j'}^{(h)}(z)}}{q^2} \cdot \kappa_1 \left(\frac{\sum_{a=-\frac{q-1}{2}}^{\frac{q-1}{2}} \sum_{b=-\frac{q-1}{2}}^{\frac{q-1}{2}} \Gamma_{i+a,j+b,i'+a,j'+b}^{(h-1)}(y, z)}{\sqrt{N_{i,j}^{(h)}(y) \cdot N_{i',j'}^{(h)}(z)}} \right) \\ &\leq \frac{\sqrt{N_{i,j}^{(h)}(y) \cdot N_{i',j'}^{(h)}(z)}}{q^2} \cdot \kappa_1(1) \\ &= \frac{\sqrt{N_{i,j}^{(h)}(y) \cdot N_{i',j'}^{(h)}(z)}}{q^2}, \end{aligned}$$

where the second line above follows because of the fact that $\kappa_1(\cdot)$ is a monotonically increasing function. This completes the inductive step for the first statement of lemma. Now we prove the inductive step for the second statement as follows,

$$\begin{aligned} \Gamma_{i,j,i,j}^{(h)}(y, y) &\equiv \frac{N_{i,j}^{(h)}(y)}{q^2} \cdot \kappa_1 \left(\frac{\sum_{a=-\frac{q-1}{2}}^{\frac{q-1}{2}} \sum_{b=-\frac{q-1}{2}}^{\frac{q-1}{2}} \Gamma_{i+a,j+b,i+a,j+b}^{(h-1)}(y, y)}{N_{i,j}^{(h)}(y)} \right) \\ &= \frac{N_{i,j}^{(h)}(y)}{q^2} \cdot \kappa_1(1) \\ &= \frac{N_{i,j}^{(h)}(y)}{q^2} \geq 0, \end{aligned}$$

where we used Corollary 2 to conclude that $\sum_{a=-\frac{q-1}{2}}^{\frac{q-1}{2}} \sum_{b=-\frac{q-1}{2}}^{\frac{q-1}{2}} \Gamma_{i+a, j+b, i+a, j+b}^{(h-1)}(y, y) = N_{i,j}^{(h)}(y)$ and then used the fact that $N_{i,j}^{(h)}(y)$ is non-negative. This completes the inductive proof of the lemma. \square

We also describes some of the basic properties of the function $\dot{\Gamma}^{(h)}(y, z)$ defined in (16) in the following lemma,

Lemma 9 (Properties of $\dot{\Gamma}^{(h)}(y, z)$). *For every images $y, z \in \mathbb{R}^{d_1 \times d_2 \times c}$, every integer $h \geq 0$ and every $i, i' \in [d_1]$ and $j, j' \in [d_2]$ the following properties are satisfied by function $\dot{\Gamma}^{(h)}$ defined in (16) of Definition 4.1:*

1. **Cauchy–Schwarz inequality:** $|\dot{\Gamma}_{i,j,i',j'}^{(h)}(y, z)| \leq \frac{1}{q^2}$.
2. **Norm value:** $\dot{\Gamma}_{i,j,i,j}^{(h)}(y, y) = \frac{1}{q^2} \geq 0$.

Proof. First, note that by Lemma 8 and the definition of $N^{(h)}$ in (14) we have,

$$\left| \frac{\sum_{a=-\frac{q-1}{2}}^{\frac{q-1}{2}} \sum_{b=-\frac{q-1}{2}}^{\frac{q-1}{2}} \Gamma_{i+a, j+b, i'+a, j'+b}^{(h-1)}(y, z)}{\sqrt{N_{i,j}^{(h)}(y) \cdot N_{i',j'}^{(h)}(z)}} \right| \leq \frac{\sum_{a=-\frac{q-1}{2}}^{\frac{q-1}{2}} \sum_{b=-\frac{q-1}{2}}^{\frac{q-1}{2}} \sqrt{\frac{N_{i+a, j+b}^{(h-1)}(y)}{q^2} \cdot \frac{N_{i'+a, j'+b}^{(h-1)}(z)}{q^2}}}{\sqrt{N_{i,j}^{(h)}(y) \cdot N_{i',j'}^{(h)}(z)}} \leq 1.$$

Thus, by monotonicity of function $\kappa_0 : [-1, 1] \rightarrow \mathbb{R}$ and using (16), we can write, $\dot{\Gamma}_{i,j,i',j'}^{(h)}(y, z) \leq \frac{1}{q^2} \cdot \kappa_0(1) = \frac{1}{q^2}$. Moreover, the equality is achieved when $y = z$ and $i = i'$ and $j = j'$. This proves both statements of the lemma. \square

We also need to use some properties of $\Pi^{(h)}(y, z)$ defined in (17) and (18). We present these properties in the next lemma,

Lemma 10 (Properties of $\Pi^{(h)}$). *For every images $y, z \in \mathbb{R}^{d_1 \times d_2 \times c}$, every integer $h \geq 0$ and every $i \in [d_1]$ and $j \in [d_2]$ the following properties are satisfied by the function $\Pi^{(h)}$ defined in (17) and (18) of Definition 4.1:*

1. **Cauchy–Schwarz inequality:** $\Pi_{i,j,i',j'}^{(h)}(y, z) \leq \sqrt{\Pi_{i,j,i,j}^{(h)}(y, y) \cdot \Pi_{i',j',i',j'}^{(h)}(z, z)}$.
2. **Norm value:** $\Pi_{i,j,i,j}^{(h)}(y, y) = \begin{cases} h \cdot N_{i,j}^{(h+1)}(y) & \text{if } h < L \\ \frac{L-1}{q^2} \cdot N_{i,j}^{(L)}(y) & \text{if } h = L \end{cases}$.

Proof. The proof is by induction on h . The base of induction corresponds to $h = 0$. By definition of $\Pi_{i,j,i,j}^{(0)} \equiv 0$ in (17), the base of induction for both statements of the lemma follow immediately.

Now we prove the inductive hypothesis. Suppose that the lemma statement holds for $h - 1$. We prove that conditioned on this, the statements of the lemma hold for h . There are two cases. The first case corresponds to $h < L$. In this case, by definition of $\Pi_{i,j,i,j}^{(h)}(x, x)$ in (17) and using

Lemma 8 and Lemma 9 we can write,

$$\begin{aligned}
\left| \Pi_{i,j,i',j'}^{(h)}(y, z) \right| &\equiv \left| \sum_{a=-\frac{q-1}{2}}^{\frac{q-1}{2}} \sum_{b=-\frac{q-1}{2}}^{\frac{q-1}{2}} \left[\Pi^{(h-1)}(y, z) \odot \dot{\Gamma}^{(h)}(y, z) + \Gamma^{(h)}(y, z) \right]_{i+a, j+b, i'+a, j'+b} \right| \\
&\leq \sum_{a=-\frac{q-1}{2}}^{\frac{q-1}{2}} \sum_{b=-\frac{q-1}{2}}^{\frac{q-1}{2}} \frac{\sqrt{\Pi_{i+a, j+b, i+a, j+b}^{(h-1)}(y, y) \cdot \Pi_{i'+a, j'+b, i'+a, j'+b}^{(h-1)}(z, z)}}{q^2} + \frac{\sqrt{N_{i+a, j+b}^{(h)}(y) \cdot N_{i'+a, j'+b}^{(h)}(z)}}{q^2} \\
&\leq \sum_{a=-\frac{q-1}{2}}^{\frac{q-1}{2}} \sum_{b=-\frac{q-1}{2}}^{\frac{q-1}{2}} \sqrt{\frac{\Pi_{i+a, j+b, i+a, j+b}^{(h-1)}(y, y) + N_{i+a, j+b}^{(h)}(y)}{q^2}} \cdot \sqrt{\frac{\Pi_{i'+a, j'+b, i'+a, j'+b}^{(h-1)}(z, z) + N_{i'+a, j'+b}^{(h)}(z)}{q^2}} \\
&\leq \sqrt{\Pi_{i,j,i,j}^{(h)}(y, y)} \cdot \sqrt{\Pi_{i',j',i',j'}^{(h)}(z, z)},
\end{aligned}$$

where the second line above follows from inductive hypothesis along with Lemma 8 and Lemma 9. The third and fourth lines above follow by Cauchy–Schwarz inequality. The second case corresponds to $h = L$. In this case, by definition of $\Pi_{i,j,i',j'}^{(L)}(y, z)$ in (18) and using Lemma 8 and Lemma 9 along with the inductive hypothesis we can write,

$$\begin{aligned}
\left| \Pi_{i,j,i',j'}^{(L)}(y, z) \right| &\equiv \left| \Pi_{i,j,i',j'}^{(L-1)}(y, z) \cdot \dot{\Gamma}_{i,j,i',j'}^{(L)}(y, z) \right| \\
&\leq \frac{\sqrt{\Pi_{i,j,i,j}^{(L-1)}(y, y) \cdot \Pi_{i',j',i',j'}^{(L-1)}(z, z)}}{q^2} \\
&= \sqrt{\Pi_{i,j,i,j}^{(L)}(y, y)} \cdot \sqrt{\Pi_{i',j',i',j'}^{(L)}(z, z)},
\end{aligned}$$

where the second line above follows from inductive hypothesis along with Lemma 9. This completes the inductive step and in turn proves the first statement of the lemma.

To prove the inductive step for the second statement of lemma we consider two cases again. The first case is $h < L$. In this case, note that by using inductive hypothesis together with Lemma 8 and Lemma 9 we can write,

$$\begin{aligned}
\Pi_{i,j,i,j}^{(h)}(y, y) &\equiv \sum_{a=-\frac{q-1}{2}}^{\frac{q-1}{2}} \sum_{b=-\frac{q-1}{2}}^{\frac{q-1}{2}} \left[\Pi^{(h-1)}(y, y) \odot \dot{\Gamma}^{(h)}(y, y) + \Gamma^{(h)}(y, y) \right]_{i+a, j+b, i+a, j+b} \\
&= \sum_{a=-\frac{q-1}{2}}^{\frac{q-1}{2}} \sum_{b=-\frac{q-1}{2}}^{\frac{q-1}{2}} \frac{(h-1) \cdot N_{i+a, j+b}^{(h)}(y)}{q^2} + \frac{N_{i+a, j+b}^{(h)}(y)}{q^2} \\
&= h \cdot \sum_{a=-\frac{q-1}{2}}^{\frac{q-1}{2}} \sum_{b=-\frac{q-1}{2}}^{\frac{q-1}{2}} \frac{N_{i+a, j+b}^{(h)}(y)}{q^2} \\
&= h \cdot N_{i,j}^{(h+1)}(y),
\end{aligned}$$

where the last line above follows from definition of $N^{(h)}$ in (14). The second case corresponds to $h = L$. In this case, by inductive hypothesis together with Lemma 8 and Lemma 9 we can write,

$$\begin{aligned}
\Pi_{i,j,i,j}^{(L)}(y, y) &\equiv \Pi_{i,j,i,j}^{(L-1)}(y, y) \cdot \dot{\Gamma}_{i,j,i,j}^{(L)}(y, y) \\
&= \frac{(L-1) \cdot N_{i,j}^{(L)}(y)}{q^2}.
\end{aligned}$$

This completes the inductive step for the second statement and in turn proves the second statement of the lemma. \square

F CNTK Sketch: Claims and Invariants

In this section we prove our main result on sketching the CNTK kernel, i.e., Theorem 3.

In the following lemma, we analyze the correctness of the CNTK Sketch method by giving the invariants that the algorithm maintains at all times,

Lemma 11 (Invariants of the CNTK Sketch). *For every positive integers d_1, d_2, c , and L , every $\epsilon, \delta > 0$, every images $y, z \in \mathbb{R}^{d_1 \times d_2 \times c}$, if we let $N^{(h)} : \mathbb{R}^{d_1 \times d_2 \times c} \rightarrow \mathbb{R}^{d_1 \times d_2}$, $\Gamma^{(h)}(y, z) \in \mathbb{R}^{d_1 \times d_2 \times d_1 \times d_2}$ and $\Pi^{(h)}(y, z) \in \mathbb{R}^{d_1 \times d_2 \times d_1 \times d_2}$ be the tensor functions defined in (14), (15), (17), and (18) of Definition 4.1, respectively, then with probability at least $1 - \delta$ the following invariants are maintained simultaneously for all $i, i' \in [d_1]$ and $j, j' \in [d_2]$ and every $h = 0, 1, 2, \dots, L$:*

1. *The mapping $\phi_{i,j}^{(h)}(\cdot)$ computed by the CNTK Sketch algorithm in (20) and (21) of Definition 4.2 satisfy the following,*

$$\left| \left\langle \phi_{i,j}^{(h)}(y), \phi_{i',j'}^{(h)}(z) \right\rangle - \Gamma_{i,j,i',j'}^{(h)}(y, z) \right| \leq (h+1) \cdot \frac{\epsilon^2}{60L^3} \cdot \frac{\sqrt{N_{i,j}^{(h)}(y) \cdot N_{i',j'}^{(h)}(z)}}{q^2}.$$

2. *The mapping $\psi_{i,j}^{(h)}(\cdot)$ computed by the CNTK Sketch algorithm in (23) and (24) of Definition 4.2 satisfy the following,*

$$\left| \left\langle \psi_{i,j}^{(h)}(y), \psi_{i',j'}^{(h)}(z) \right\rangle - \Pi_{i,j,i',j'}^{(h)}(y, z) \right| \leq \begin{cases} \frac{\epsilon}{10} \cdot \frac{h^2}{L+1} \cdot \sqrt{N_{i,j}^{(h+1)}(y) \cdot N_{i',j'}^{(h+1)}(z)} & \text{if } h < L \\ \frac{\epsilon}{10} \cdot \frac{L-1}{q^2} \cdot \sqrt{N_{i,j}^{(L)}(y) \cdot N_{i',j'}^{(L)}(z)} & \text{if } h = L \end{cases}.$$

Proof. The proof is by induction on the value of $h = 0, 1, 2, \dots, L$. More formally, consider the following statements for every $h = 0, 1, 2, \dots, L$:

P₁(h) : Simultaneously for all $i, i' \in [d_1]$ and $j, j' \in [d_2]$:

$$\begin{aligned} \left| \left\langle \phi_{i,j}^{(h)}(y), \phi_{i',j'}^{(h)}(z) \right\rangle - \Gamma_{i,j,i',j'}^{(h)}(y, z) \right| &\leq (h+1) \cdot \frac{\epsilon^2}{60L^3} \cdot \frac{\sqrt{N_{i,j}^{(h)}(y) \cdot N_{i',j'}^{(h)}(z)}}{q^2}, \\ \left| \left\| \phi_{i,j}^{(h)}(y) \right\|_2^2 - \Gamma_{i,j,i,j}^{(h)}(y, y) \right| &\leq \frac{(h+1) \cdot \epsilon^2}{60L^3} \cdot \frac{N_{i,j}^{(h)}(y)}{q^2}, \\ \left| \left\| \phi_{i',j'}^{(h)}(z) \right\|_2^2 - \Gamma_{i',j',i',j'}^{(h)}(z, z) \right| &\leq \frac{(h+1) \cdot \epsilon^2}{60L^3} \cdot \frac{N_{i',j'}^{(h)}(z)}{q^2}. \end{aligned}$$

P₂(h) : Simultaneously for all $i, i' \in [d_1]$ and $j, j' \in [d_2]$:

$$\begin{aligned} \left| \left\langle \psi_{i,j}^{(h)}(y), \psi_{i',j'}^{(h)}(z) \right\rangle - \Pi_{i,j,i',j'}^{(h)}(y, z) \right| &\leq \begin{cases} \frac{\epsilon}{10} \cdot \frac{h^2}{L+1} \cdot \sqrt{N_{i,j}^{(h+1)}(y) \cdot N_{i',j'}^{(h+1)}(z)} & \text{if } h < L \\ \frac{\epsilon}{10} \cdot \frac{L-1}{q^2} \cdot \sqrt{N_{i,j}^{(L)}(y) \cdot N_{i',j'}^{(L)}(z)} & \text{if } h = L \end{cases}, \\ (\text{only for } h < L) : \quad \left| \left\| \psi_{i,j}^{(h)}(y) \right\|_2^2 - \Pi_{i,j,i,j}^{(h)}(y, y) \right| &\leq \frac{\epsilon}{10} \cdot \frac{h^2}{L+1} \cdot N_{i,j}^{(h+1)}(y), \\ (\text{only for } h < L) : \quad \left| \left\| \psi_{i',j'}^{(h)}(z) \right\|_2^2 - \Pi_{i',j',i',j'}^{(h)}(z, z) \right| &\leq \frac{\epsilon}{10} \cdot \frac{h^2}{L+1} \cdot N_{i',j'}^{(h+1)}(z). \end{aligned}$$

We prove that probabilities $\Pr[P_1(0)]$ and $\Pr[P_2(0)|P_1(0)]$ are both greater than $1 - O(\delta/L)$. Additionally, for every $h = 1, 2, \dots, L$, we prove that the conditional probabilities $\Pr[P_1(h)|P_1(h-1)]$ and $\Pr[P_2(h)|P_2(h-1), P_1(h), P_1(h-1)]$ are greater than $1 - O(\delta/L)$.

The **base of induction** corresponds to $h = 0$. By (20), $\phi_{i,j}^{(0)}(y) = S \cdot y_{(i,j,:)}$ and $\phi_{i',j'}^{(0)}(z) = S \cdot z_{(i',j',:)}$, thus, Lemma 2 implies the following

$$\Pr \left[\left| \left\langle \phi_{i,j}^{(0)}(y), \phi_{i',j'}^{(0)}(z) \right\rangle - \left\langle y_{(i,j,:)}, z_{(i',j',:)} \right\rangle \right| \leq O \left(\epsilon^2 / L^3 \right) \cdot \|y_{(i,j,:)}\|_2 \|z_{(i',j',:)}\|_2 \right] \geq 1 - O \left(\frac{\delta}{d_1^2 d_2^2 L} \right),$$

therefore, by using (14) and (15) we have

$$\Pr \left[\left| \left\langle \phi_{i,j}^{(0)}(y), \phi_{i',j'}^{(0)}(z) \right\rangle - \Gamma_{i,j,i',j'}^{(0)}(y, z) \right| \leq O \left(\epsilon^2 / L^3 \right) \cdot \frac{\sqrt{N_{i,j}^{(0)}(y) \cdot N_{i',j'}^{(0)}(z)}}{q^2} \right] \geq 1 - O \left(\frac{\delta}{d_1^2 d_2^2 L} \right).$$

Similarly, we can prove that with probability at least $1 - O \left(\frac{\delta}{d_1^2 d_2^2 L} \right)$, the following hold

$$\begin{aligned} \left| \left\| \phi_{i,j}^{(0)}(y) \right\|_2^2 - \Gamma_{i,j,i,j}^{(0)}(y, y) \right| &\leq O \left(\epsilon^2 / L^3 \right) \cdot \frac{N_{i,j}^{(0)}(y)}{q^2}, \\ \left| \left\| \phi_{i',j'}^{(0)}(z) \right\|_2^2 - \Gamma_{i',j',i',j'}^{(0)}(z, z) \right| &\leq O \left(\epsilon^2 / L^3 \right) \cdot \frac{N_{i',j'}^{(0)}(z)}{q^2}. \end{aligned}$$

By union bounding over all $i, i' \in [d_1]$ and $j, j' \in [d_2]$, this proves the base of induction for statement $P_1(h)$, i.e., $\Pr[P_1(0)] \geq 1 - O(\delta/L)$.

Moreover, by (23), we have that $\psi_{i,j}^{(0)}(y) = 0$ and $\psi_{i',j'}^{(0)}(z) = 0$, thus, by (17), it trivially holds that $\Pr[P_2(0)|P_1(0)] = 1 \geq 1 - O(\delta/L)$. This completes the base of induction.

We proceed by proving the **inductive step**. That is, by assuming the inductive hypothesis for $h-1$, we prove that statements $P_1(h)$ and $P_2(h)$ hold. More precisely, first we condition on the statement $P_1(h-1)$ being true for some $h \geq 1$, and then prove that $P_1(h)$ holds with probability at least $1 - O(\delta/L)$. Next we show that conditioned on statements $P_2(h-1), P_1(h), P_1(h-1)$ being true, $P_2(h)$ holds with probability at least $1 - O(\delta/L)$. This will complete the induction.

First, note that by Lemma 2, union bound, and using (21), the following holds simultaneously for all $i, i' \in [d_1]$ and all $j, j' \in [d_2]$, with probability at least $1 - O \left(\frac{\delta}{L} \right)$,

$$\left| \left\langle \phi_{i,j}^{(h)}(y), \phi_{i',j'}^{(h)}(z) \right\rangle - \frac{\sqrt{N_{i,j}^{(h)}(y) N_{i',j'}^{(h)}(z)}}{q^2} \cdot \sum_{l=0}^{2p+2} e_l \left\langle \left[Z_{i,j}^{(h)}(y) \right]_l, \left[Z_{i',j'}^{(h)}(z) \right]_l \right\rangle \right| \leq O \left(\frac{\epsilon^2}{L^3} \right) \cdot A, \quad (48)$$

where $A := \frac{\sqrt{N_{i,j}^{(h)}(y) N_{i',j'}^{(h)}(z)}}{q^2} \cdot \sqrt{\sum_{l=0}^{2p+2} e_l \left\| \left[Z_{i,j}^{(h)}(y) \right]_l \right\|_2^2} \cdot \sqrt{\sum_{l=0}^{2p+2} e_l \left\| \left[Z_{i',j'}^{(h)}(z) \right]_l \right\|_2^2}$ and the collection of vectors $\left\{ \left[Z_{i,j}^{(h)}(y) \right]_l \right\}_{l=0}^{2p+2}$ and $\left\{ \left[Z_{i',j'}^{(h)}(z) \right]_l \right\}_{l=0}^{2p+2}$ and coefficients $e_0, e_1, e_2, \dots, e_{2p+2}$ are defined as per (21). Additionally, by Lemma 1 and union bound, the following inequalities hold, with probability at least $1 - O \left(\frac{\delta}{L} \right)$, simultaneously for all $l = 0, 1, 2, \dots, 2p+2$, all $i, i' \in [d_1]$ and all $j, j' \in [d_2]$:

$$\begin{aligned} \left| \left\langle \left[Z_{i,j}^{(h)}(y) \right]_l, \left[Z_{i',j'}^{(h)}(z) \right]_l \right\rangle - \left\langle \mu_{i,j}^{(h)}(y), \mu_{i',j'}^{(h)}(z) \right\rangle^l \right| &\leq O \left(\frac{\epsilon^2}{L^3} \right) \left\| \mu_{i,j}^{(h)}(y) \right\|_2^l \left\| \mu_{i',j'}^{(h)}(z) \right\|_2^l \\ \left\| \left[Z_{i,j}^{(h)}(y) \right]_l \right\|_2^2 &\leq \frac{11}{10} \cdot \left\| \mu_{i,j}^{(h)}(y) \right\|_2^{2l} \\ \left\| \left[Z_{i',j'}^{(h)}(z) \right]_l \right\|_2^2 &\leq \frac{11}{10} \cdot \left\| \mu_{i',j'}^{(h)}(z) \right\|_2^{2l} \end{aligned} \quad (49)$$

Therefore, by plugging (49) back to (48) and using union bound and triangle inequality as well as Cauchy–Schwarz inequality, we find that with probability at least $1 - O\left(\frac{\delta}{L}\right)$, the following holds simultaneously for all $i, i' \in [d_1]$ and $j, j' \in [d_2]$

$$\left| \left\langle \phi_{i,j}^{(h)}(y), \phi_{i',j'}^{(h)}(z) \right\rangle - \frac{\sqrt{N_{i,j}^{(h)}(y)N_{i',j'}^{(h)}(z)}}{q^2} \cdot P_{\text{relu}}^{(p)}\left(\left\langle \mu_{i,j}^{(h)}(y), \mu_{i',j'}^{(h)}(z) \right\rangle\right) \right| \leq O\left(\frac{\epsilon^2}{L^3}\right) \cdot B, \quad (50)$$

where $B := \frac{\sqrt{N_{i,j}^{(h)}(y)N_{i',j'}^{(h)}(z)}}{q^2} \cdot \sqrt{P_{\text{relu}}^{(p)}\left(\|\mu_{i,j}^{(h)}(y)\|_2^2\right) \cdot P_{\text{relu}}^{(p)}\left(\|\mu_{i',j'}^{(h)}(z)\|_2^2\right)}$ and $P_{\text{relu}}^{(p)}(\alpha) = \sum_{l=0}^{2p+2} e_l \cdot \alpha^l$ is the polynomial defined in (8). By using the definition of $\mu_{i,j}^{(h)}(\cdot)$ in (21) we have,

$$\begin{aligned} \left\langle \mu_{i,j}^{(h)}(y), \mu_{i',j'}^{(h)}(z) \right\rangle &= \frac{\sum_{a=-\frac{q-1}{2}}^{\frac{q-1}{2}} \sum_{b=-\frac{q-1}{2}}^{\frac{q-1}{2}} \left\langle \phi_{i+a,j+b}^{(h-1)}(y), \phi_{i'+a,j'+b}^{(h-1)}(z) \right\rangle}{\sqrt{N_{i,j}^{(h)}(y)N_{i',j'}^{(h)}(z)}}, \\ \left\| \mu_{i,j}^{(h)}(y) \right\|_2^2 &= \frac{\sum_{a=-\frac{q-1}{2}}^{\frac{q-1}{2}} \sum_{b=-\frac{q-1}{2}}^{\frac{q-1}{2}} \left\| \phi_{i+a,j+b}^{(h-1)}(y) \right\|_2^2}{N_{i,j}^{(h)}(y)}, \\ \left\| \mu_{i',j'}^{(h)}(z) \right\|_2^2 &= \frac{\sum_{a=-\frac{q-1}{2}}^{\frac{q-1}{2}} \sum_{b=-\frac{q-1}{2}}^{\frac{q-1}{2}} \left\| \phi_{i'+a,j'+b}^{(h-1)}(z) \right\|_2^2}{N_{i',j'}^{(h)}(z)}. \end{aligned} \quad (51)$$

Hence, by conditioning on the inductive hypothesis $P_1(h-1)$ and using (51) and Corollary 2 we have,

$$\left| \left\| \mu_{i,j}^{(h)}(y) \right\|_2^2 - 1 \right| \leq h \cdot \frac{\epsilon^2}{60L^3}, \quad \text{and} \quad \left| \left\| \mu_{i',j'}^{(h)}(z) \right\|_2^2 - 1 \right| \leq h \cdot \frac{\epsilon^2}{60L^3}.$$

Therefore, by invoking Lemma 4, it follows that $\left| P_{\text{relu}}^{(p)}\left(\|\mu_{i,j}^{(h)}(y)\|_2^2\right) - P_{\text{relu}}^{(p)}(1) \right| \leq h \cdot \frac{\epsilon^2}{60L^3}$ and $\left| P_{\text{relu}}^{(p)}\left(\|\mu_{i',j'}^{(h)}(z)\|_2^2\right) - P_{\text{relu}}^{(p)}(1) \right| \leq h \cdot \frac{\epsilon^2}{60L^3}$. Consequently, because $P_{\text{relu}}^{(p)}(1) \leq P_{\text{relu}}^{(+\infty)}(1) = 1$, we find that

$$B \leq \frac{11}{10} \cdot \frac{\sqrt{N_{i,j}^{(h)}(y)N_{i',j'}^{(h)}(z)}}{q^2}.$$

For shorthand we use the notation $\beta := \frac{\sqrt{N_{i,j}^{(h)}(y)N_{i',j'}^{(h)}(z)}}{q^2}$. By plugging this into (50) and using the notation β , we find that the following holds simultaneously for all $i, i' \in [d_1]$ and all $j, j' \in [d_2]$, with probability at least $1 - O\left(\frac{\delta}{L}\right)$,

$$\left| \left\langle \phi_{i,j}^{(h)}(y), \phi_{i',j'}^{(h)}(z) \right\rangle - \beta \cdot P_{\text{relu}}^{(p)}\left(\left\langle \mu_{i,j}^{(h)}(y), \mu_{i',j'}^{(h)}(z) \right\rangle\right) \right| \leq O\left(\frac{\epsilon^2}{L^3}\right) \cdot \beta. \quad (52)$$

Furthermore, by conditioning on the inductive hypothesis $P_1(h-1)$ and combining it with (51) and

applying Cauchy–Schwarz inequality and invoking Corollary 2 we find that,

$$\begin{aligned}
& \left| \left\langle \mu_{i,j}^{(h)}(y), \mu_{i',j'}^{(h)}(z) \right\rangle - \frac{\sum_{a=-\frac{q-1}{2}}^{\frac{q-1}{2}} \sum_{b=-\frac{q-1}{2}}^{\frac{q-1}{2}} \Gamma_{i+a,j+b,i'+a,j'+b}^{(h-1)}(y, z)}{\sqrt{N_{i,j}^{(h)}(y) \cdot N_{i',j'}^{(h)}(z)}} \right| \\
& \leq \frac{\sum_{a=-\frac{q-1}{2}}^{\frac{q-1}{2}} \sum_{b=-\frac{q-1}{2}}^{\frac{q-1}{2}} \sqrt{N_{i+a,j+b}^{(h-1)}(y) \cdot N_{i'+a,j'+b}^{(h-1)}(z)}}{q^2 \cdot \sqrt{N_{i,j}^{(h)}(y) \cdot N_{i',j'}^{(h)}(z)}} \cdot h \cdot \frac{\epsilon^2}{60L^3} \\
& \leq \frac{\sqrt{\sum_{a=-\frac{q-1}{2}}^{\frac{q-1}{2}} \sum_{b=-\frac{q-1}{2}}^{\frac{q-1}{2}} N_{i+a,j+b}^{(h-1)}(y)/q^2} \cdot \sqrt{\sum_{a=-\frac{q-1}{2}}^{\frac{q-1}{2}} \sum_{b=-\frac{q-1}{2}}^{\frac{q-1}{2}} N_{i'+a,j'+b}^{(h-1)}(z)/q^2}}{\sqrt{N_{i,j}^{(h)}(y) \cdot N_{i',j'}^{(h)}(z)}} \cdot h \cdot \frac{\epsilon^2}{60L^3} \\
& = h \cdot \frac{\epsilon^2}{60L^3},
\end{aligned} \tag{53}$$

where the last line follows from (14).

For shorthand, we use the notation $\gamma := \frac{\sum_{a=-\frac{q-1}{2}}^{\frac{q-1}{2}} \sum_{b=-\frac{q-1}{2}}^{\frac{q-1}{2}} \Gamma_{i+a,j+b,i'+a,j'+b}^{(h-1)}(y, z)}{\sqrt{N_{i,j}^{(h)}(y) \cdot N_{i',j'}^{(h)}(z)}}$. Note that by Lemma 8 and (14), $-1 \leq \gamma \leq 1$. Hence, we can invoke Lemma 4 and use (53) to find that,

$$\left| P_{\text{relu}}^{(p)} \left(\left\langle \mu_{i,j}^{(h)}(y), \mu_{i',j'}^{(h)}(z) \right\rangle \right) - P_{\text{relu}}^{(p)}(\gamma) \right| \leq h \cdot \frac{\epsilon^2}{60L^3}.$$

By incorporating the above inequality into (52) using triangle inequality we find that, with probability at least $1 - O\left(\frac{\delta}{L}\right)$, the following holds simultaneously for all $i, i' \in [d_1]$ and all $j, j' \in [d_2]$:

$$\left| \left\langle \phi_{i,j}^{(h)}(y), \phi_{i',j'}^{(h)}(z) \right\rangle - \beta \cdot P_{\text{relu}}^{(p)}(\gamma) \right| \leq \left(O\left(\frac{\epsilon^2}{L^4}\right) + \frac{h \cdot \epsilon^2}{60L^3} \right) \cdot \beta. \tag{54}$$

Additionally, since $-1 \leq \gamma \leq 1$, we can invoke Lemma 3 and use the fact that $p = \lceil 2L^2/\epsilon^{4/3} \rceil$ to conclude,

$$\left| P_{\text{relu}}^{(p)}(\gamma) - \kappa_1(\gamma) \right| \leq \frac{\epsilon^2}{76L^3}.$$

By combining the above inequality with (54) via triangle inequality and using the fact that, by (15), $\beta \cdot \kappa_1(\gamma) \equiv \Gamma_{i,j,i',j'}^{(h)}(y, z)$ we get the following inequality, with probability at least $1 - O\left(\frac{\delta}{L}\right)$

$$\left| \left\langle \phi_{i,j}^{(h)}(y), \phi_{i',j'}^{(h)}(z) \right\rangle - \Gamma_{i,j,i',j'}^{(h)}(y, z) \right| \leq (h+1) \cdot \frac{\epsilon^2}{60L^3} \cdot \frac{\sqrt{N_{i,j}^{(h)}(y)N_{i',j'}^{(h)}(z)}}{q^2}.$$

Similarly, we can prove that with probability at least $1 - O\left(\frac{\delta}{L}\right)$ the following hold, simultaneously for all $i, i' \in [d_1]$ and $j, j' \in [d_2]$,

$$\left| \left\| \phi_{i,j}^{(h)}(y) \right\|_2^2 - \Gamma_{i,j,i,j}^{(h)}(y, y) \right| \leq \frac{(h+1)\epsilon^2}{60L^3} \cdot \frac{N_{i,j}^{(h)}(y)}{q^2}, \text{ and } \left| \left\| \phi_{i',j'}^{(h)}(z) \right\|_2^2 - \Gamma_{i',j',i',j'}^{(h)}(z, z) \right| \leq \frac{(h+1)\epsilon^2}{60L^3} \cdot \frac{N_{i',j'}^{(h)}(z)}{q^2}.$$

This is sufficient to prove the inductive step for statement $P_1(h)$, i.e., $\Pr[P_1(h)|P_1(h-1)] \geq 1 - O(\delta/L)$.

Now we prove the inductive step for statement $P_2(h)$. That is, we prove that conditioned on $P_2(h-1), P_1(h), P_1(h-1)$, $P_2(h)$ holds with probability at least $1 - O(\delta/L)$. First, note that by Lemma 2 and using (22) and union bound, we have the following simultaneously for all $i, i' \in [d_1]$ and all $j, j' \in [d_2]$, with probability at least $1 - O\left(\frac{\delta}{L}\right)$,

$$\left| \left\langle \dot{\phi}_{i,j}^{(h)}(y), \dot{\phi}_{i',j'}^{(h)}(z) \right\rangle - \frac{1}{q^2} \sum_{l=0}^{2p'+1} f_l \left\langle \left[Y_{i,j}^{(h)}(y) \right]_l, \left[Y_{i',j'}^{(h)}(z) \right]_l \right\rangle \right| \leq O\left(\frac{\epsilon}{L}\right) \hat{A}, \quad (55)$$

where $\hat{A} := \frac{1}{q^2} \cdot \sqrt{\sum_{l=0}^{2p'+1} f_l \left\| \left[Y_{i,j}^{(h)}(y) \right]_l \right\|_2^2} \cdot \sqrt{\sum_{l=0}^{2p'+1} f_l \left\| \left[Y_{i',j'}^{(h)}(z) \right]_l \right\|_2^2}$ and the collection of vectors $\left\{ \left[Y_{i,j}^{(h)}(y) \right]_l \right\}_{l=0}^{2p'+1}$ and $\left\{ \left[Y_{i',j'}^{(h)}(z) \right]_l \right\}_{l=0}^{2p'+1}$ and coefficients $f_0, f_1, f_2, \dots, f_{2p'+1}$ are defined as per (22). By Lemma 1 and union bound, with probability at least $1 - O\left(\frac{\delta}{L}\right)$, the following inequalities hold true simultaneously for all $l \in \{0, 1, 2, \dots, 2p'+1\}$, all $i, i' \in [d_1]$ and all $j, j' \in [d_2]$,

$$\begin{aligned} & \left| \left\langle \left[Y_{i,j}^{(h)}(y) \right]_l, \left[Y_{i',j'}^{(h)}(z) \right]_l \right\rangle - \left\langle \mu_{i,j}^{(h)}(y), \mu_{i',j'}^{(h)}(z) \right\rangle^l \right| \leq O\left(\frac{\epsilon}{L}\right) \cdot \left\| \mu_{i,j}^{(h)}(y) \right\|_2^l \left\| \mu_{i',j'}^{(h)}(z) \right\|_2^l \\ & \left\| \left[Y_{i,j}^{(h)}(y) \right]_l \right\|_2^2 \leq \frac{11}{10} \cdot \left\| \mu_{i,j}^{(h)}(y) \right\|_2^{2l} \\ & \left\| \left[Y_{i',j'}^{(h)}(z) \right]_l \right\|_2^2 \leq \frac{11}{10} \cdot \left\| \mu_{i',j'}^{(h)}(z) \right\|_2^{2l} \end{aligned} \quad (56)$$

Therefore, by plugging (56) into (55) and using union bound and triangle inequality as well as Cauchy–Schwarz inequality, we find that with probability at least $1 - O\left(\frac{\delta}{L}\right)$, the following holds simultaneously for all $i, i' \in [d_1]$ and $j, j' \in [d_2]$

$$\left| \left\langle \dot{\phi}_{i,j}^{(h)}(y), \dot{\phi}_{i',j'}^{(h)}(z) \right\rangle - \frac{1}{q^2} \cdot \dot{P}_{\text{relu}}^{(p')} \left(\left\langle \mu_{i,j}^{(h)}(y), \mu_{i',j'}^{(h)}(z) \right\rangle \right) \right| \leq O\left(\frac{\epsilon}{L}\right) \cdot \hat{B}, \quad (57)$$

where $\hat{B} := \frac{1}{q^2} \cdot \sqrt{\dot{P}_{\text{relu}}^{(p')} \left(\left\| \mu_{i,j}^{(h)}(y) \right\|_2^2 \right) \cdot \dot{P}_{\text{relu}}^{(p')} \left(\left\| \mu_{i',j'}^{(h)}(z) \right\|_2^2 \right)}$ and $\dot{P}_{\text{relu}}^{(p)}(\alpha) = \sum_{l=0}^{2p'+1} f_l \cdot \alpha^l$ is the polynomial defined in (8). By conditioning on the inductive hypothesis $P_1(h-1)$ and using (51) and Corollary 2 we have $\left| \left\| \mu_{i,j}^{(h)}(y) \right\|_2^2 - 1 \right| \leq h \cdot \frac{\epsilon^2}{60L^3}$ and $\left| \left\| \mu_{i',j'}^{(h)}(z) \right\|_2^2 - 1 \right| \leq h \cdot \frac{\epsilon^2}{60L^3}$. Therefore, using the fact that $p' = \lceil 9L^2/\epsilon^2 \rceil$ and by invoking Lemma 4, it follows that $\left| \dot{P}_{\text{relu}}^{(p')} \left(\left\| \mu_{i,j}^{(h)}(y) \right\|_2^2 \right) - \dot{P}_{\text{relu}}^{(p')}(1) \right| \leq \frac{h \cdot \epsilon}{20L^2}$ and $\left| \dot{P}_{\text{relu}}^{(p')} \left(\left\| \mu_{i',j'}^{(h)}(z) \right\|_2^2 \right) - \dot{P}_{\text{relu}}^{(p')}(1) \right| \leq \frac{h \cdot \epsilon}{20L^2}$. Consequently, because $\dot{P}_{\text{relu}}^{(p')}(1) \leq \dot{P}_{\text{relu}}^{(+\infty)}(1) = 1$, we find that

$$\hat{B} \leq \frac{11}{10 \cdot q^2}.$$

By plugging this into (57) we get the following, with probability at least $1 - O\left(\frac{\delta}{L}\right)$,

$$\left| \left\langle \dot{\phi}_{i,j}^{(h)}(y), \dot{\phi}_{i',j'}^{(h)}(z) \right\rangle - \frac{1}{q^2} \cdot \dot{P}_{\text{relu}}^{(p')} \left(\left\langle \mu_{i,j}^{(h)}(y), \mu_{i',j'}^{(h)}(z) \right\rangle \right) \right| \leq O\left(\frac{\epsilon}{q^2 \cdot L}\right). \quad (58)$$

Furthermore, recall the notation $\gamma = \frac{\sum_{a=-\frac{q-1}{2}}^{\frac{q-1}{2}} \sum_{b=-\frac{q-1}{2}}^{\frac{q-1}{2}} \Gamma_{i+a, j+b, i'+a, j'+b}^{(h-1)}(y, z)}{\sqrt{N_{i,j}^{(h)}(y) \cdot N_{i',j'}^{(h)}(z)}}$ and note that by Lemma 8

and (14), $-1 \leq \gamma \leq 1$. Hence, we can invoke Lemma 4 and use the fact that $p' = \lceil 9L^2/\epsilon^2 \rceil$ to find that (53) implies the following,

$$\left| \dot{P}_{\text{relu}}^{(p')} \left(\left\langle \mu_{i,j}^{(h)}(y), \mu_{i',j'}^{(h)}(z) \right\rangle \right) - \dot{P}_{\text{relu}}^{(p')}(\gamma) \right| \leq \frac{h \cdot \epsilon}{20L^2}.$$

By incorporating the above inequality into (58) using triangle inequality, we find that, with probability at least $1 - O\left(\frac{\delta}{L}\right)$, the following holds simultaneously for all $i, i' \in [d_1]$ and all $j, j' \in [d_2]$:

$$\left| \left\langle \dot{\phi}_{i,j}^{(h)}(y), \dot{\phi}_{i',j'}^{(h)}(z) \right\rangle - \frac{1}{q^2} \cdot \dot{P}_{relu}^{(p')}\left(\gamma\right) \right| \leq O\left(\frac{\epsilon}{q^2 L^2}\right) + \frac{h}{q^2} \cdot \frac{\epsilon}{20L^2}. \quad (59)$$

Since $-1 \leq \gamma \leq 1$, we can invoke Lemma 3 and use the fact that $p' = \lceil 9L^2/\epsilon^2 \rceil$ to conclude,

$$\left| \dot{P}_{relu}^{(p')}\left(\gamma\right) - \kappa_0\left(\gamma\right) \right| \leq \frac{\epsilon}{15L}.$$

By combining above inequality with (59) via triangle inequality and using the fact that, by (16), $\frac{1}{q^2} \cdot \kappa_0(\gamma) \equiv \dot{\Gamma}_{i,j,i',j'}^{(h)}(y, z)$ we get the following bound simultaneously for all $i, i' \in [d_1]$ and all $j, j' \in [d_2]$, with probability at least $1 - O\left(\frac{\delta}{L}\right)$:

$$\left| \left\langle \dot{\phi}_{i,j}^{(h)}(y), \dot{\phi}_{i',j'}^{(h)}(z) \right\rangle - \dot{\Gamma}_{i,j,i',j'}^{(h)}(y, z) \right| \leq \frac{1}{q^2} \cdot \frac{\epsilon}{8L}. \quad (60)$$

Similarly we can prove that with probability at least $1 - O\left(\frac{\delta}{L}\right)$, the following hold simultaneously for all $i, i' \in [d_1]$ and all $j, j' \in [d_2]$,

$$\left| \left\| \dot{\phi}_{i,j}^{(h)}(y) \right\|_2^2 - \dot{\Gamma}_{i,j,i,j}^{(h)}(y, y) \right| \leq \frac{1}{q^2} \cdot \frac{\epsilon}{8L}, \text{ and } \left| \left\| \dot{\phi}_{i',j'}^{(h)}(z) \right\|_2^2 - \dot{\Gamma}_{i',j',i',j'}^{(h)}(z, z) \right| \leq \frac{1}{q^2} \cdot \frac{\epsilon}{8L}. \quad (61)$$

We will use (60) and (61) to prove the inductive step for $P_2(h)$.

Next, we consider two cases for the value of h . When $h < L$, the vectors $\psi_{i,j}^{(h)}(y), \psi_{i',j'}^{(h)}(z)$ are defined in (23) and when $h = L$, these vectors are defined differently in (24). First we consider the case of $h < L$. Note that in this case, if we let $\eta_{i,j}^{(h)}(y)$ and $\eta_{i',j'}^{(h)}(z)$ be the vectors defined in (23), then by Lemma 2 and union bound, the following holds simultaneously for all $i, i' \in [d_1]$ and all $j, j' \in [d_2]$, with probability at least $1 - O\left(\frac{\delta}{L}\right)$:

$$\left| \left\langle \psi_{i,j}^{(h)}(y), \psi_{i',j'}^{(h)}(z) \right\rangle - \sum_{a=-\frac{q-1}{2}}^{\frac{q-1}{2}} \sum_{b=-\frac{q-1}{2}}^{\frac{q-1}{2}} \left\langle \eta_{i+a,j+b}^{(h)}(y), \eta_{i'+a,j'+b}^{(h)}(z) \right\rangle \right| \leq O\left(\epsilon/L\right) \cdot D, \quad (62)$$

where $D := \sqrt{\sum_{a=-\frac{q-1}{2}}^{\frac{q-1}{2}} \sum_{b=-\frac{q-1}{2}}^{\frac{q-1}{2}} \|\eta_{i+a,j+b}^{(h)}(y)\|_2^2} \cdot \sqrt{\sum_{a=-\frac{q-1}{2}}^{\frac{q-1}{2}} \sum_{b=-\frac{q-1}{2}}^{\frac{q-1}{2}} \|\eta_{i'+a,j'+b}^{(h)}(z)\|_2^2}$. Now, if we let $f_{i,j} := \psi_{i,j}^{(h-1)}(y) \otimes \dot{\phi}_{i,j}^{(h)}(y)$ and $g_{i',j'} := \psi_{i',j'}^{(h-1)}(z) \otimes \dot{\phi}_{i',j'}^{(h)}(z)$, then by (23), $\eta_{i,j}^{(h)}(y) = (Q^2 \cdot f_{i,j}) \oplus \phi_{i,j}^{(h)}(y)$ and $\eta_{i',j'}^{(h)}(z) = (Q^2 \cdot g_{i',j'}) \oplus \phi_{i',j'}^{(h)}(z)$. Thus by Lemma 1 and union bound, with probability at least $1 - O\left(\frac{\delta}{L}\right)$, we have the following inequalities simultaneously for all $i, i' \in [d_1]$ and $j, j' \in [d_2]$:

$$\begin{aligned} & \left| \left\langle \eta_{i,j}^{(h)}(y), \eta_{i',j'}^{(h)}(z) \right\rangle - \langle f_{i,j}, g_{i',j'} \rangle - \left\langle \phi_{i,j}^{(h)}(y), \phi_{i',j'}^{(h)}(z) \right\rangle \right| \leq O\left(\frac{\epsilon}{L}\right) \cdot \|f_{i,j}\|_2 \|g_{i',j'}\|_2 \\ & \left\| \eta_{i,j}^{(h)}(y) \right\|_2^2 \leq \frac{11}{10} \cdot \|f_{i,j}\|_2^2 + \left\| \phi_{i,j}^{(h)}(y) \right\|_2^2 \\ & \left\| \eta_{i',j'}^{(h)}(z) \right\|_2^2 \leq \frac{11}{10} \cdot \|g_{i',j'}\|_2^2 + \left\| \phi_{i',j'}^{(h)}(z) \right\|_2^2 \end{aligned} \quad (63)$$

Therefore, if we condition on inductive hypotheses $P_1(h)$ and $P_2(h-1)$, then by using Corollary 2, Lemma 10, inequality (61) and Lemma 9 along with the fact that $\|f_{i,j}\|_2^2 = \|\psi_{i,j}^{(h-1)}(y)\|_2^2 \cdot \|\dot{\phi}_{i,j}^{(h)}(y)\|_2^2$, we have:

$$\begin{aligned}
& \sum_{a=-\frac{q-1}{2}}^{\frac{q-1}{2}} \sum_{b=-\frac{q-1}{2}}^{\frac{q-1}{2}} \|\eta_{i+a,j+b}^{(h)}(y)\|_2^2 \\
& \leq \sum_{a=-\frac{q-1}{2}}^{\frac{q-1}{2}} \sum_{b=-\frac{q-1}{2}}^{\frac{q-1}{2}} \frac{11}{10} \|f_{i+a,j+b}\|_2^2 + \Gamma_{i+a,j+b,i+a,j+b}^{(h)}(y, y) + \frac{N_{i+a,j+b}^{(h)}(y)}{10q^2} \\
& = \frac{11}{10} \cdot \sum_{a=-\frac{q-1}{2}}^{\frac{q-1}{2}} \sum_{b=-\frac{q-1}{2}}^{\frac{q-1}{2}} \|\psi_{i+a,j+b}^{(h-1)}(y)\|_2^2 \cdot \|\dot{\phi}_{i+a,j+b}^{(h)}(y)\|_2^2 + \Gamma_{i+a,j+b,i+a,j+b}^{(h)}(y, y) \\
& \leq \frac{12}{10} \sum_{a=-\frac{q-1}{2}}^{\frac{q-1}{2}} \sum_{b=-\frac{q-1}{2}}^{\frac{q-1}{2}} \Pi_{i+a,j+b,i+a,j+b}^{(h-1)}(y, y) \cdot \dot{\Gamma}_{i+a,j+b,i+a,j+b}^{(h)}(y, y) + \Gamma_{i+a,j+b,i+a,j+b}^{(h)}(y, y) \\
& = \frac{12}{10} \cdot \Pi_{i,j,i,j}^{(h)}(y, y) = \frac{12}{10} \cdot h \cdot N_{i,j}^{(h+1)}(y),
\end{aligned}$$

where the fourth line above follows from the inductive hypothesis $P_2(h-1)$ along with (61) and Lemma 9 and Lemma 10. The last line above follows from (17) and Lemma 10. Similarly we can prove, $\sum_{a=-\frac{q-1}{2}}^{\frac{q-1}{2}} \sum_{b=-\frac{q-1}{2}}^{\frac{q-1}{2}} \|\eta_{i'+a,j'+b}^{(h)}(z)\|_2^2 \leq \frac{12}{10} \cdot h \cdot N_{i',j'}^{(h+1)}(z)$, thus conditioned on $P_2(h-1), P_1(h), P_1(h-1)$, with probability at least $1 - O\left(\frac{\delta}{L}\right)$:

$$D \leq \frac{12}{10} \cdot h \cdot \sqrt{N_{i,j}^{(h+1)}(y) \cdot N_{i',j'}^{(h+1)}(z)}.$$

By incorporating this into (62) it follows that if we condition on $P_2(h-1), P_1(h), P_1(h-1)$, then, with probability at least $1 - O\left(\frac{\delta}{L}\right)$, the following holds simultaneously for all $i, i' \in [d_1]$ and all $j, j' \in [d_2]$,

$$\begin{aligned}
& \left| \left\langle \psi_{i,j}^{(h)}(y), \psi_{i',j'}^{(h)}(z) \right\rangle - \sum_{a=-\frac{q-1}{2}}^{\frac{q-1}{2}} \sum_{b=-\frac{q-1}{2}}^{\frac{q-1}{2}} \left\langle \eta_{i+a,j+b}^{(h)}(y), \eta_{i'+a,j'+b}^{(h)}(z) \right\rangle \right| \\
& \leq O(\epsilon h / L) \cdot \sqrt{N_{i,j}^{(h+1)}(y) \cdot N_{i',j'}^{(h+1)}(z)}.
\end{aligned} \tag{64}$$

Now we bound the term $\left| \left\langle \eta_{i,j}^{(h)}(y), \eta_{i',j'}^{(h)}(z) \right\rangle - \langle f_{i,j}, g_{i',j'} \rangle - \left\langle \phi_{i,j}^{(h)}(y), \phi_{i',j'}^{(h)}(z) \right\rangle \right|$ using (63), (61), and Lemma 9 along with inductive hypotheses $P_2(h-1)$ and Lemma 10. With probability at least $1 - O\left(\frac{\delta}{L}\right)$ the following holds simultaneously for all $i, i' \in [d_1]$ and all $j, j' \in [d_2]$:

$$\begin{aligned}
& \left| \left\langle \eta_{i,j}^{(h)}(y), \eta_{i',j'}^{(h)}(z) \right\rangle - \langle f_{i,j}, g_{i',j'} \rangle - \left\langle \phi_{i,j}^{(h)}(y), \phi_{i',j'}^{(h)}(z) \right\rangle \right| \\
& \leq O\left(\frac{\epsilon}{L}\right) \cdot \sqrt{\Pi_{i,j,i,j}^{(h-1)}(y, y) \cdot \dot{\Gamma}_{i,j,i,j}^{(h)}(y, y) \cdot \Pi_{i',j',i',j'}^{(h-1)}(z, z) \cdot \dot{\Gamma}_{i',j',i',j'}^{(h)}(z, z)} \\
& = O\left(\frac{\epsilon \cdot h}{L}\right) \cdot \frac{\sqrt{N_{i,j}^{(h)}(y) \cdot N_{i',j'}^{(h)}(z)}}{q^2},
\end{aligned}$$

where the last line above follows from Lemma 10 together with the fact that $\dot{\Gamma}_{i,j,i,j}^{(h)}(y, y) = \dot{\Gamma}_{i',j',i',j'}^{(h)}(z, z) = \frac{1}{q^2}$.

By combining the above with inductive hypotheses $P_1(h), P_2(h-1)$ and (60) via triangle inequality and invoking Lemma 10 we get that the following holds simultaneously for all $i, i' \in [d_1]$ and all $j, j' \in [d_2]$, with probability at least $1 - O\left(\frac{\delta}{L}\right)$,

$$\begin{aligned}
& \left| \left\langle \eta_{i,j}^{(h)}(y), \eta_{i',j'}^{(h)}(z) \right\rangle - \Pi_{i,j,i',j'}^{(h-1)}(y, z) \cdot \dot{\Gamma}_{i,j,i',j'}^{(h)}(y, z) - \Gamma_{i,j,i',j'}^{(h)}(y, z) \right| \\
& \leq \frac{\epsilon}{10} \cdot \frac{(h-1)^2}{L+1} \cdot \sqrt{N_{i,j}^{(h)}(y) \cdot N_{i',j'}^{(h)}(z)} \cdot \left(\left| \dot{\Gamma}_{i,j,i',j'}^{(h)}(y, z) \right| + \frac{1}{q^2} \cdot \frac{\epsilon}{8L} \right) + \frac{1}{q^2} \cdot \frac{\epsilon}{8L} \cdot \left| \Pi_{i,j,i',j'}^{(h-1)}(y, z) \right| \\
& + \frac{(h+1) \cdot \epsilon^2}{60L^3} \cdot \frac{\sqrt{N_{i,j}^{(h)}(y) \cdot N_{i',j'}^{(h)}(z)}}{q^2} + O\left(\frac{\epsilon \cdot h}{L}\right) \cdot \frac{\sqrt{N_{i,j}^{(h)}(y) \cdot N_{i',j'}^{(h)}(z)}}{q^2} \\
& \leq \frac{\epsilon}{10} \cdot \frac{(h-1)^2}{L+1} \cdot \frac{\sqrt{N_{i,j}^{(h)}(y) \cdot N_{i',j'}^{(h)}(z)}}{q^2} \cdot \left(1 + \frac{\epsilon}{8L} \right) + \frac{h-1}{q^2} \cdot \frac{\epsilon}{8L} \cdot \sqrt{N_{i,j}^{(h)}(y) \cdot N_{i',j'}^{(h)}(z)} \\
& + \left(\frac{(h+1) \cdot \epsilon^2}{60L^3} + O\left(\frac{\epsilon \cdot h}{L}\right) \right) \cdot \frac{\sqrt{N_{i,j}^{(h)}(y) \cdot N_{i',j'}^{(h)}(z)}}{q^2} \\
& \leq \frac{\epsilon}{10} \cdot \frac{h^2 - h/2}{L+1} \cdot \frac{\sqrt{N_{i,j}^{(h)}(y) \cdot N_{i',j'}^{(h)}(z)}}{q^2}.
\end{aligned}$$

By plugging the above bound into (64) using triangle inequality and using (17) we get the following with probability at least $1 - O\left(\frac{\delta}{L}\right)$:

$$\begin{aligned}
& \left| \left\langle \psi_{i,j}^{(h)}(y), \psi_{i',j'}^{(h)}(z) \right\rangle - \Pi_{i,j,i',j'}^{(h)}(y, z) \right| \\
& \leq O(\epsilon h / L) \cdot \sqrt{N_{i,j}^{(h+1)}(y) \cdot N_{i',j'}^{(h+1)}(z)} \\
& + \frac{\epsilon}{10} \cdot \frac{h^2 - h/2}{L+1} \cdot \sum_{a=-\frac{q-1}{2}}^{\frac{q-1}{2}} \sum_{b=-\frac{q-1}{2}}^{\frac{q-1}{2}} \frac{\sqrt{N_{i+a,j+b}^{(h)}(y) \cdot N_{i'+a,j'+b}^{(h)}(z)}}{q^2} \\
& \leq O(\epsilon h / L) \cdot \sqrt{N_{i,j}^{(h+1)}(y) \cdot N_{i',j'}^{(h+1)}(z)} \\
& + \frac{\epsilon}{10} \cdot \frac{h^2 - h/2}{L+1} \cdot \sqrt{\sum_{a=-\frac{q-1}{2}}^{\frac{q-1}{2}} \sum_{b=-\frac{q-1}{2}}^{\frac{q-1}{2}} \frac{N_{i+a,j+b}^{(h)}(y)}{q^2}} \cdot \sqrt{\sum_{a=-\frac{q-1}{2}}^{\frac{q-1}{2}} \sum_{b=-\frac{q-1}{2}}^{\frac{q-1}{2}} \frac{N_{i'+a,j'+b}^{(h)}(z)}{q^2}} \\
& \leq \frac{\epsilon}{10} \cdot \frac{h^2}{L+1} \cdot \sqrt{N_{i,j}^{(h+1)}(y) \cdot N_{i',j'}^{(h+1)}(z)}.
\end{aligned} \tag{65}$$

Similarly, we can prove that with probability at least $1 - O\left(\frac{\delta}{L}\right)$ the following hold simultaneously for all $i, i' \in [d_1]$ and all $j, j' \in [d_2]$,

$$\begin{aligned}
& \left| \left\| \psi_{i,j}^{(h)}(y) \right\|_2^2 - \Pi_{i,j,i,j}^{(h)}(y, y) \right| \leq \frac{\epsilon}{10} \cdot \frac{h^2}{L+1} \cdot N_{i,j}^{(h+1)}(y), \\
& \left| \left\| \psi_{i',j'}^{(h)}(z) \right\|_2^2 - \Pi_{i',j',i',j'}^{(h)}(z, z) \right| \leq \frac{\epsilon}{10} \cdot \frac{h^2}{L+1} \cdot N_{i',j'}^{(h+1)}(z).
\end{aligned}$$

This is sufficient to prove the inductive step for statement $P_2(h)$, in the case of $h < L$, i.e., $\Pr[P_2(h) | P_2(h-1), P_1(h), P_1(h-1)] \geq 1 - O(\delta/L)$.

Now we prove the inductive step for $P_2(h)$ in the case of $h = L$. Similar to before, if we let $f_{i,j} := \psi_{i,j}^{(L-1)}(y) \otimes \dot{\phi}_{i,j}^{(L)}(y)$ and $g_{i',j'} := \psi_{i',j'}^{(L-1)}(z) \otimes \dot{\phi}_{i',j'}^{(L)}(z)$, then by (24), we have $\psi_{i,j}^{(L)}(y) = (Q^2 \cdot f_{i,j})$ and $\psi_{i',j'}^{(L)}(z) = (Q^2 \cdot g_{i',j'})$. Thus by Lemma 1 and union bound, we find that, with probability at least $1 - O\left(\frac{\delta}{L}\right)$, the following inequality holds simultaneously for all $i, i' \in [d_1]$ and $j, j' \in [d_2]$:

$$\left| \left\langle \psi_{i,j}^{(L)}(y), \psi_{i',j'}^{(L)}(z) \right\rangle - \langle f_{i,j}, g_{i',j'} \rangle \right| \leq O\left(\frac{\epsilon}{L}\right) \cdot \|f_{i,j}\|_2 \|g_{i',j'}\|_2.$$

Therefore, using (61) and Lemma 9 along with inductive hypotheses $P_2(L-1)$ and Lemma 10, with probability at least $1 - O\left(\frac{\delta}{L}\right)$, the following holds simultaneously for all $i, i' \in [d_1]$ and $j, j' \in [d_2]$,

$$\begin{aligned} \left| \left\langle \psi_{i,j}^{(L)}(y), \psi_{i',j'}^{(L)}(z) \right\rangle - \langle f_{i,j}, g_{i',j'} \rangle \right| &\leq O\left(\frac{\epsilon}{L}\right) \cdot \sqrt{\Pi_{i,j,i,j}^{(L-1)}(y, y) \cdot \dot{\Gamma}_{i,j,i,j}^{(L)}(y, y) \cdot \Pi_{i',j',i',j'}^{(L-1)}(z, z) \cdot \dot{\Gamma}_{i',j',i',j'}^{(L)}(z, z)} \\ &= O(\epsilon) \cdot \frac{\sqrt{N_{i,j}^{(L)}(y) \cdot N_{i',j'}^{(L)}(z)}}{q^2}. \end{aligned}$$

By combining the above with inductive hypotheses $P_1(L), P_2(L-1)$ and (60) via triangle inequality and invoking Lemma 10 and also using the definition of $\Pi^{(L)}(y, z)$ given in (18), we get that the following holds, simultaneously for all $i, i' \in [d_1]$ and $j, j' \in [d_2]$, with probability at least $1 - O\left(\frac{\delta}{L}\right)$,

$$\begin{aligned} &\left| \left\langle \psi_{i,j}^{(L)}(y), \psi_{i',j'}^{(L)}(z) \right\rangle - \Pi_{i,j,i',j'}^{(L)}(y, z) \right| \\ &\leq \frac{\epsilon}{10} \cdot \frac{(L-1)^2}{L+1} \cdot \sqrt{N_{i,j}^{(L)}(y) \cdot N_{i',j'}^{(L)}(z)} \cdot \left(\left| \dot{\Gamma}_{i,j,i',j'}^{(L)}(y, z) \right| + \frac{1}{q^2} \cdot \frac{\epsilon}{8L} \right) + \frac{1}{q^2} \cdot \frac{\epsilon}{8L} \cdot \left| \Pi_{i,j,i',j'}^{(L-1)}(y, z) \right| \\ &\quad + \frac{(L+1) \cdot \epsilon^2}{60L^3} \cdot \frac{\sqrt{N_{i,j}^{(L)}(y) \cdot N_{i',j'}^{(L)}(z)}}{q^2} + O(\epsilon) \cdot \frac{\sqrt{N_{i,j}^{(L)}(y) \cdot N_{i',j'}^{(L)}(z)}}{q^2} \\ &\leq \frac{\epsilon}{10} \cdot \frac{(L-1)^2}{L+1} \cdot \frac{\sqrt{N_{i,j}^{(L)}(y) \cdot N_{i',j'}^{(L)}(z)}}{q^2} \cdot \left(1 + \frac{\epsilon}{8L} \right) + \frac{\epsilon}{8q^2} \cdot \sqrt{N_{i,j}^{(L)}(y) \cdot N_{i',j'}^{(L)}(z)} \\ &\quad + \left(\frac{(L+1) \cdot \epsilon^2}{60L^3} + O(\epsilon) \right) \cdot \frac{\sqrt{N_{i,j}^{(L)}(y) \cdot N_{i',j'}^{(L)}(z)}}{q^2} \\ &\leq \frac{\epsilon \cdot (L-1)}{10} \cdot \frac{\sqrt{N_{i,j}^{(L)}(y) \cdot N_{i',j'}^{(L)}(z)}}{q^2}. \end{aligned}$$

This proves the inductive step for statement $P_2(h)$, in the case of $h = L$, i.e., $\Pr[P_2(L)|P_2(L-1), P_1(L), P_1(L-1)] \geq 1 - O(\delta/L)$. The induction is complete and hence the statements of lemma are proved by union bounding over all $h = 0, 1, 2, \dots, L$. \square

In the following lemma we analyze the runtime of the CNTK Sketch algorithm,

Lemma 12 (Runtime of the CNTK Sketch). *For every positive integers d_1, d_2, c , and L , every $\epsilon, \delta > 0$, every image $x \in \mathbb{R}^{d_1 \times d_2 \times c}$, the time to compute the CNTK Sketch $\Psi_{\text{cntk}}^{(L)}(x) \in \mathbb{R}^{s^*}$, for $s^* = O\left(\frac{1}{\epsilon^2} \cdot \log \frac{1}{\delta}\right)$, using the procedure given in Definition 4.2 is bounded by $O\left(\frac{L^{11}}{\epsilon^7} \cdot (d_1 d_2) \cdot \log^3 \frac{d_1 d_2 L}{\epsilon \delta}\right)$.*

Proof. First note that the total time to compute $N_{i,j}^{(h)}(x)$ for all $i \in [d_1]$ and $j \in [d_2]$ and $h = 0, 1, \dots, L$ as per (14) is bounded by $O(q^2 L \cdot d_1 d_2)$. Besides the time to compute $N_{i,j}^{(h)}(x)$, there are two other main components to the runtime of this procedure. The first heavy operation corresponds to

computing vectors $\left[Z_{i,j}^{(h)}(x)\right]_l = Q^{2p+2} \cdot \left(\left[\mu_{i,j}^{(h)}(x)\right]^{\otimes l} \otimes \mathbf{e}_1^{\otimes 2p+2-l}\right)$ for $l = 0, 1, 2, \dots, 2p+2$ and $h = 1, 2, \dots, L$ and all indices $i \in [d_1]$ and $j \in [d_2]$, in (21). By Lemma 1, the time to compute $\left[Z_{i,j}^{(h)}(x)\right]_l$ for a fixed h , fixed $i \in [d_1]$ and $j \in [d_2]$, and all $l = 0, 1, 2, \dots, 2p+2$ is bounded by,

$$O\left(L^{10}/\epsilon^{20/3} \cdot \log^2 \frac{L}{\epsilon} \log^3 \frac{d_1 d_2 L}{\epsilon \delta} + q^2 \cdot L^8/\epsilon^{16/3} \cdot \log^3 \frac{d_1 d_2 L}{\epsilon \delta}\right) = O\left(\frac{L^{10}}{\epsilon^7} \cdot \log^3 \frac{d_1 d_2 L}{\epsilon \delta}\right).$$

The total time to compute vectors $\left[Z_{i,j}^{(h)}(x)\right]_l$ for all $h = 1, 2, \dots, L$ and all $l = 0, 1, 2, \dots, 2p+2$ and all indices $i \in [d_1]$ and $j \in [d_2]$ is thus bounded by $O\left(\frac{L^{11}}{\epsilon^7} \cdot (d_1 d_2) \cdot \log^3 \frac{d_1 d_2 L}{\epsilon \delta}\right)$. The next computationally expensive operation is computing vectors $\left[Y_{i,j}^{(h)}(x)\right]_l$ for $l = 0, 1, 2, \dots, 2p'+1$ and $h = 1, 2, \dots, L$, and all indices $i \in [d_1]$ and $j \in [d_2]$, in (22). By Lemma 1, the runtime of computing $\left[Y_{i,j}^{(h)}(x)\right]_l$ for a fixed h , fixed $i \in [d_1]$ and $j \in [d_2]$, and all $l = 0, 1, 2, \dots, 2p'+1$ is bounded by,

$$O\left(\frac{L^6}{\epsilon^6} \cdot \log^2 \frac{L}{\epsilon} \log^3 \frac{d_1 d_2 L}{\epsilon \delta} + \frac{q^2 \cdot L^8}{\epsilon^6} \cdot \log^3 \frac{d_1 d_2 L}{\epsilon \delta}\right) = O\left(\frac{L^8}{\epsilon^6} \log^2 \frac{L}{\epsilon} \cdot \log^3 \frac{d_1 d_2 L}{\epsilon \delta}\right).$$

Hence, the total time to compute vectors $\left[Y_{i,j}^{(h)}(x)\right]_l$ for all $h = 1, 2, \dots, L$ and $l = 0, 1, 2, \dots, 2p'+1$ and all indices $i \in [d_1]$ and $j \in [d_2]$ is $O\left(\frac{L^9}{\epsilon^6} \log^2 \frac{L}{\epsilon} \cdot (d_1 d_2) \cdot \log^3 \frac{d_1 d_2 L}{\epsilon \delta}\right)$. The total runtime bound is obtained by summing up these three contributions. \square

Now we are ready to prove Theorem 3,

Proof of Theorem 3: Let $\psi^{(L)} : \mathbb{R}^{d_1 \times d_2 \times c} \rightarrow \mathbb{R}^{d_1 \times d_2 \times s}$ for $s = O\left(\frac{L^4}{\epsilon^2} \cdot \log^3 \frac{d_1 d_2 L}{\epsilon \delta}\right)$ be the mapping defined in (24) of Definition 4.2. By (25), the CNTK Sketch $\Psi_{cntk}^{(L)}(x)$ is defined as

$$\Psi_{ntk}^{(L)}(x) := \frac{1}{d_1 d_2} \cdot G \cdot \left(\sum_{i \in [d_1]} \sum_{j \in [d_2]} \psi_{i,j}^{(L)}(x) \right).$$

The matrix G is defined in (25) to be a matrix of i.i.d. normal entries with $s^* = C \cdot \frac{1}{\epsilon^2} \cdot \log \frac{1}{\delta}$ rows for large enough constant C . [DG03] shows that G is a JL transform and hence $\Psi_{cntk}^{(L)}$ satisfies the following,

$$\Pr \left[\left| \left\langle \Psi_{cntk}^{(L)}(y), \Psi_{cntk}^{(L)}(z) \right\rangle - \frac{1}{d_1^2 d_2^2} \cdot \sum_{i,i' \in [d_1]} \sum_{j,j' \in [d_2]} \left\langle \psi_{i,j}^{(L)}(y), \psi_{i',j'}^{(L)}(z) \right\rangle \right| \leq O(\epsilon) \cdot A \right] \geq 1 - O(\delta),$$

where $A := \frac{1}{d_1^2 d_2^2} \cdot \left\| \sum_{i \in [d_1]} \sum_{j \in [d_2]} \psi_{i,j}^{(L)}(y) \right\|_2 \cdot \left\| \sum_{i \in [d_1]} \sum_{j \in [d_2]} \psi_{i,j}^{(L)}(z) \right\|_2$. By triangle inequality together with Lemma 11 and Lemma 10, the following bounds hold with probability at least $1 - O(\delta)$:

$$\begin{aligned} \left\| \sum_{i \in [d_1]} \sum_{j \in [d_2]} \psi_{i,j}^{(L)}(y) \right\|_2 &\leq \frac{11}{10} \cdot \frac{\sqrt{L-1}}{q} \cdot \sum_{i \in [d_1]} \sum_{j \in [d_2]} \sqrt{N_{i,j}^{(L)}(y)}, \\ \sum_{i \in [d_1]} \sum_{j \in [d_2]} \left\| \psi_{i,j}^{(L)}(z) \right\|_2^2 &\leq \frac{11}{10} \cdot \frac{\sqrt{L-1}}{q} \cdot \sum_{i \in [d_1]} \sum_{j \in [d_2]} \sqrt{N_{i,j}^{(L)}(z)}, \end{aligned}$$

Therefore, by union bound we find that, with probability at least $1 - O(\delta)$:

$$\begin{aligned} & \left| \left\langle \Psi_{cntk}^{(L)}(y), \Psi_{cntk}^{(L)}(z) \right\rangle - \frac{1}{d_1^2 d_2^2} \cdot \sum_{i, i' \in [d_1]} \sum_{j, j' \in [d_2]} \left\langle \psi_{i,j}^{(L)}(y), \psi_{i',j'}^{(L)}(z) \right\rangle \right| \\ & \leq O\left(\frac{\epsilon L}{q^2 \cdot d_1^2 d_2^2}\right) \cdot \sum_{i, i' \in [d_1]} \sum_{j, j' \in [d_2]} \sqrt{N_{i,j}^{(L)}(y) \cdot N_{i',j'}^{(L)}(z)}. \end{aligned}$$

Be combining the above with Lemma 11 using triangle inequality and union bound and also using (19), the following holds with probability at least $1 - O(\delta)$:

$$\left| \left\langle \Psi_{cntk}^{(L)}(y), \Psi_{cntk}^{(L)}(z) \right\rangle - \Theta_{cntk}^{(L)}(y, z) \right| \leq \frac{\epsilon \cdot (L-1)}{9q^2 \cdot d_1^2 d_2^2} \cdot \sum_{i, i' \in [d_1]} \sum_{j, j' \in [d_2]} \sqrt{N_{i,j}^{(L)}(y) \cdot N_{i',j'}^{(L)}(z)}. \quad (66)$$

Now we prove that $\Theta_{cntk}^{(L)}(y, z) \geq \frac{L-1}{9q^2 d_1^2 d_2^2} \cdot \sum_{i, i' \in [d_1]} \sum_{j, j' \in [d_2]} \sqrt{N_{i,j}^{(L)}(y) \cdot N_{i',j'}^{(L)}(z)}$ for every $L \geq 2$. First note that, it follows from (15) that $\Gamma_{i,j,i',j'}^{(1)}(y, z) \geq 0$ for any i, i', j, j' because the function κ_1 is non-negative everywhere on $[-1, 1]$. This also implies that $\Gamma_{i,j,i',j'}^{(2)}(y, z) \geq \frac{\sqrt{N_{i,j}^{(2)}(y) \cdot N_{i',j'}^{(2)}(z)}}{\pi \cdot q^2}$ because $\kappa_1(\alpha) \geq \frac{1}{\pi}$ for every $\alpha \in [0, 1]$. Since, $\kappa_1(\cdot)$ is a monotone increasing function, by recursively using (14) and (15) along with Lemma 8, we can show that for every $h \geq 1$, the value of $\Gamma_{i,j,i',j'}^{(h)}(y, z)$ is lower bounded by $\frac{\sqrt{N_{i,j}^{(h)}(y) \cdot N_{i',j'}^{(h)}(z)}}{q^2} \cdot \Sigma_{relu}^{(h)}(-1)$, where $\Sigma_{relu}^{(h)} : [-1, 1] \rightarrow \mathbb{R}$ is the function defined in (5).

Furthermore, it follows from (16) that $\dot{\Gamma}_{i,j,i',j'}^{(1)}(y, z) \geq 0$ for any i, i', j, j' because the function κ_0 is non-negative everywhere on $[-1, 1]$. Additionally, $\dot{\Gamma}_{i,j,i',j'}^{(2)}(y, z) \geq \frac{1}{2q^2}$ because $\kappa_0(\alpha) \geq \frac{1}{2}$ for every $\alpha \in [0, 1]$. By using the inequality $\Gamma_{i,j,i',j'}^{(h)}(y, z) \geq \frac{\sqrt{N_{i,j}^{(h)}(y) \cdot N_{i',j'}^{(h)}(z)}}{q^2} \cdot \Sigma_{relu}^{(h)}(-1)$ that we proved above along with the fact that $\kappa_0(\cdot)$ is a monotone increasing function and recursively using (16) and Lemma 8, it follows that for every $h \geq 1$, we have $\dot{\Gamma}_{i,j,i',j'}^{(h)}(y, z) \geq \frac{1}{q^2} \cdot \dot{\Sigma}_{relu}^{(h)}(-1)$.

By using these inequalities and Definition of $\Pi^{(h)}$ in (17) together with (14), recursively, it follows that, for every i, i', j, j' and $h = 2, \dots, L-1$:

$$\Pi_{i,j,i',j'}^{(h)}(y, z) \geq \frac{h}{4} \cdot \sqrt{N_{i,j}^{(h+1)}(y) \cdot N_{i',j'}^{(h+1)}(z)},$$

Therefore, using this inequality and (18) we have that for every $L \geq 2$:

$$\begin{aligned} \Pi_{i,j,i',j'}^{(L)}(y, z) & \geq \frac{L-1}{4} \cdot \sqrt{N_{i,j}^{(L)}(y) \cdot N_{i',j'}^{(L)}(z)} \cdot \frac{\dot{\Sigma}_{relu}^{(L)}(-1)}{q^2} \\ & \geq \frac{L-1}{9q^2} \cdot \sqrt{N_{i,j}^{(L)}(y) \cdot N_{i',j'}^{(L)}(z)}. \end{aligned}$$

Now using this inequality and (19), the following holds for every $L \geq 2$:

$$\Theta_{cntk}^{(L)}(y, z) \geq \frac{L-1}{9q^2 d_1^2 d_2^2} \cdot \sum_{i, i' \in [d_1]} \sum_{j, j' \in [d_2]} \sqrt{N_{i,j}^{(L)}(y) \cdot N_{i',j'}^{(L)}(z)}.$$

Therefore, by incorporating the above into (66) we get that,

$$\Pr \left[\left| \left\langle \Psi_{cntk}^{(L)}(y), \Psi_{cntk}^{(L)}(z) \right\rangle - \Theta_{cntk}^{(L)}(y, z) \right| \leq \epsilon \cdot \Theta_{cntk}^{(L)}(y, z) \right] \geq 1 - \delta.$$

Runtime: By Lemma 12, time to compute the CNTK Sketch is $O \left(\frac{L^{11}}{\epsilon^7} \cdot (d_1 d_2) \cdot \log^3 \frac{d_1 d_2 L}{\epsilon \delta} \right)$.
 \square